PL-TR-95-2177

SSS-TR-95-14980

A Comparative Analysis of the Seismic Characteristics of Cavity Decoupled Nuclear and Chemical Explosions

John R. Murphy
Brian W. Barker

Maxwell Laboratories, Incorporated
S-CUBED Division
P.O. Box 1620
La Jolla, CA 92038-1620

March 1995

Final Report
1 November 1992 - 31 October 1994

Approved for Public Release; Distribution Unlimited

PHILLIPS LABORATORY
Directorate of Geophysics
AIR FORCE MATERIEL COMMAND
HANSCOM AIR FORCE BASE, MA 01731-3010

"This technical report has been reviewed and is approved for publication."

JAMES F. LEWKOWICZ
Contract Manager

JAMES F. LEWKOWICZ
Director
Earth Sciences Division

This report has been reviewed by the ESD Public Affairs Office (PA) and is releasable to the National Technical Information Service (NTIS).

Qualified requestors may obtain additional copies from the Defense Technical Information Center. All others should apply to the National Technical Information Service.

If your address has changed, or if you wish to be removed from the mailing list, or if the addressee is no longer employed by your organization, please notify PL/IM, 29 Randolph Road, Hanscom AFB, MA 01731-3010. This will assist us in maintaining a current mailing list.

Do not return copies of this report unless contractual obligations or notices on a specific document requires that it be returned.

REPORT DOCUMENTATION PAGE

Form Approved OMB No. 0704-0188

1. AGENCY USE ONLY *(Leave blank)*	2. REPORT DATE	3. REPORT TYPE AND DATES COVERED
	March 1995	Final 11/1/92 - 10/31/94

4. TITLE AND SUBTITLE

A COMPARATIVE ANALYSIS OF THE SEISMIC CHARACTERISTICS OF CAVITY DECOUPLED NUCLEAR AND CHEMICAL EXPLOSIONS

5. FUNDING NUMBERS

Contract:
F19628-91-C-0186

PE 61102F
PR 2309
TA G2
WU BL

6. AUTHOR(S)

John R. Murphy and Brian W. Barker

7. PERFORMING ORGANIZATION NAME(S) AND ADDRESS(ES)

Maxwell Laboratories, Inc.
S-CUBED Division
P.O. Box 1620
La Jolla, CA 92038-1620

8. PERFORMING ORGANIZATION REPORT NUMBER

SSS-TR-95-14980

9. SPONSORING/MONITORING AGENCY NAME(S) AND ADDRESS(ES)

Phillips Laboratory
29 Randolph Road
Hanscom AFB, MA 01731-3010

Contracting Manager: James F. Lewkowicz/GPE

10. SPONSORING/MONITORING AGENCY REPORT NUMBER

PL-TR-95-2177

11. SUPPLEMENTARY NOTES

12a. DISTRIBUTION/AVAILABILITY STATEMENT

Approved for public release; distribution unlimited

12b. DISTRIBUTION CODE

13. ABSTRACT *(Maximum 200 words)*

Successful seismic monitoring of any eventual Comprehensive Test Ban Treaty will require the development of a capability to identify signals from small cavity decoupled nuclear explosions from among the numerous signals to be expected from earthquakes, rockbursts and chemical explosion (CE) events of comparable magnitude. The investigations summarized in this report center on a variety of comparative analyses of observed and simulated seismic data corresponding to decoupled nuclear explosions with data recorded from both tamped and near-surface, ripple-fired CE events. More specifically, seismic data recorded from cavity decoupled nuclear tests in both the U.S. and former Soviet Union are used to assess the relative seismic coupling efficiencies of the different types of CE events and to evaluate potential seismic discriminants which might be used to identify the various source types. The results of these comparison studies incidate that tamped CE events with yields on the order of 7 tons and ripple-fired CE events with yields in the 70-100 ton range can be expected to produce near-regional ground motion levels comparable to those expected from fully decoupled 1 kt nuclear explosions at Azgir.

14. SUBJECT TERMS

Seismic, Explosion, Cavity Decoupling, STERLING, Discrimination, Nuclear, Mine Blast, Azgir

15. NUMBER OF PAGES 96

16. PRICE CODE

17. SECURITY CLASSIFICATION OF REPORT	18. SECURITY CLASSIFICATION OF THIS PAGE	19. SECURITY CLASSIFICATION OF ABSTRACT	20. LIMITATION OF ABSTRACT
UNCLASSIFIED	UNCLASSIFIED	UNCLASSIFIED	UNLIMITED

Table of Contents

List of Illustrations

1. INTRODUCTION

A central issue in current discussions of the seismic monitoring capability required to adequately verify any eventual Comprehensive Test Ban Treaty (CTBT) concerns the definition of the threshold level of seismic event size or magnitude down to which seismic events will have to be detected and identified. It is generally agreed that the capability currently exists to unambiguously identify almost all seismic events having magnitudes characteristic of well-coupled underground nuclear explosions with yields greater than a few kilotons (i.e., $m_b \sim 4$, OTA (1988)). However, in the context of monitoring a CTBT, consideration has to be given to the requirement to characterize the much smaller signals which would be expected to result from various evasive testing practices which might be employed by a nation pursuing a clandestine nuclear weapons development program. The most challenging of such proposed evasive testing practices are those associated with cavity decoupling. That is, since the U.S. nuclear cavity decoupling experiment STERLING established that it is possible to reduce the amplitude of the radiated seismic signal by at least a factor of 70 using this testing procedure, it follows that comprehensive monitoring of underground nuclear tests in the 1 to 10 kt range will necessarily involve identification analyses of small seismic events with magnitudes in the range $2.0 < m_b < 3.5$. At such low magnitudes, seismic activity associated with naturally occurring earthquakes is supplemented by seismic events of similar size which are associated with chemical explosions (CE) routinely being carried out in most developed areas of the world in conjunction with a variety of quarrying, mining and construction projects. For this reason, it is important to characterize the types and sizes of CE events which will have to be detected and identified in order to effectively monitor a CTBT. The objective of the research program described in this report has been to improve the capability to distinguish between small cavity decoupled nuclear explosions and CE events of comparable magnitude through analyses of observed and simulated seismic data representative of the two source types.

This report presents a summary of the investigations which have been conducted on this project over the past year. Preliminary results of the first year of this study were described in a previous report by Murphy and Barker (1994). In Section 2, near-regional seismic data recorded from tamped and partially

decoupled nuclear explosions at the Soviet Azgir test site are theoretically scaled to the nominal 1 kt fully decoupled scenario and then used to estimate the yields of both fully tamped and near-surface, ripple-fired CE events which would be expected to produce comparable ground motion levels. This is followed in Section 3 by an identification analysis of selected seismic data recorded from the various source types in which the time dependent spectral compositions of the signals from tamped and decoupled nuclear explosions and CE events are compared. The report concludes with Section 4 which contains a summary and statement of conclusions regarding the current capability to discriminate between the seismic signals produced by cavity decoupled nuclear and CE events.

2. PRELIMINARY ASSESSMENT OF THE RELATIVE SEISMIC COUPLING EFFICIENCY OF CAVITY DECOUPLED NUCLEAR AND CHEMICAL EXPLOSIONS

2.1 Overview of Cavity Decoupling Phenomenology

Surrounding every fully coupled underground nuclear explosion is a region within which the material response is nonlinear. This corresponds to the regime where the induced shock pressure is high enough to cause vaporization, crushing and cracking of the medium. As the range from the detonation point increases, however, the shock pressure decays to a level (P_{el}) at which the response is linear and it is the forcing function acting at this boundary which defines the characteristics of the radiated seismic waves which are used for detection and discrimination purposes. For the spherically symmetric case, the radius of this boundary is commonly called the elastic radius and is denoted as r_{el}. Consider the simplest approximation in which the pressure function acting at r_{el} is taken to be a step in pressure, $P_{el}\ H(\tau)$. Then it can be shown (Mueller and Murphy, 1971) that the amplitude of the seismic source function, $S(\omega)$, in the low frequency limit is given by

$$\lim_{\omega \to 0} \quad S(\omega) \sim P_{el}\, r_{el}^3 \qquad (1)$$

Now, for explosions at a fixed depth, P_{el} is generally taken to be a medium dependent constant which is independent of yield and, consequently, the low frequency seismic coupling efficiency for explosions at a fixed depth will depend only on r_{el}. It follows that, since the peak shock pressure in the nonlinear regime decreases with distance as r^{-n} where n is the medium dependent attenuation rate, r_{el} decreases as n increases and the reason that cavity decoupling works is that for strong shocks in air n = 3, while in rock $n \approx 2$ (Brode, 1968; Rodean, 1971). An explosion is said to be fully decoupled if it is detonated in a cavity which is large enough that the surrounding medium undergoes no nonlinear deformation. It follows from the above discussion that the radius of the cavity required to fully decouple an explosion is smaller than the elastic radius associated with a fully tamped shot of the same yield and, consequently, by equation (1), its low frequency coupling efficiency is lower.

The U.S. nuclear decoupling experiment STERLING which was conducted in Mississippi in December, 1966 confirmed the applicability of this theory and indicated that the amplitudes of the low frequency seismic signals produced by a fully decoupled nuclear test in salt are at least a factor of 70 smaller than those expected from a fully tamped nuclear explosion of the same yield at that same detonation point (Springer *et al.*, 1968). That is, while the observed low frequency decoupling factor for STERLING was about 70, the evidence suggests that STERLING was not fully decoupled and theoretical simulations which accurately predict the observed STERLING factor predict somewhat larger factors (100-200) for fully decoupled conditions in significantly larger cavities (Stevens *et al.*, 1991; Glenn and Goldstein, 1994). However, for the purposes of this report, we will defer to the limited experimental data and use the observed STERLING factor of 70 to represent full decoupling. The implications of such cavity decoupling effectiveness with respect to seismic monitoring are illustrated graphically in Figure 1, where approximate m_b/yield curves corresponding to different testing conditions are compared. In this case, the upper reference curve labeled "Good Coupling/Stable Region" is taken to be the nominal Semipalatinsk hardrock relation

$$m_b = 4.45 + 0.75 \log W \quad . \tag{2}$$

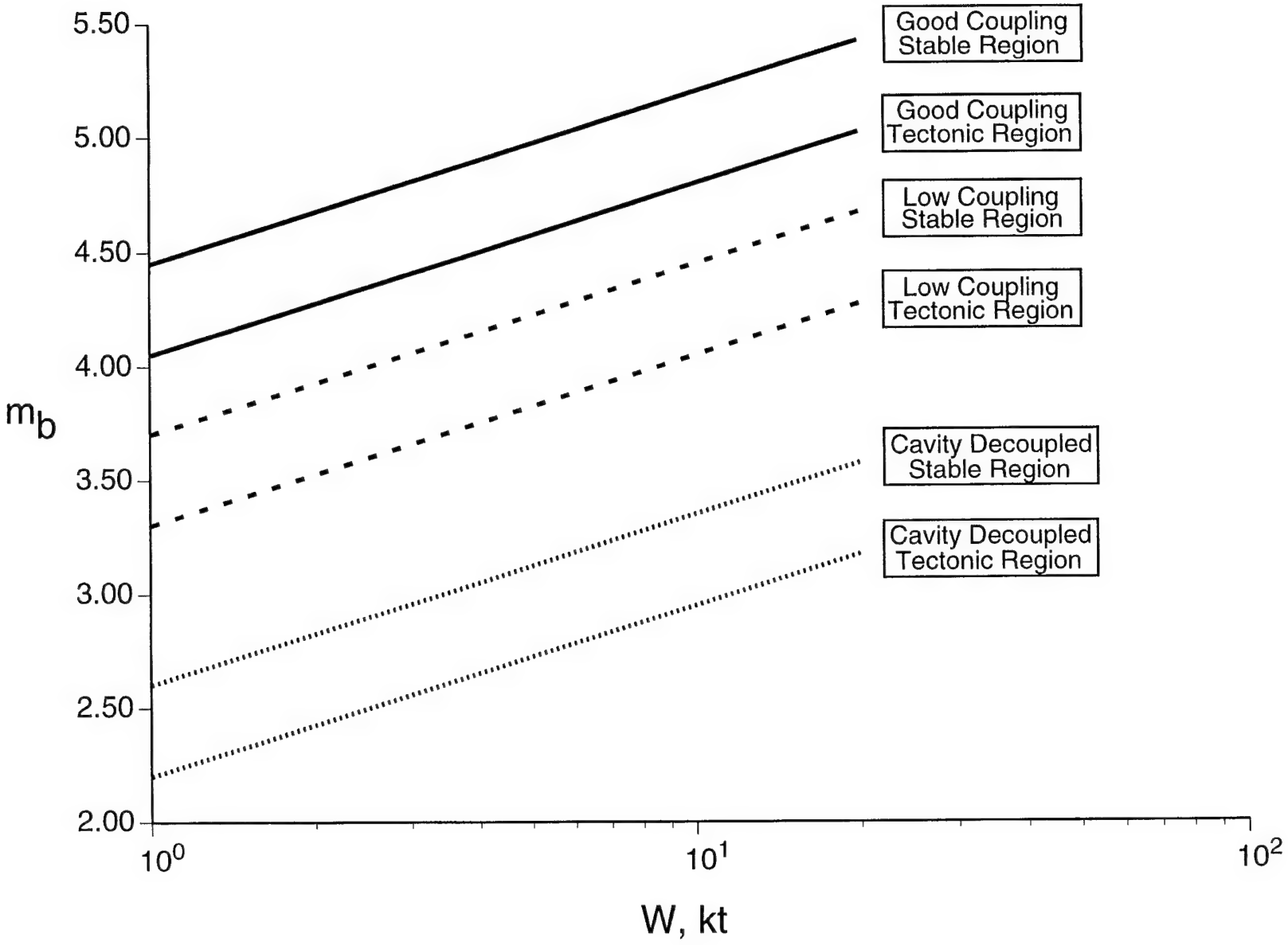

Figure 1. Comparison of m_b/yield relations for underground nuclear explosions illustrating the effects of test site tectonic environment and cavity decoupling.

The corresponding "Good Coupling/Tectonic Region" curve was obtained from this reference relation by subtracting 0.40 units m_b to account for upper mantle attenuation bias such as that observed between NTS and Semipalatinsk. The curves labeled "Low Coupling" in this figure are meant to be representative of explosions in dry, porous media such as the dry alluvium and tuff media at NTS and are offset below the corresponding reference hardrock curves by 0.75 units m_b. Finally, the curves labeled "Cavity Decoupled" are shown offset below the reference hardrock curves by 1.85 units m_b (i.e., the logarithm of 70). Thus, 1 kt fully decoupled tests in stable and tectonic regions are expected to correspond on average to m_b values of 2.6 and 2.2, respectively. Similarly, 10 kt fully decoupled explosions in stable and tectonic regions are expected to correspond on average to m_b values of 3.35 and 2.95, respectively. As a further point of reference, 1 kt and 10 kt fully decoupled explosions in good coupling media at NTS would be expected to correspond on average to m_b values of about 2.1 and 2.9, respectively. It follows that comprehensive monitoring of underground nuclear tests in the 1 to 10 kt range will necessarily involve identification analyses of small seismic events with magnitudes in the range $2.0 < m_b < 3.5$, at least in regions where cavity decoupling is considered to be feasible over this yield range.

The above discussion applies only in the low frequency limit. The reason for this is illustrated in Figure 2 which shows a comparison of schematic seismic source approximations for coupled and fully decoupled 10 kt explosions at a depth of 1 km in salt. It can be seen that both of these source function estimates are approximately flat at low frequencies and decrease as ω^{-2} above their respective characteristic corner frequencies. Moreover, since the characteristic corner frequency is inversely proportional to r_{el}, it is larger for the decoupled explosion than it is for the tamped explosion. Taking the ratio of the tamped to decoupled source approximations gives the frequency dependent decoupling factor shown in Figure 3. It can be seen that this approximation to the decoupling factor is roughly constant up to the corner frequency of the tamped source function, above which it decreases as ω^{-2} up to the corner frequency of the decoupled source function. Beyond this frequency, the decoupling remains at a constant (lower) value, or at least begins to decrease less rapidly, depending on the details of the high frequency character of the decoupled source function. Somewhat surprisingly, it has been found that such simple approximations to the

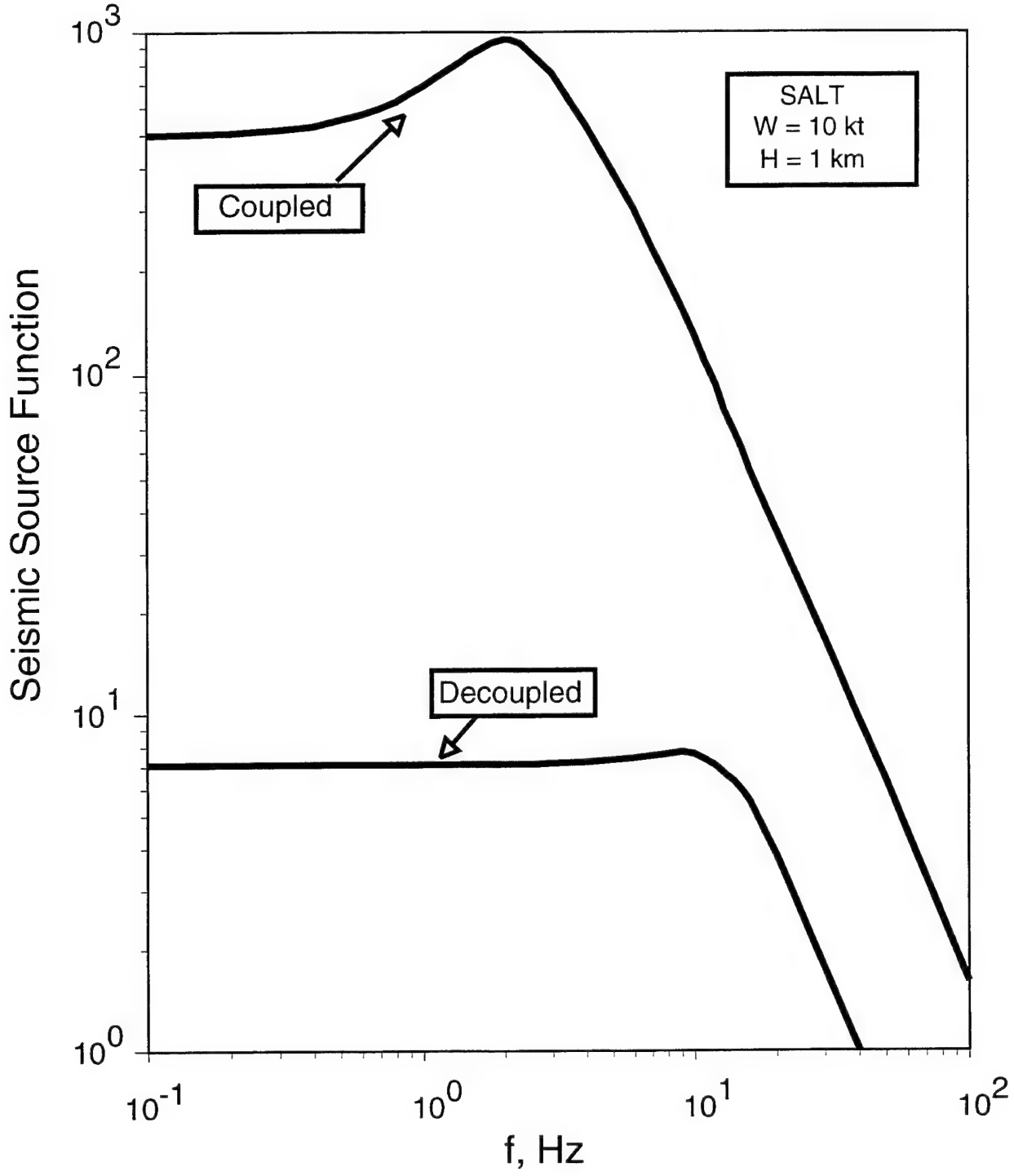

Figure 2. Comparison of approximate seismic source functions for coupled and fully decoupled explosions of the same yield.

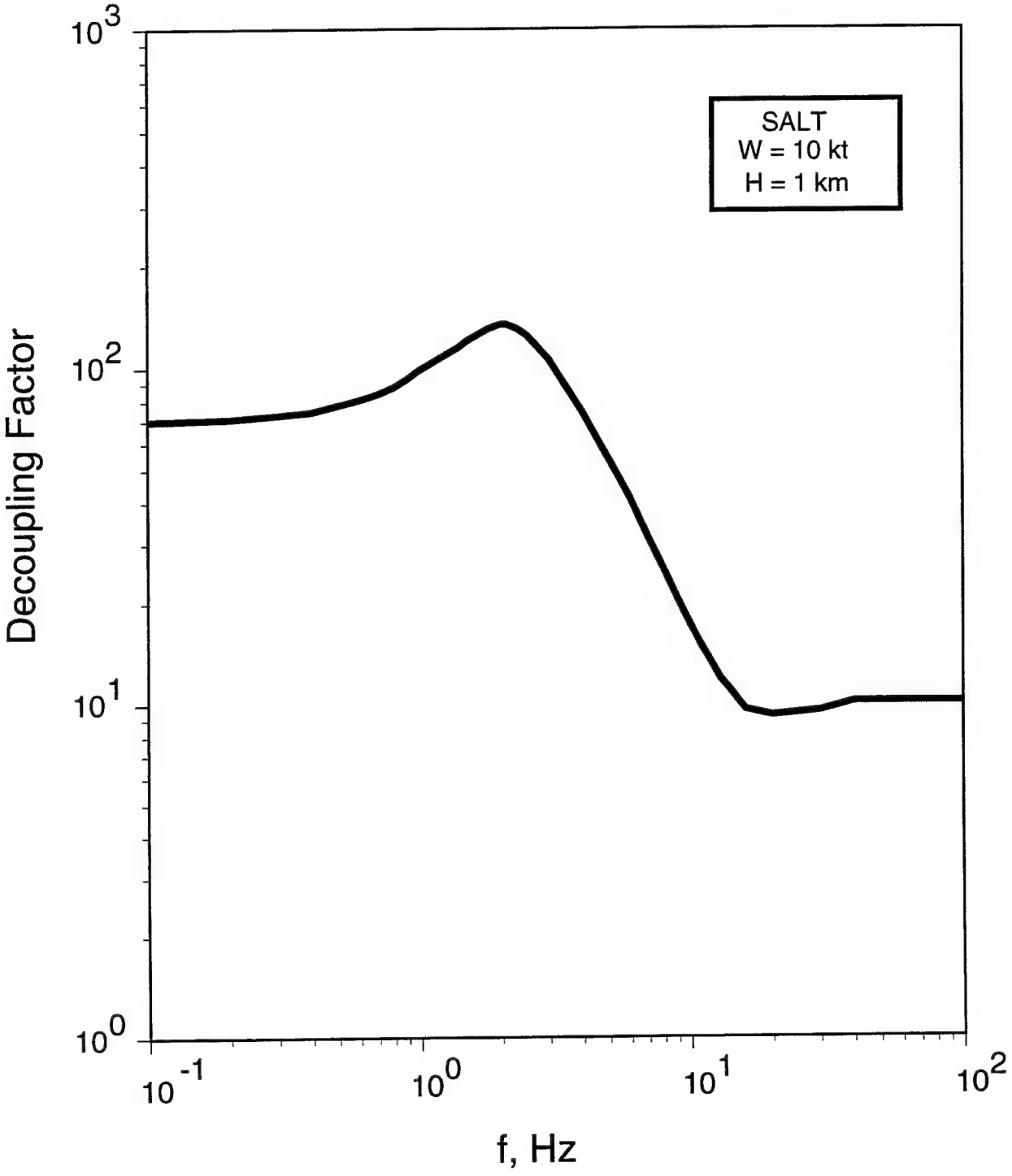

Figure 3. Decoupling factor as a function of frequency corresponding to the approximate seismic source functions of Figure 2.

frequency dependent effects of cavity decoupling describe the observed short-period data remarkably well. This fact is illustrated in Figure 4, where the seismic data observed from STERLING (top) at a station located 16 km from the source has been theoretically transformed into the seismic signal expected from the tamped 5.3 kt SALMON explosion at that same station (center) using a simple source spectral ratio comparable to that shown in Figure 3. Comparison of this synthetic with the corresponding observed SALMON data at that station (bottom) reveals excellent agreement with respect to amplitude level, waveform and relative spectral composition.

Despite the fact that the simple decoupled seismic source approximation described above has been shown to be quite successful in some applications, it is important to recognize that its application to higher frequency ranges or different yield/cavity volume ratios may be subject to significant uncertainties. The reason for this is illustrated in Figure 5 which shows the computed time history of pressure on the wall of a spherical cavity estimated from a nonlinear finite difference simulation of a nuclear explosion in the center of the cavity. It can be seen that this computed pressure contains an initial high amplitude spike associated with the shock reflection from the cavity wall, which is followed by a series of oscillations related to the reverberation of the air shock in the cavity. At late times, these pressure oscillations damp out and the pressure attains the steady-state value P, which is related to the yield W and cavity radius r_c by the expression (Latter *et al.*, 1961)

$$P = \frac{(\gamma - 1)\, W}{\frac{4}{3}\pi\, r_c^3} \qquad (3)$$

where γ is the adiabatic expansion constant for air. It is this steady-state pressure given by equation (3) which is generally used in the simple step function approximation to the cavity decoupled seismic source function. Now, if the response of the cavity wall is strictly linear, then this simple steady-state approximation provides an adequate description of the low frequency seismic coupling efficiency. However, Stevens *et al.* (1991) have shown that for most cavity decoupling scenarios of practical interest, the large initial pressure spike on the cavity wall induces nonlinear response in the surrounding medium and this

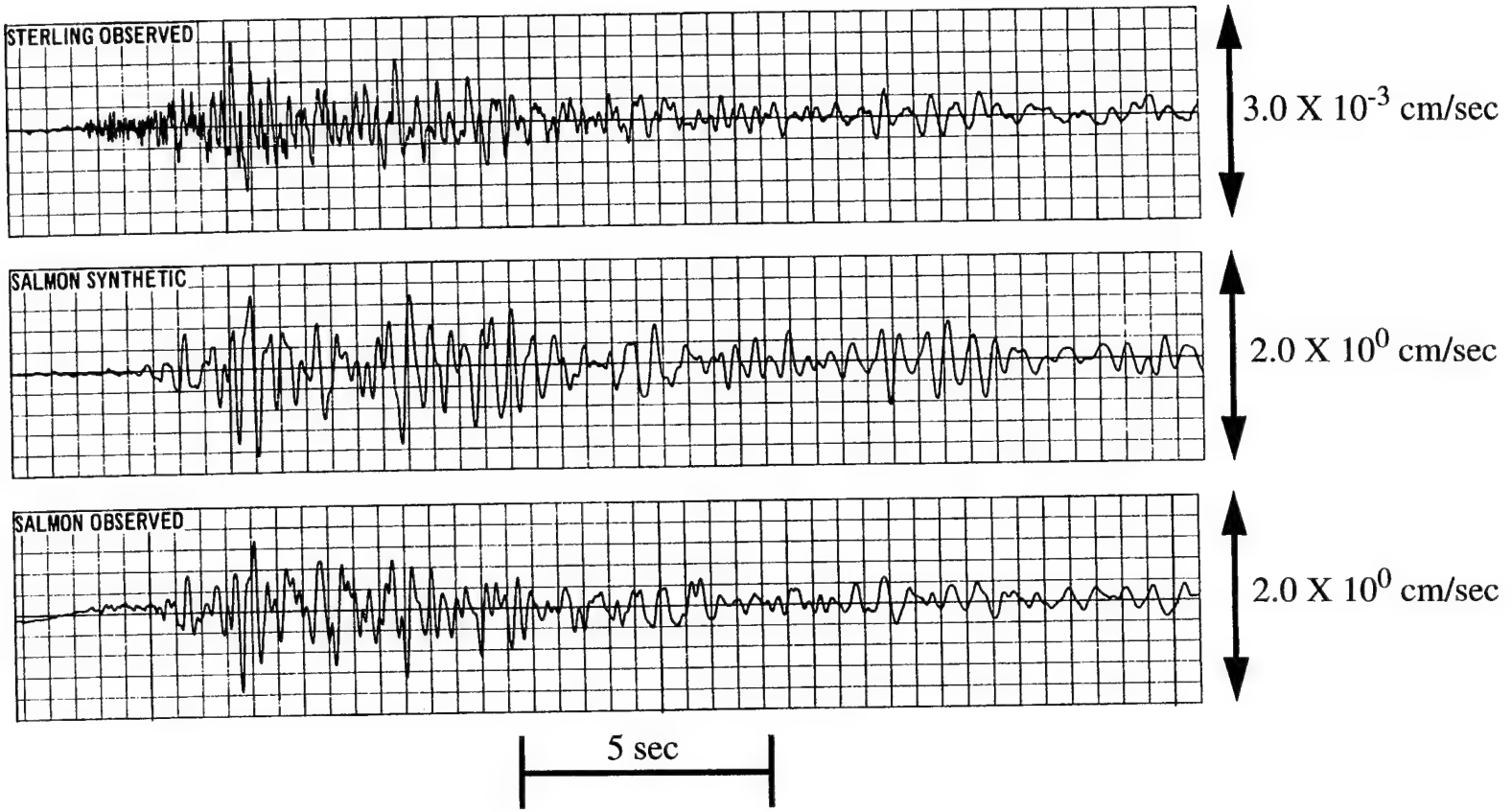

Figure 4. Comparison of observed SALMON and scaled STERLING seismograms, radial component, R = 16 km.

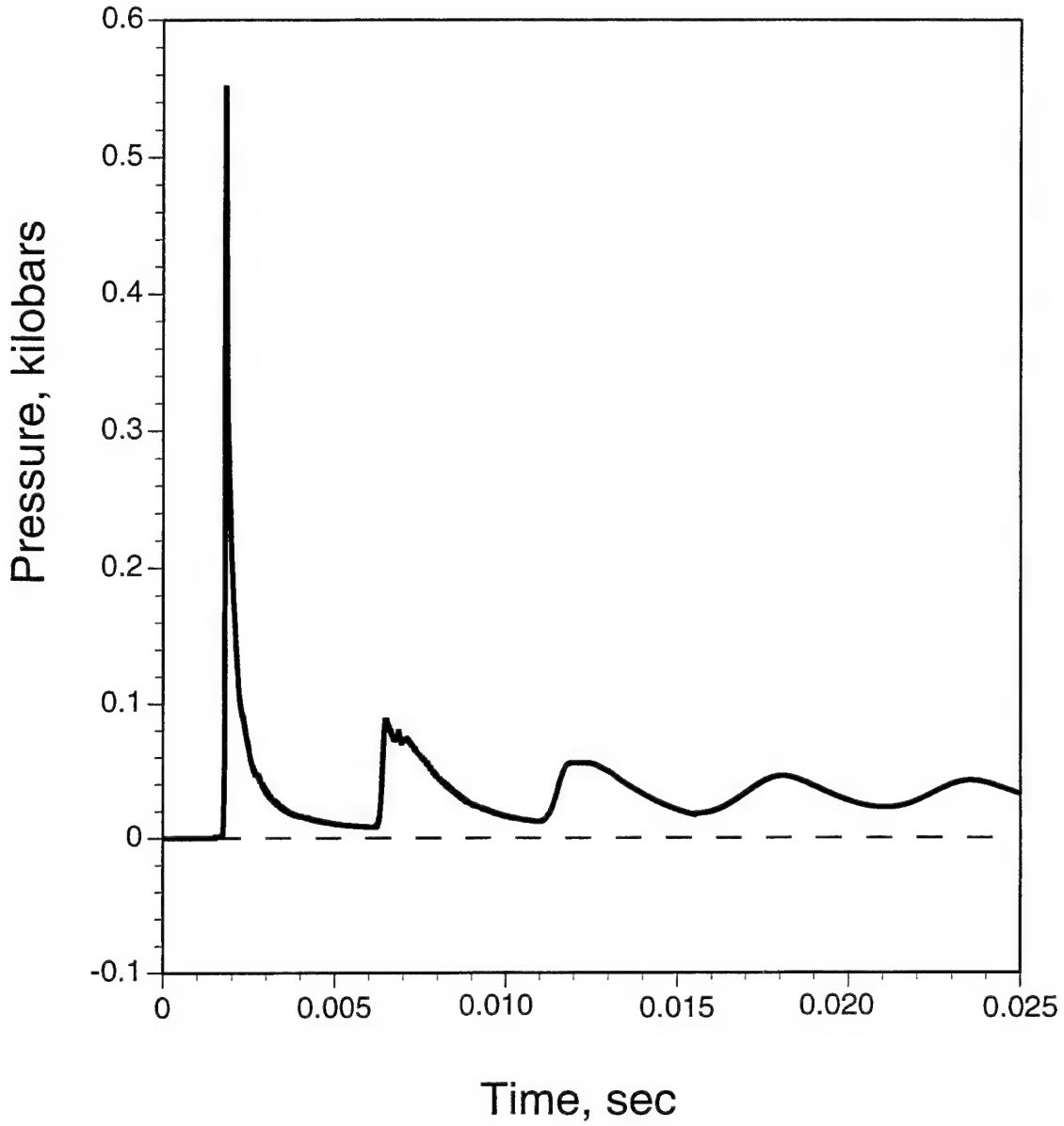

Figure 5. Nonlinear, finite difference simulation of the time dependent pressure on the wall of a spherical cavity produced by a nuclear explosion in the center of the cavity.

affects the seismic source characteristics at all frequencies. This fact is illustrated in Figure 6, which shows a comparison of the seismic source functions determined from a nonlinear finite difference simulation with the equivalent step function approximation for the same nuclear explosion in a spherical cavity. It can be seen that the nonlinear finite, difference solution shows enhanced high frequency spectral content and spectral modulations associated with the medium response to the initial pressure spike and subsequent reverberations of the air shock in the cavity. Moreover, because of the nonlinear response induced by the initial pressure spike, these differences persist to low frequencies. It follows that extrapolations outside the limited range of experimental experience which are based on simple, analytical models need to be cautiously evaluated on a case by case basis.

2.2 Simulation of Near-Regional Ground Motions Corresponding to 1 kt Fully Decoupled Explosions at the Soviet Azgir Test Site

During the period 1966-1979 the Soviet Union conducted a total of 17 underground nuclear explosions at the Azgir test site in the North Caspian Basin. These tests encompassed a yield range extending from less than 1 to about 100 kt and included the partially decoupled 8 kt explosion which was detonated at a depth of 987 m in a 38 m radius cavity on 3/29/76 (Adushkin *et al.*, 1992). Broadband seismic data were recorded from this latter test at near-regional distances ranging from about 1 to 113 km and, in our previous preliminary analysis (Murphy and Barker, 1994), these data were theoretically scaled to the ground motions to be expected from a 1 kt fully decoupled explosion using an approximate analytical source model similar to that described above in conjunction with the discussion of Figures 2-4. The resulting scaled ground motion data are reproduced in Figure 7 for the 8 stations located in the distance range 17.8 to 113 km. The peak vertical displacements measured from these 8 scaled seismograms are shown plotted as a function of distance in Figure 8, together with the average attenuation relation determined from a least-squares fit to these data. In our previous analysis (Murphy and Barker, 1994), these estimates of the near-regional ground motion amplitude levels to be expected from a 1 kt fully decoupled explosion at Azgir were used as a basis for

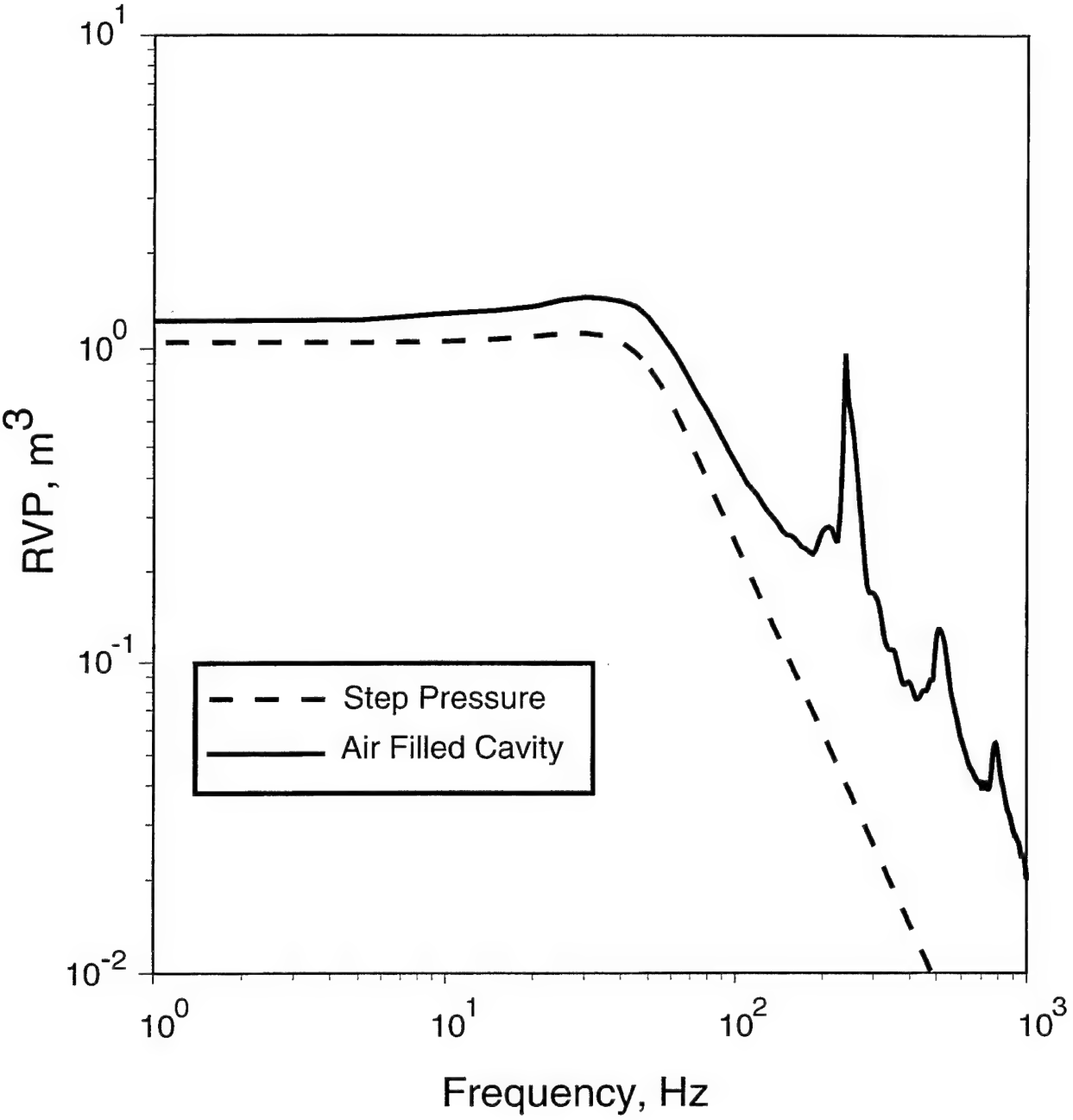

Figure 6. Computed decoupled seismic source functions corresponding to a nonlinear air shock and a step pressure approximation.

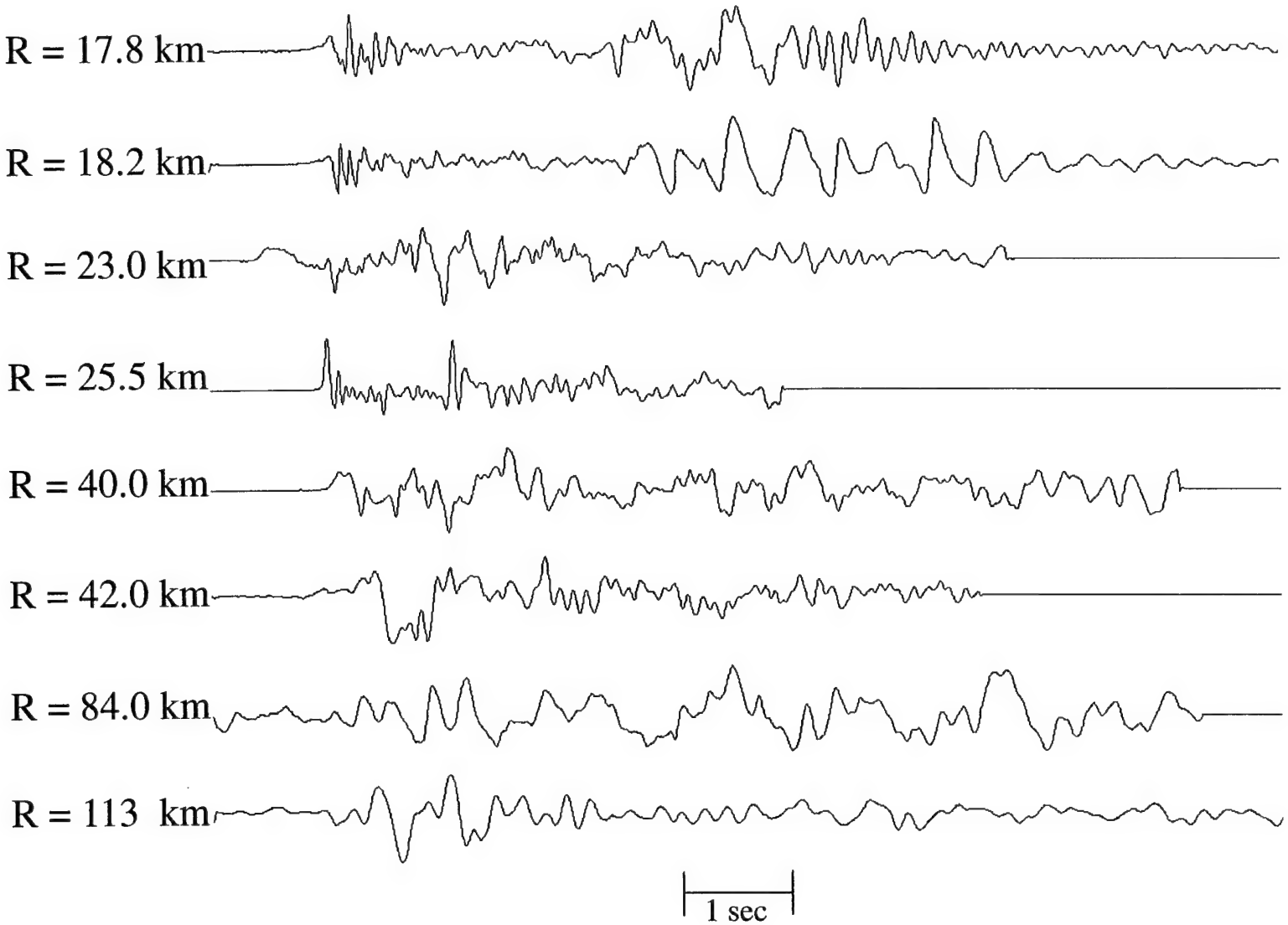

Figure 7. Theoretically scaled vertical component ground motions corresponding to a 1 kt fully decoupled explosion at the source location of the 8 kt Azgir decoupling test of 3/29/76.

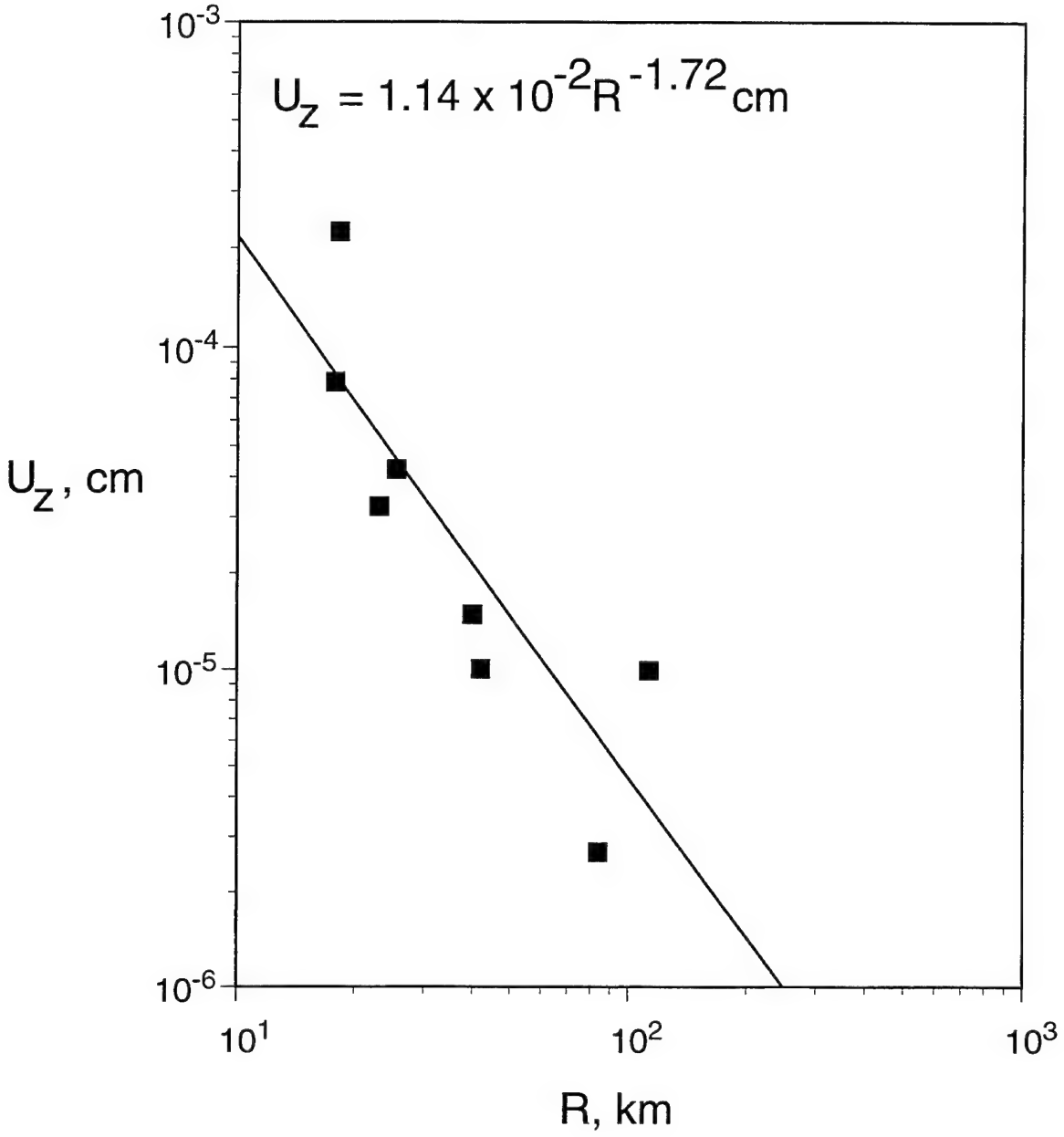

Figure 8. Estimated peak vertical displacements as a function of distance for a fully decoupled 1 kt nuclear explosion at a depth of 987m at Azgir.

conducting a preliminary assessment of the relative seismic coupling efficiency of various CE events.

While the above referenced analysis of the seismic data recorded from the partially decoupled Azgir test employed reasonable approximations, the final results are somewhat sensitive to the estimates of the yield and associated partial decoupling effectiveness for that cavity test, both of which are considered to be uncertain to some extent (Sykes, 1994). Consequently, in the present study, the simulation analysis has been extended to include data recorded from the tamped Azgir explosions. More specifically, near-regional ground motion data recorded from the 1.1 kt tamped explosion which was detonated at a depth of 161 m in salt at Azgir on 4/22/66 have been theoretically scaled to approximate the ground motions to be expected from a fully decoupled 1 kt explosion at that source location. Now since this explosion was detonated at a much shallower depth than STERLING (i.e., 161 m vs. 828 m), the source spectral ratio approximation used to scale these observed Azgir data had to be modified to account for this depth difference. This was accomplished using the following reasoning. According to the Latter criterion (Latter *et al.*, 1961), an explosion of yield W will be fully decoupled if it is detonated in a cavity which is large enough that the late time pressure in the cavity, which is given by equation (3), is equal to one half the overburden pressure (i.e., ρgh) at source depth h. That is,

$$\frac{(\gamma - 1)\, W}{\frac{4}{3}\pi\, r_c^3} = \frac{1}{2}\, \rho g h \quad . \tag{4}$$

It follows that the cavity radius required for full decoupling according to this criterion scales with explosion yield and depth of burial as

$$r_c \sim \frac{W^{1/3}}{h^{1/3}} \quad . \tag{5}$$

Thus, according to this scaling law, the cavity radius required for full decoupling increases with decreasing source depth and a cavity with a radius of about 40 m would be required to decouple 1 kt at a depth of 161 m to the same degree as that achieved for the 0.38 kt STERLING explosion, which was detonated in a 17 m

radius cavity at a depth of 828 m. Moreover, according to the model of Mueller and Murphy (1971), the elastic radius of the corresponding tamped 1 kt explosion would also be expected to increase with decreasing source depth. The implications of this depth dependent scaling with respect to the predicted decoupling source spectral ratios are illustrated in Figure 9, which shows a comparison of various estimates of the decoupled to tamped source spectral ratios for 1 kt decoupled explosions at the two depths. The curves labeled "Rimer/Cherry Salt, h = 828m" and "Laboratory Salt, h = 828m" in this figure correspond to results obtained from nonlinear finite difference simulations of 1 kt decoupling in a 23.5 m radius cavity at a depth of 828 m in two significantly different salt models (Stevens *et al.*, 1991). The curves labeled "Analytic, h = 828m" and "Analytic, h = 161m" correspond to our simple analytic approximations to the source spectral ratios for 1 kt decoupled explosions at depths of 828 m and 161 m, respectively. It can be seen from the figure that all these source spectral ratio estimates are consistent with a low frequency decoupling factor of about 70, in agreement with STERLING experience. Moreover, while the analytic spectral ratio approximation for the 828 m depth case is bounded by the two finite difference solutions for decoupling at that depth, that for the 161 m depth case is shown shifted to lower frequency, in accord with the depth dependent source scaling laws described above.

The vertical component displacement waveforms recorded from the 1.1 kt tamped Azgir test of 4/22/66 in the near-regional distance range extending from 69 to 180 km are shown in Figure 10 and the results of scaling these data to those to be expected from a 1 kt fully decoupled explosion at that location using the approximate 161 m source spectral ratio from Figure 9 are shown in Figure 11. Comparing Figures 10 and 11, it can be seen that the scaling has enhanced the high frequency components (both signal and noise) relative to the lower frequency components, as would be expected on the basis of the highpass nature of this source scaling operator. The synthetic decoupled waveforms of Figure 11, together with those shown previously in Figure 7, will be further analyzed in Section 3 where they will be compared in detail with corresponding data recorded in the same distance range from selected CE events.

With respect to the amplitude levels of the ground motions expected from fully decoupled 1 kt explosions at Azgir, data recorded from the complete sample

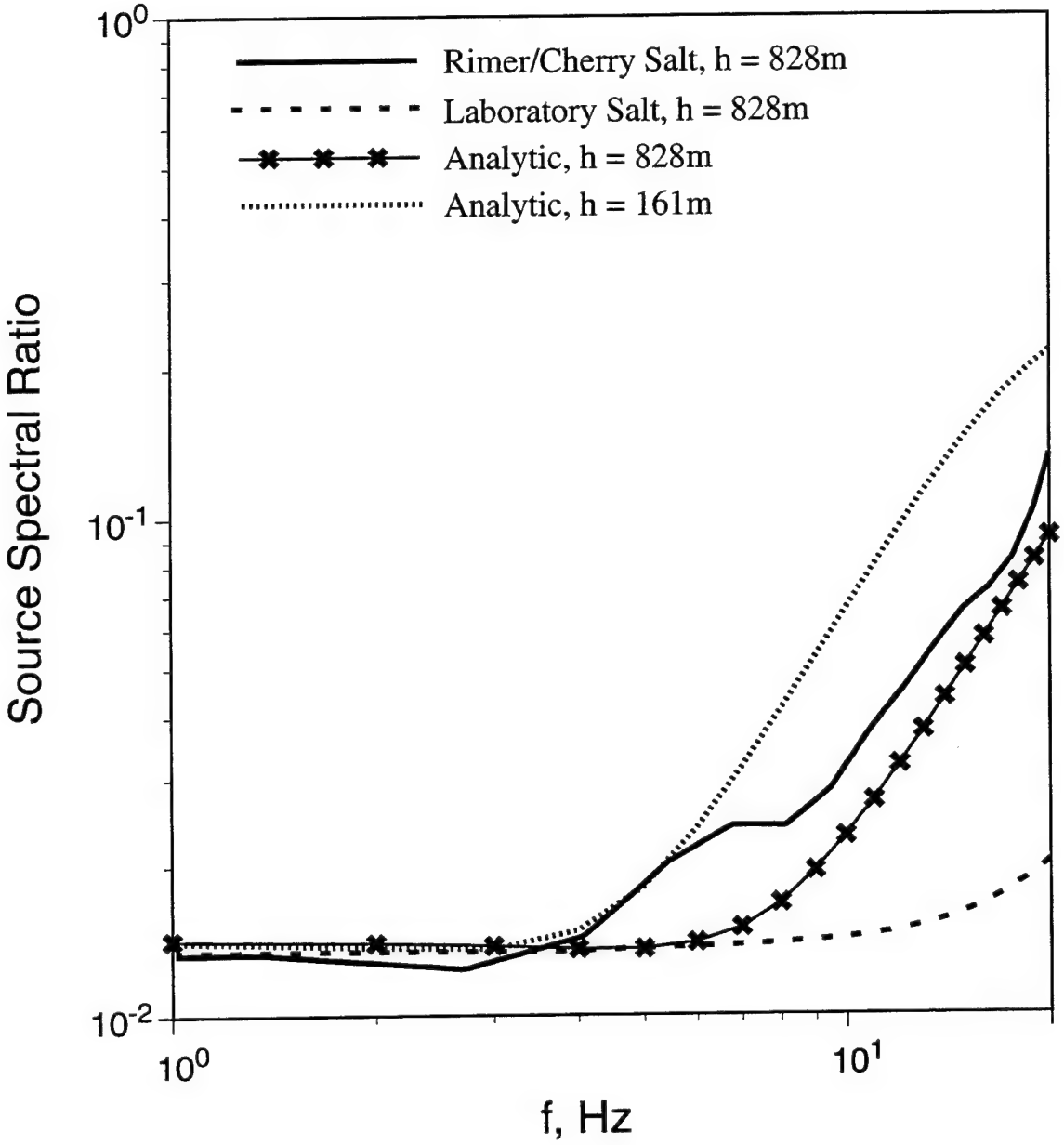

Figure 9. Comparison of estimates of the source spectral ratios (decoupled/tamped) corresponding to fully decoupled 1 kt nuclear explosions at different depths at the Azgir test site.

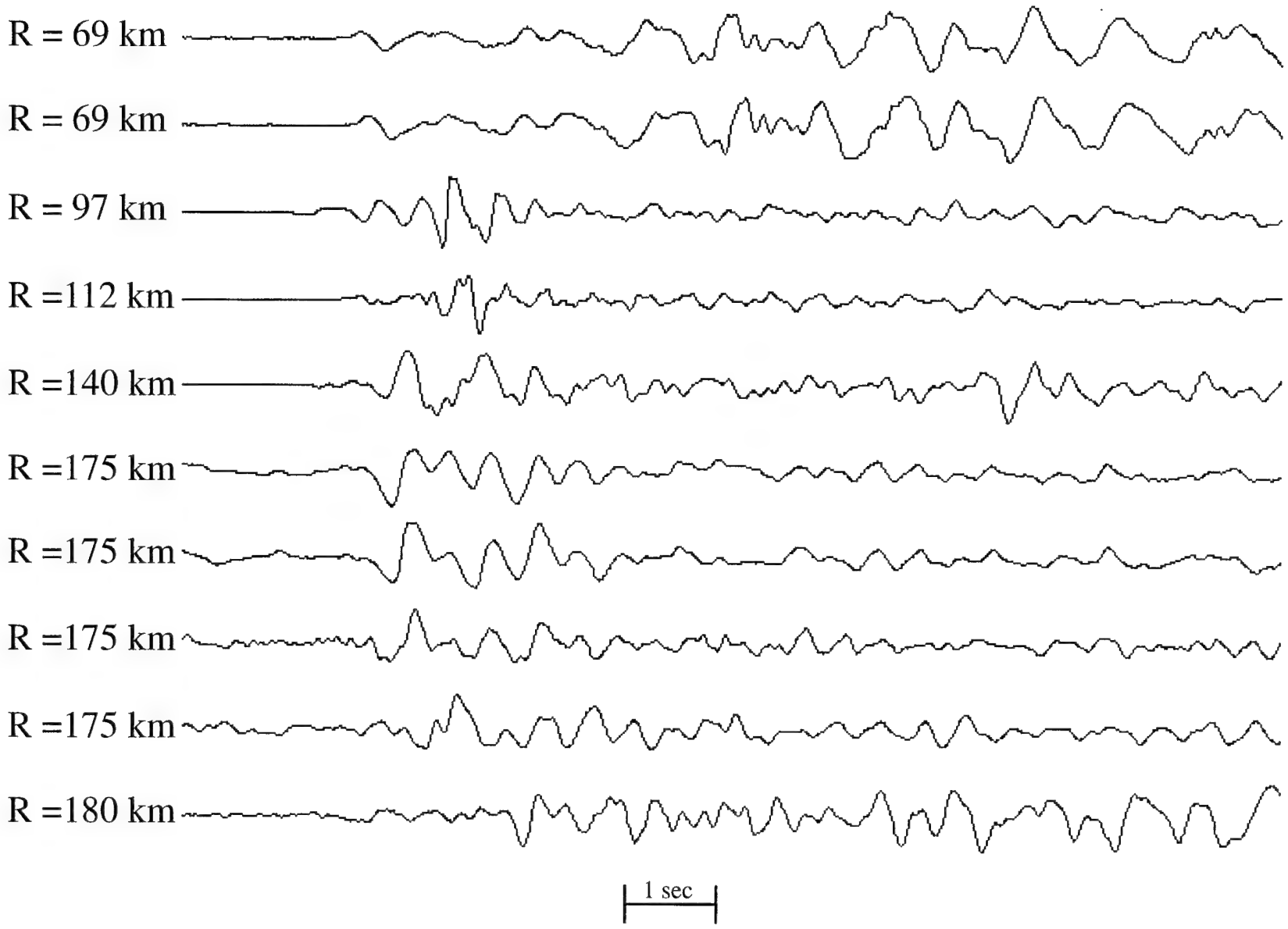

Figure 10. Vertical component ground motions recorded from the tamped 1.1 kt Azgir nuclear test of 4/22/66.

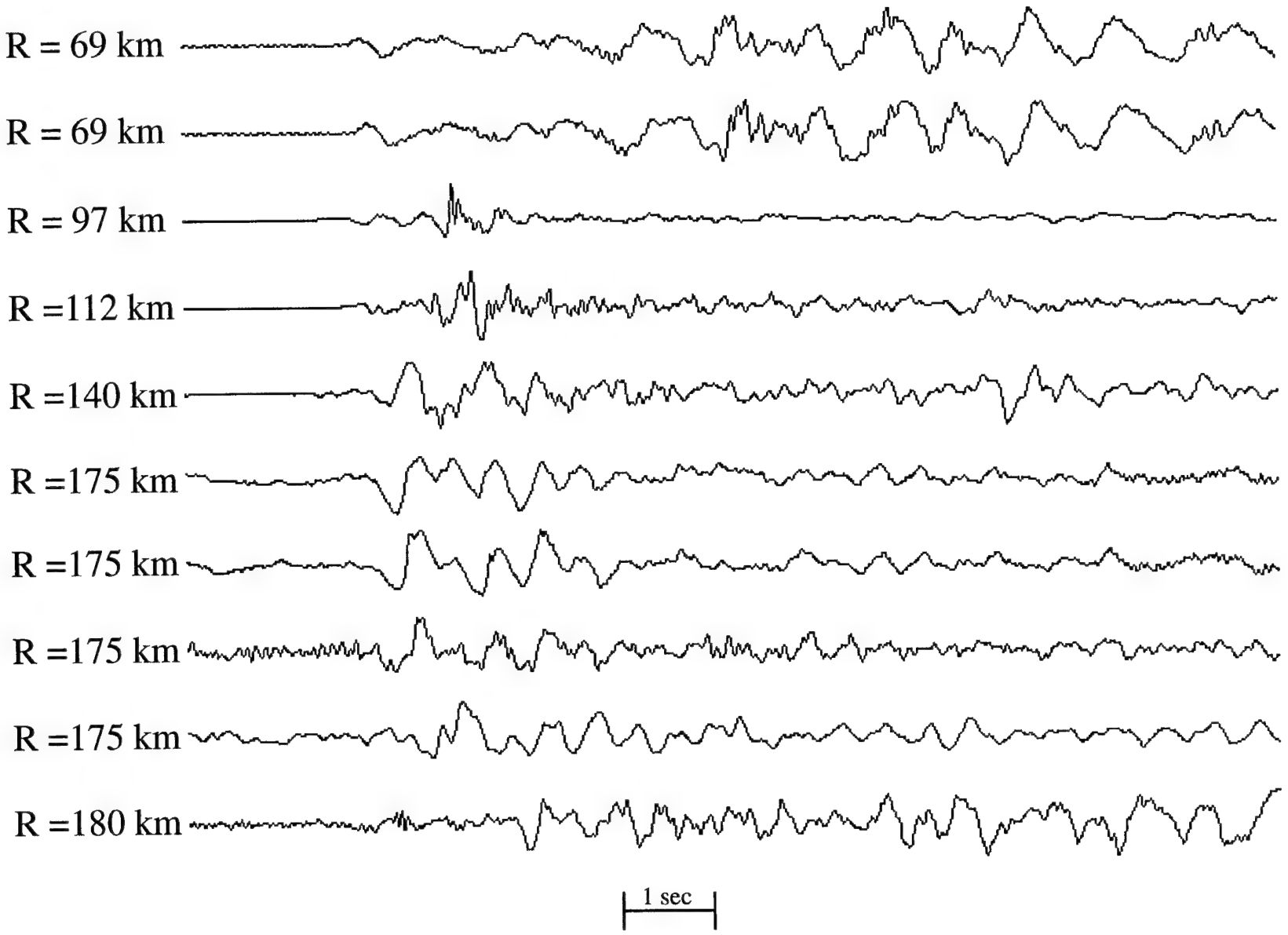

Figure 11. Theoretically scaled vertical component ground motions corresponding to a 1 kt fully decoupled explosion at the source location of the 1.1 kt tamped Azgir nuclear test of 4/22/66.

of tamped explosions at that site can provide the basis for a more reliable average estimate than that obtained using data from any single explosion. Thus, Adushkin *et al.* (1992) report that a statistical fit to the peak vertical displacement data (U_Z) observed from tamped Azgir explosions in the 1-100 kt range supports a scaling law of the form:

$$U_Z = 1.0\ W^{0.8}\ R^{-1.7} \quad \text{cm} \tag{6}$$

where W is the yield in kt, R is the range in km and the average scaled depth of the explosions used in the statistical analysis is about 245 m/kt$^{1/3}$. Evaluating this expression at W = 1 kt and dividing by the nominal decoupling factor of 70 gives

$$U_Z = 1.4\ X\ 10^{-2}\ R^{-1.7} \quad \text{cm} \tag{7}$$

for the predicted vertical displacement as a function of range corresponding to a 1 kt fully decoupled nuclear test at a depth of 245 m at Azgir. The peak vertical displacement levels as a function of range predicted for tamped and fully decoupled 1 kt explosions at 245 m depth using equations (6) and (7) are shown in Figure 12 where they are compared with that corresponding to the 1 kt fully decoupled estimate of Figure 8. Since this latter estimate was obtained by scaling observed data from the 8 kt partially decoupled Azgir test of 3/29/76, it is representative of a decoupled explosion at a depth of 987 m and has been labeled as such in this figure. It can be seen that while these two estimates of the 1 kt decoupled ground motion levels are very consistent, the estimated peak displacement values for the deeper explosion are somewhat lower, in qualitative agreement with the source depth scaling model of Mueller and Murphy (1971). That is, if it is assumed that the nominal full decoupling factor of 70 applies independent of source depth, then at a fixed yield the low frequency displacement amplitudes corresponding to a cavity decoupled explosion are expected to decrease somewhat with increasing source depth. In any case, it is reassuring that these two estimates of the ground motion amplitude levels expected from 1 kt fully decoupled explosions at Azgir are consistent to this degree.

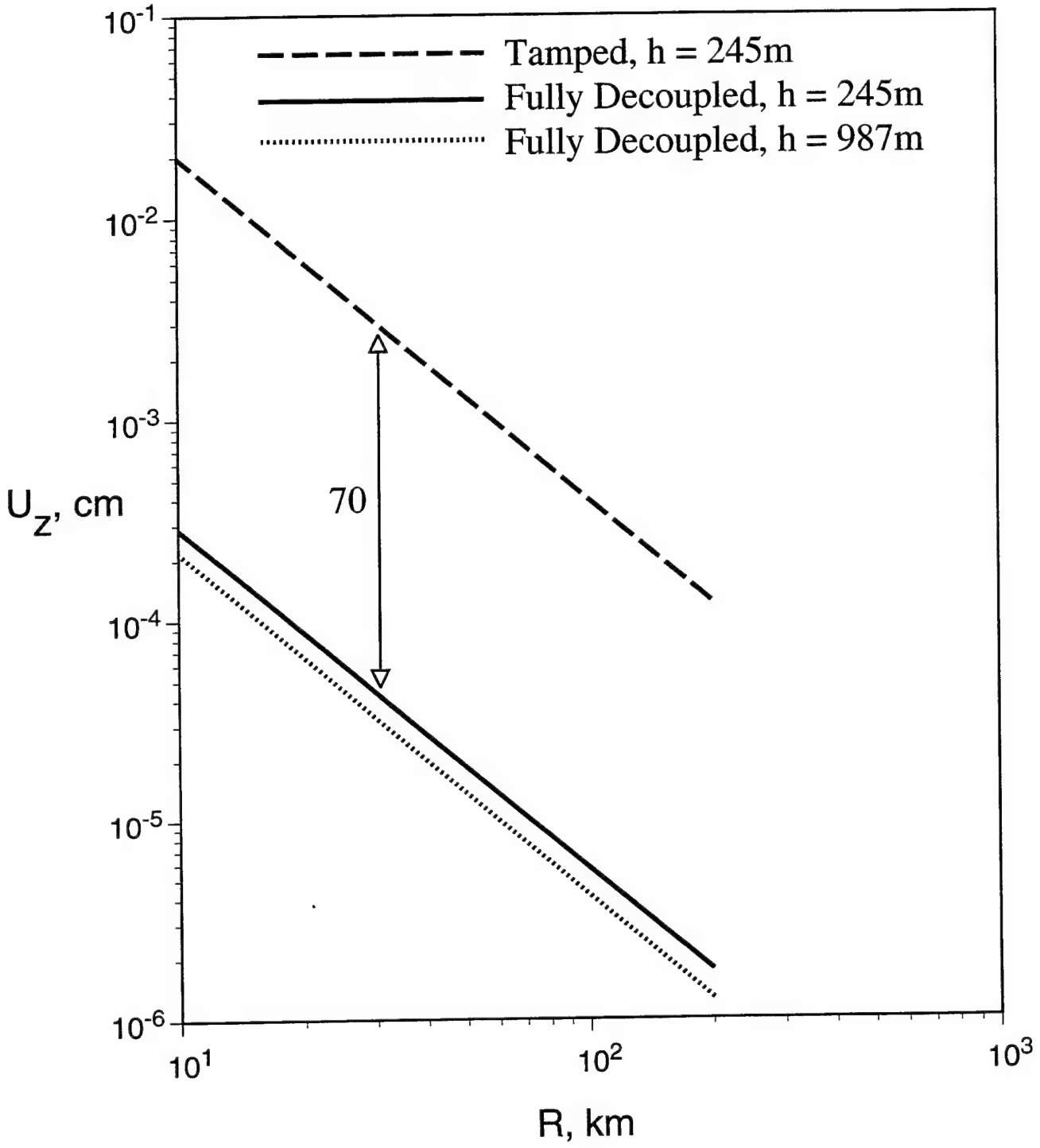

Figure 12. Comparison of average peak vertical displacement levels as a function of range corresponding to fully decoupled 1 kt nuclear explosions at depths of 245m (solid) and 987m (dotted) at Azgir.

2.3 Analysis of the Yield Equivalence of Cavity Decoupled Nuclear and Chemical Explosions

It follows from the preceding discussion that definitive verification of any eventual CTBT will involve the characterization of small seismic events which might correspond to evasive testing of low yield nuclear devices. More specifically, in situations where cavity decoupling is feasible, comprehensive monitoring of underground nuclear tests in the 1 to 10 kt range will require the routine identification of many small seismic events with magnitudes in the range $2.0 < m_b < 3.5$. Thus, an important issue in the assessment of monitoring requirements concerns the definition of the numbers and types of CE events which will generate seismic signals in this magnitude range. This has proved to be a difficult question to answer with any real degree of confidence, because the magnitude values reported for most CE events are based on a variety of regional magnitude scales which may not be consistent with the teleseismic m_b magnitude scale which is used to specify seismic monitoring capability. That is, since such small events are not detected teleseismically, their equivalent m_b values are generally estimated using rather uncertain conversions between local and teleseismic magnitude measures. In this study, we have the advantage of having derived reasonable approximations to the near-regional ground motions expected from cavity decoupled nuclear explosions and, consequently, we have pursued an alternate approach in which we have attempted to directly identify the types and associated yields of CE events which produce comparable near-regional ground motion amplitude levels to those expected from cavity decoupled nuclear explosions of various yields.

In considering the relative seismic coupling efficiency of CE events, it is necessary to distinguish between the fully tamped explosions which are used in some underground mining operations and the more numerous near-surface, ripple-fired explosions which are routinely employed in strip mining, quarrying and construction applications. With regard to fully tamped CE events, the analysis of seismic coupling efficiency is relatively straightforward. That is, assuming that the low frequency seismic amplitudes scale directly with yield for nuclear explosions at a fixed depth, then the tamped nuclear yield which would produce ground motion amplitudes equivalent to a fully decoupled explosion of yield W is simply W/70. Thus, a 1 kt fully decoupled explosion is expected to

produce seismic signals with amplitude levels comparable to those associated with a 14.3 ton tamped nuclear explosion at that location. Furthermore, comparisons of the ground motions observed from nearby chemical and nuclear explosions indicate that tamped CE events have a higher seismic coupling efficiency than nuclear explosions of the same total yield. For example, analyses of the seismic signals recorded from STERLING and STERLING HE (Springer *et al.*, 1968) and from the Non-Proliferation Experiment and nearby NTS nuclear explosions of comparable yield (Walter *et al.*, 1994) indicate that the seismic coupling efficiency of a tamped CE event is about twice that of a tamped nuclear explosion of the same yield at that location. It follows that a tamped CE event with a yield of about 7 tons would be expected to produce seismic signals with amplitudes comparable to those expected from a 1 kt fully decoupled nuclear explosion. Moreover, available data suggest that this equivalence factor is roughly independent of yield and, therefore, a tamped CE event with a yield of about 70 tons would be expected to have a seismic coupling efficiency comparable to a 10 kt fully decoupled nuclear explosion. However, as has been noted by Richards *et al.* (1992) and others, tamped CE events of this size appear to be rare in current mining practice.

Establishing the relative seismic coupling efficiency of near-surface, ripple-fired CE events is a more difficult problem, because such explosions are designed to move large volumes of surface material and, as a result, are much less efficient at generating seismic signals than tamped explosions of the same yield. In addition, the large variations in blasting practice between mines, and even between different explosions at a particular mine, makes it difficult to arrive at any general conclusions. The most direct procedure for estimating the relative seismic coupling efficiency of such CE events would be to compare ground motions observed from these events with those recorded from nearby nuclear explosions of known yield. Unfortunately, no data from ripple-fired CE events have been recorded at the stations used to monitor the STERLING and Azgir nuclear decoupling tests. However, numerous mine blasts have been recorded in the same near-regional distance range at IRIS station KIV which is located west of the Caspian Sea at Kislovodsk, approximately 600 km southwest of Azgir. The location of station KIV with respect to Azgir is shown in Figure 13, which also shows in expanded scale the locations of two mines near KIV, as well as the locations of five satellite stations surrounding KIV which have recorded seismic

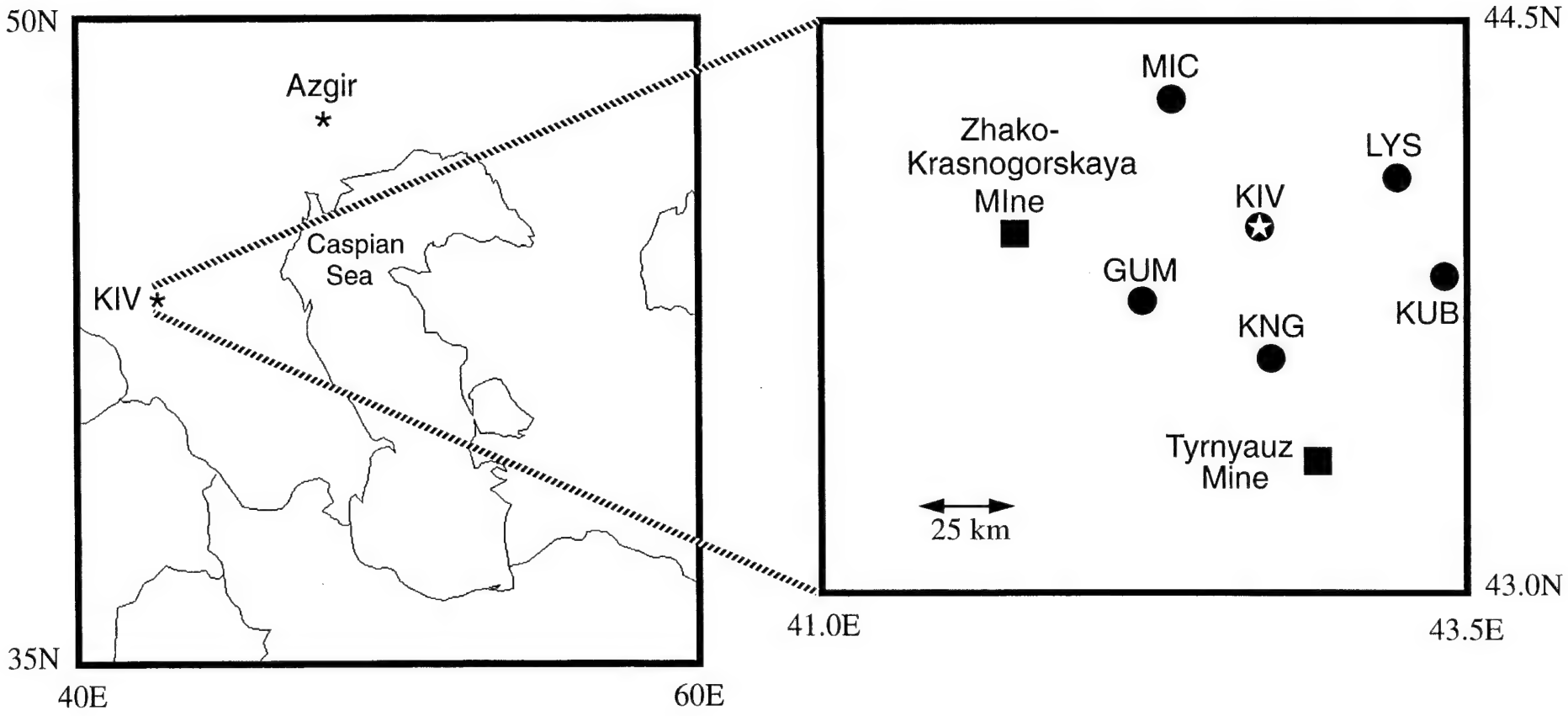

Figure 13. Map location of IRIS station KIV with respect to the Azgir test site. The expanded display at the right shows the locations of selected mines and broadband recording stations around KIV.

data from blasts at these two mines (Rivière-Barbier, 1993). These stations recorded data at an extended sampling rate of 125 samples/second from two well-documented explosions at the Tyrnyauz mine and one at the Zhako-Krasnogorskaya mine, which provide a broadband, near-regional seismic data base comparable to the Azgir nuclear decoupling data recorded in the same distance range. According to Rivière-Barbier (1993), the two well-documented Tyrnyauz mine blasts were conducted about one minute apart on 4/12/92. Both were ripple-fired explosions detonated in multiple boreholes extending to a depth of 15.6 m below the surface of the open pit mine. The first, denoted 4/12/92(1), had a total yield of 27 tons of CE, while the second, denoted 4/12/92(2), had a total yield of 70 tons CE. The documented blast at the Zhako-Krasnogorskaya mine occurred on 5/8/92 and was also a ripple-fired, multiple borehole explosion at the surface of this gypsum pit mine, having a total yield of 11.9 tons CE.

The peak vertical displacements observed at the KIV station array from these three well-documented mine blasts are displayed as a function of range in Figure 14, where they are compared with the corresponding ground motion levels expected from 1 kt fully decoupled explosions at Azgir. On these figures, the dashed and dotted lines correspond to the average 1 kt fully decoupled amplitude-distance relations from Figure 12 and the solid lines represent the attenuation relations of the same slope which provide the best fits to the observed ground motion amplitudes for these three mine blasts. Now, on the basis of the preceding discussion, a 1 kt fully decoupled explosion is expected to produce low frequency seismic motions having amplitudes comparable to those expected from a 7 ton fully tamped CE event. Thus, if these three mine blasts had been fully tamped, the solid lines in Figure 14 would have been expected to lie above the dashed and dotted lines in each case. In fact, however, it can be seen that the estimated 1 kt fully decoupled ground motion levels lie above the corresponding mine blast data for each of these three CE events. These observations are consistent with both the data reported by Richards *et al.* (1992) and the theoretical simulation results reported by Barker *et al.* (1992) which indicate that the seismic coupling efficiencies of ripple-fired, excavation type CE blasts are significantly lower than those to be expected from contained underground explosions of comparable yield. Assuming first power amplitude-yield scaling, the data of Figure 14 give estimates of the yield of a ripple-fired mine blast required to produce near-regional ground motions having the same low

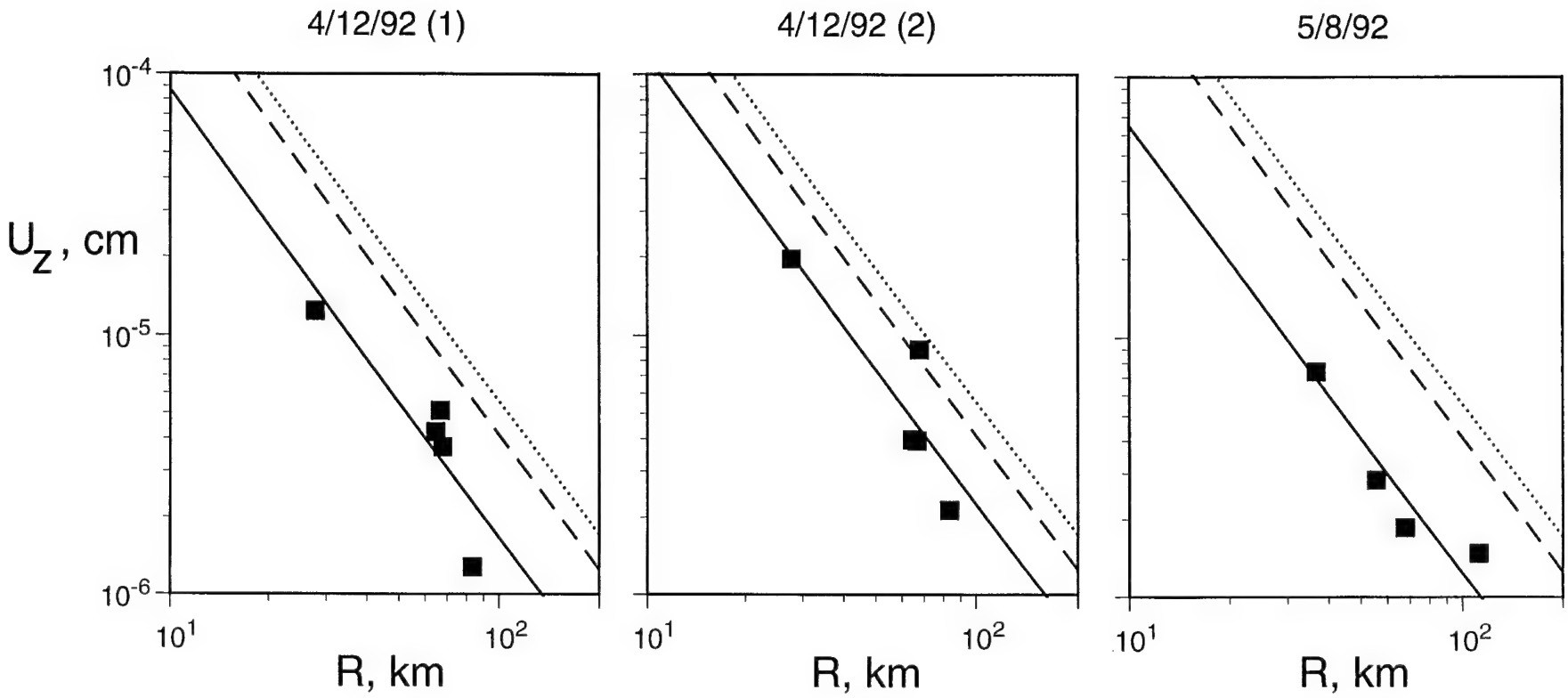

Figure 14. Comparison of peak vertical displacement levels observed from three well-documented Caspian mine blasts (solid) with the corresponding displacement levels expected from fully decoupled 1 kt nuclear explosions at depths of 245m (dotted) and 987m (dashed) at Azgir.

frequency amplitude levels as those expected from a 1 kt fully decoupled nuclear explosion at a depth of 987 m at Azgir which range from about 40 to 125 tons, with a mean of about 70 tons. The corresponding values for a 1 kt fully decoupled nuclear explosion at a depth of 245 m range from about 50 to 170 tons, with a mean of about 95 tons. That is, the average low frequency seismic coupling efficiency of these three mine blasts is on the order of a factor of 5 to 7 lower than that expected from tamped nuclear explosions of comparable yield. A simple linear extrapolation of these results would lead to the conclusion that a ripple-fired mine blast with a total yield of about 1 kt might be expected to produce ground motion amplitudes comparable to those expected from a 10 kt fully decoupled nuclear explosion. However, analyses of distant seismic signals recorded from such large mine blasts suggest that their coupling efficiency may be even lower than those of mine blasts in the 100 ton range (Paul Richards, personal communication, 1995). Moreover, it can be anticipated that there will be significant deviations from average coupling in individual cases due to variations in blasting practice. For the present, it can only be stated that ripple-fired mine blasts in the 70-100 ton yield range at two mines near KIV are expected to produce near-regional ground motions having amplitudes comparable to those expected from a 1 kt fully decoupled nuclear explosion at the Azgir test site. Thus, allowing for normal variability in seismic coupling efficiency, a cautious interpretation of the analysis results available at this time would suggest that a completely reliable CTBT seismic monitoring network will need to have the capability to routinely process and identify tamped CE events with yields greater than about 5 tons and ripple-fired CE events with yields greater than about 50 tons which occur in regions where cavity decoupling of nuclear explosions is considered to be feasible at the 1 kt yield level.

3. SEISMIC IDENTIFICATION OF CAVITY DECOUPLED NUCLEAR AND CHEMICAL EXPLOSIONS

On the basis of the analysis presented in Section 2, it appears that there will be many CE events per year which will produce regional seismic signals having amplitude levels comparable to those to be expected from fully decoupled nuclear explosions with yields in the 1 to 10 kt range. Therefore, it is important in a

global monitoring context that simple, robust discriminants be identified which can be used to routinely eliminate most CE events from further consideration. As in the preceding seismic coupling analysis, it is necessary to distinguish between the different types of chemical and nuclear explosions from a discrimination perspective. Thus, in the following discussion we will begin by comparing the seismic signals from tamped nuclear and tamped CE sources, then consider possible differences between the seismic signals produced by tamped and cavity decoupled nuclear sources and, finally, compare seismic signals from selected ripple-fired mine blasts and cavity decoupled nuclear explosions.

3.1 Seismic Characteristics of Tamped Nuclear and Chemical Explosions

Although there have been few direct comparisons of relevant seismic data recorded from these two source types, it is generally believed that the seismic discrimination between tamped nuclear and tamped chemical explosions of equivalent yield, if it is possible at all, will be a very difficult problem. That is, despite the differences in near-source phenomenology which produce the systematic differences in seismic coupling efficiency which were discussed in Section 2 above, results of both theoretical simulation analyses (Rimer *et al.*, 1993) and comparisons of experimental data indicate that the seismic source functions characteristic of these two types of explosions are very similar over the frequency range of interest in seismic monitoring. Thus, for example, Stump *et al.* (1994) and Denny *et al.* (1995) conducted detailed comparisons of seismic signals recorded from the recent 1 kt tamped CE at NTS (i.e., the Non-Proliferation Experiment, NPE) and from nearby nuclear explosions of comparable yield and concluded that there were no significant differences in the tamped CE and nuclear seismic source functions over the entire seismic frequency band extending from 0.36 - 100 Hz. More specifically, Denny *et al.* (1995) concluded that the seismic source function for the NPE was equivalent to that of a nuclear explosion of about twice that yield.

Another U.S. test series relevant to this issue is the SALMON/STERLING/STERLING HE sequence of explosions conducted in the Tatum salt dome near Hattiesburg, Mississippi between 1964 and 1966. The first

of these tests was SALMON, which was a fully tamped 5.3 kt nuclear explosion conducted at a depth of 828 m on October 22, 1964. This was followed on November 17, 1966 by STERLING HE, a 2.7 ton tamped, high explosive calibration shot which was detonated about 350 m southwest of SALMON at a depth of 831 m. The decoupled nuclear test STERLING had a yield of 0.38 kt and was detonated on December 3, 1966 in the 17 m radius semispherical cavity produced by the SALMON explosion (Perret 1968a,b; Springer *et al.*, 1968). Given that the low frequency decoupling factor for STERLING has been estimated to have been approximately 70 ± 20 (Springer *et al.*, 1968), it follows that the amplitudes of the low frequency seismic signals from STERLING were of the same order of magnitude as those to be expected from a 5.4 ton tamped nuclear explosion. Comparison of the near-regional seismic signals recorded from STERLING and STERLING HE indicated that they produced very similar ground motion amplitude levels, which suggests that the seismic coupling efficiency of the 2.7 ton STERLING HE event was approximately equivalent to that expected from a tamped 5.4 ton nuclear explosion at that location. That is, the tamped CE had about twice the seismic coupling efficiency expected from a tamped nuclear explosion of the same yield, in agreement with the NPE experience referenced above. In contrast to the NPE comparisons, however, there appear to be some frequency dependent differences in the seismic signals recorded from the tamped nuclear and tamped CE source types in this case. The differences are graphically illustrated in Figures 15 and 16 which show comparisons of the vertical component signals and associated bandpass filter outputs (0.55 to 18.4 Hz) for the two source types for stations at ranges of 16 km (10S) and 32 km (20S), respectively. As was noted previously by Murphy and Barker (1994), it can be seen that the broadband S/P amplitude ratios are significantly larger for STERLING HE than for SALMON at both these stations. At station 10S this difference seems to be roughly independent of frequency and persists over the entire band covered by the selected filters. At station 20S these same kinds of S/P differences persist out to 7 or 8 Hz, whereupon they reverse, showing larger S/P ratios for SALMON than for STERLING HE above about 10 Hz. Now, the source locations for these two explosions were offset by some 350 m and, given the geometrical complexity of the salt dome structure in which the tests were conducted, it is possible that variations in the propagation paths to these stations may be contributing to these observed differences in S/P ratios. However, in the absence of a quantitative demonstration of the potential

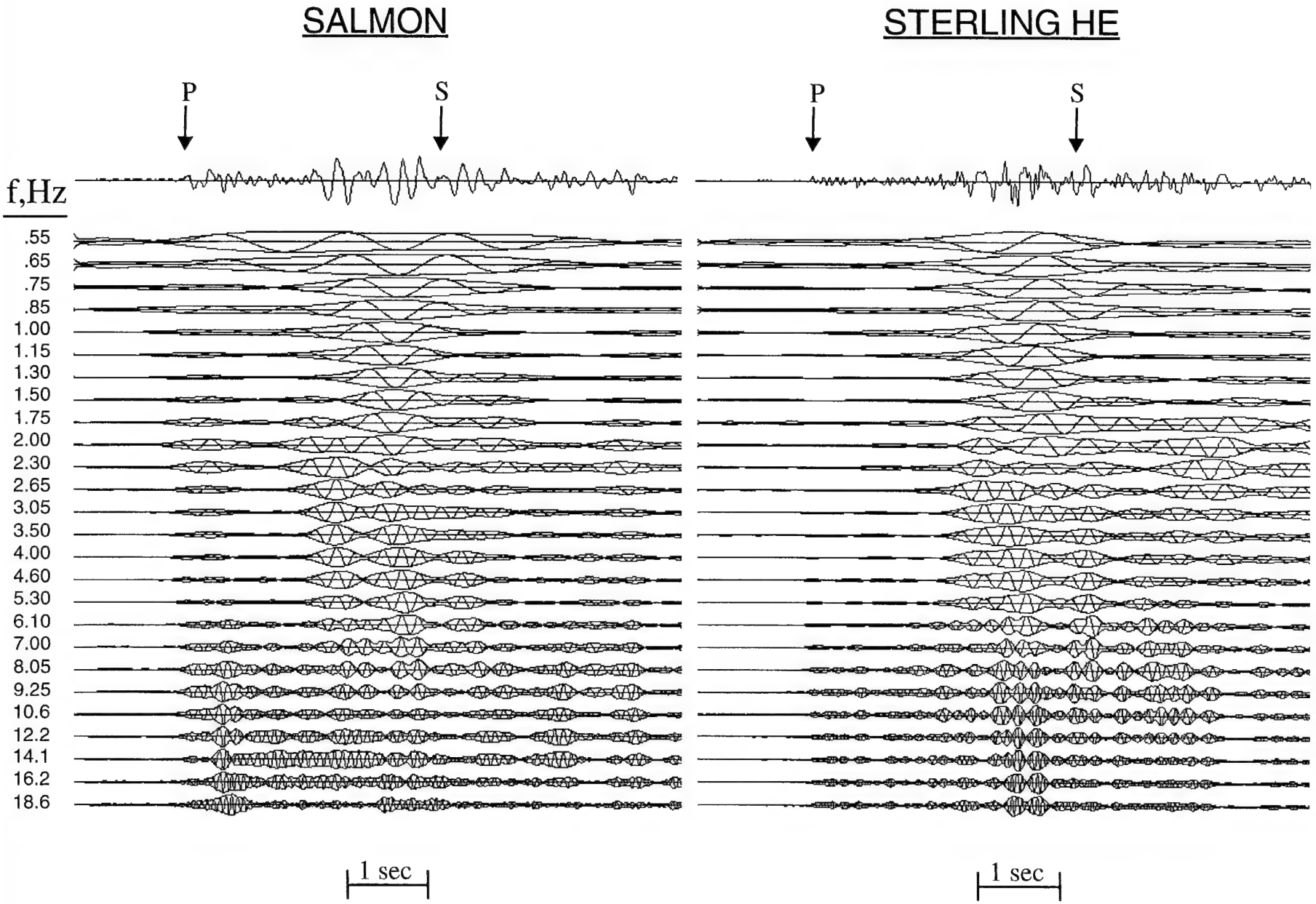

Figure 15. Comparison of vertical component waveforms and associated bandpass filter outputs for the SALMON and STERLING HE events recorded at station 10S at a range of 16 km.

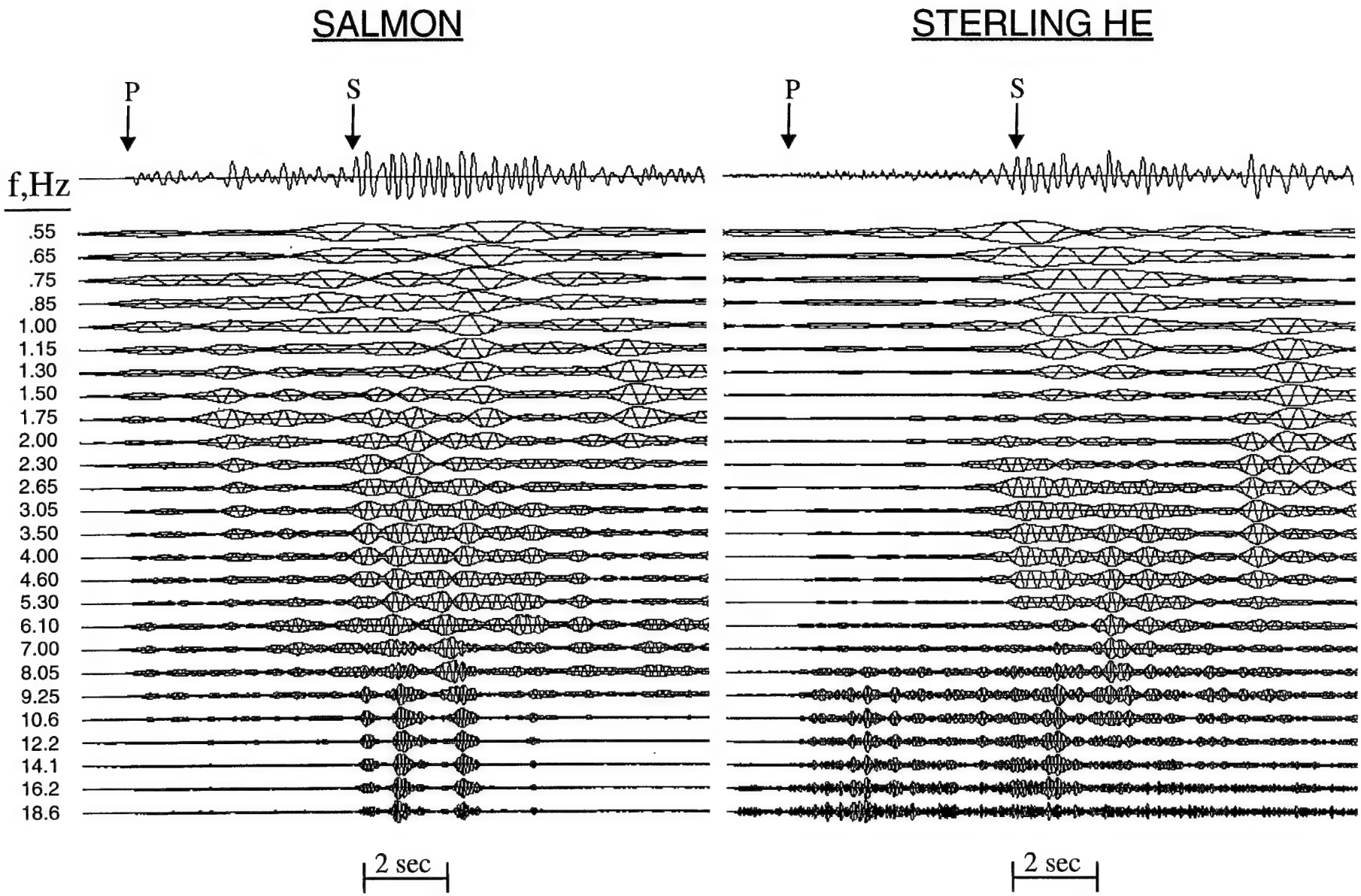

Figure 16. Comparison of vertical component waveforms and associated bandpass filter outputs for the SALMON and STERLING HE events recorded at station 20S at a range of 32 km.

importance of such effects, it is not possible at this time to rule out the hypothesis that there may also be some differences in the seismic source functions in this case.

To summarize, available evidence indicates that tamped CE have seismic coupling efficiencies comparable to tamped nuclear explosions having about twice the CE yield. Moreover, in at least some cases (e.g. NPE), the seismic source characteristics of tamped CE events appear to be indistinguishable from those of equivalent tamped nuclear explosions over the entire frequency range of interest in seismic monitoring. However, in some other instances (e.g. STERLING HE) the evidence concerning the possible seismic identification of the two source types is less clear. A combination of additional experimental data and improved theoretical insight will be required in order to address this issue in a definitive manner.

3.2 Comparison of Seismic Signals Recorded From Tamped and Cavity Decoupled Nuclear Explosions

Most assessments of seismic monitoring capability with respect to cavity decoupled nuclear explosions have proceeded under the assumption that the seismic source characteristics of such explosions are comparable to those expected from tamped nuclear explosions with suitably reduced yields (e.g. W/70 for fully decoupled explosions), at least over the limited frequency band which is typically available for seismic identification analysis. However, Blandford (1995) has recently noted that comparisons of selected seismic signals recorded from co-located tamped and cavity decoupled explosions at common stations suggest that there may be some consistent differences in the frequency dependent S/P ratios associated with these two source types. These observations are illustrated in Figure 17 where vertical component seismic signals recorded from the U.S. and Russian cavity decoupled nuclear explosions are compared with the seismic signals recorded at the same stations from the preceding tamped explosions which produced the two cavities. In these examples, the broadband (BB) signals recorded from the paired tamped and decoupled explosions are shown at the top, with the corresponding pairs of bandpass filter outputs shown beneath, extending over the frequency range from 0.5 to 25 Hz. Considering first the SALMON and

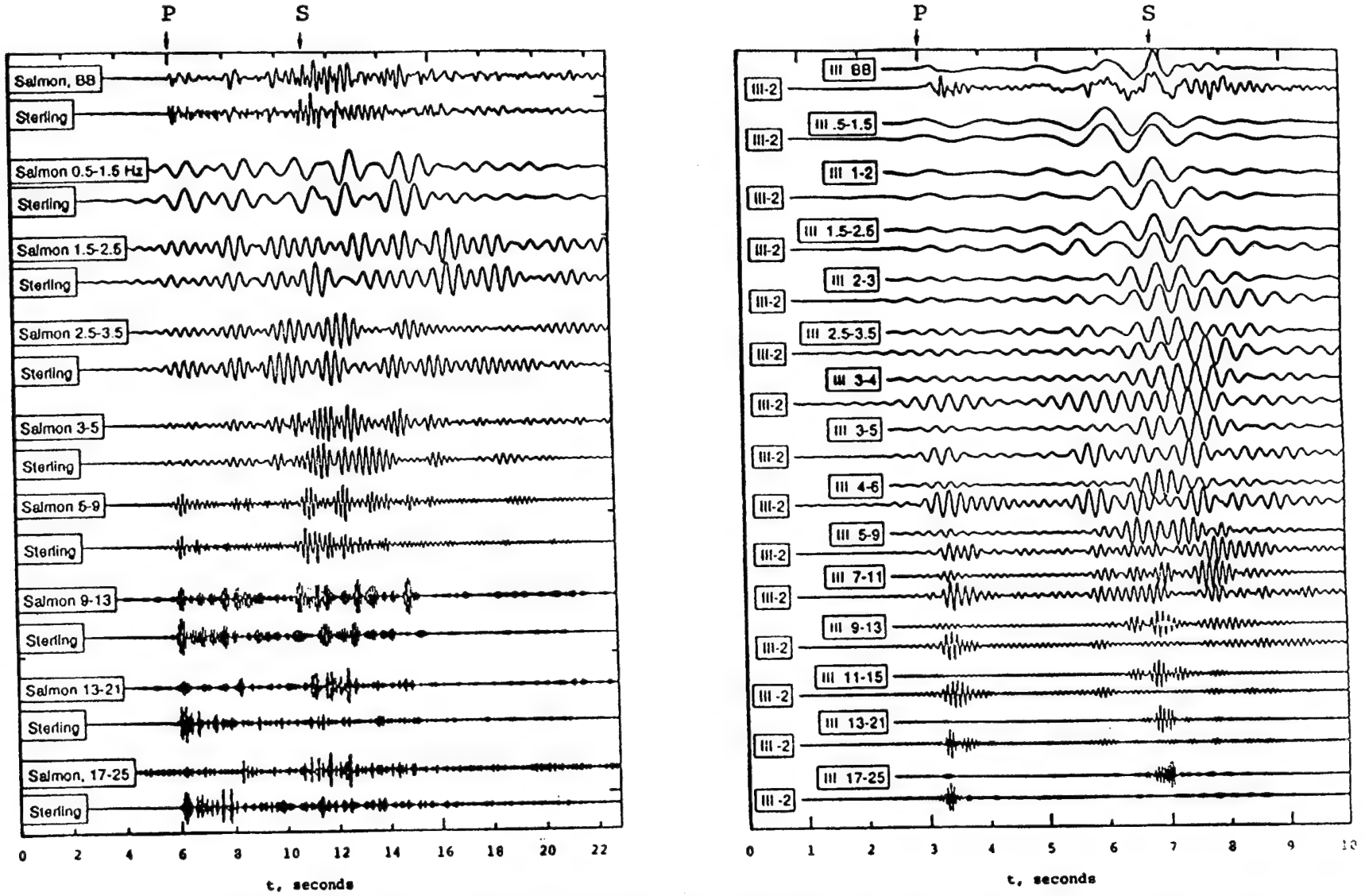

Figure 17. Comparison of vertical component waveforms and associated bandpass filter outputs for SALMON and STERLING (left) and the Soviet Azgir tamped (III) and cavity decoupled (III-2) nuclear explosions (right), Blandford (1995).

STERLING comparison for station Poplarville (Δ = 27 km) shown on the left side of this figure, it can be seen that the time dependent filter outputs for these two events are remarkably similar for the filters centered below about 10 Hz, consistent with the simple scaling results shown previously in Figure 4. However, for the filters centered above about 10 Hz, the S/P ratios observed on the time dependent filters outputs are consistently larger for SALMON than for STERLING by a factor of 5 or more. The display on the right side of Figure 17 shows a similar comparison of the seismic signals recorded at a common station at a range of 17.8 km from the 8 kt Soviet Azgir III-2 cavity decoupled nuclear explosion and the tamped 64 kt Azgir III explosion which produced the cavity. Here, the time dependent filters outputs are found to be quite similar for the filters centered below about 3 Hz, but once again the S/P ratios become progressively larger for the tamped event relative to the cavity decoupled event as the frequency increases above 3 Hz. Thus, in both these examples, there is evidence that the cavity decoupled explosions are less efficient than tamped explosions at producing high frequency S wave energy. Blandford (1995) has hypothesized that this effect may be associated with the greater extent of cracking induced in the nonlinear zone surrounding tamped explosions and, therefore, that it could be a diagnostic feature of cavity decoupled explosions which could be used for identification purposes. That is, since the high frequency S/P ratios typical of tamped nuclear explosions are generally found to be lower than those associated with other source types (i.e., earthquakes, mining blasts, rockbursts) (Bennett *et al.*, 1994), cavity decoupled nuclear explosions will appear to be very strongly "explosion-like" if Blandford's hypothesis is correct.

While the evidence presented in Figure 17 appears to be quite consistent and unambiguous, there are a number of reasons why it should be interpreted cautiously with respect to its implications for the seismic identification of cavity decoupled nuclear explosions. In the first place, the data are only representative of a single station for each explosion and, consequently, it is not obvious that the analysis results are generally applicable. Furthermore, the data for the two Azgir explosions were hand-digitized from paper records and, as a result, their reliability at high frequencies is questionable, particularly for the tamped Azgir III explosion. That is, since the Azgir III explosion had a yield of 64 kt, it is characterized by a source corner frequency on the order of a few Hertz, above which the source spectral amplitude level decreases at least as fast as ω^{-2}. Thus,

given the limited dynamic range of the paper recording, it is unlikely that the Azgir III data contain usable information at frequencies much above 5-6 Hz (personal communication, D. Sultanov, 1994). With regard to Figure 17, it can be seen that this upper frequency limit is close to the boundary where the S/P ratio becomes noticeably larger for Azgir III than for Azgir III-2, although the difference is certainly still detectable in the 3-6 Hz band where the data are considered to be reliable. In any case, given these data limitations, it seems appropriate to test the Blandford hypothesis against a larger and more diverse sample of data.

Considering first the SALMON/STERLING comparison, good data for both events were recorded at stations 20S (Δ = 32 km) and 10S (Δ = 16 km), in addition to the Poplarville (Δ = 27 km) station used by Blandford (1995). Bandpass filter outputs derived from the vertical component data recorded from these two events at station 20S are shown side by side in Figure 18, where it can be seen that they appear to be quite consistent with the Poplarville data of Figure 17, showing larger S/P ratios for SALMON than for STERLING on the time dependent filter outputs for those filters with center frequencies above about 7 Hz. The corresponding comparison for the station 10S data is shown in Figure 19. In this case there are no obvious differences between the filtered signals for the two events and, in fact, the time dependent filter outputs appear to be remarkably similar for these two recordings over the entire frequency range extending from about 0.55 to 18.6 Hz. That is, while the data recorded at the two stations located at distances of about 30 km from these two events show similar frequency dependent S/P ratio differences between the source types, the corresponding data recorded at a range of 16 km do not appear to be consistent with this simple picture. This observed inconsistency raises the possibility that this manifestation of source differences may be distance dependent. However, good quality data recorded over a wider range of distances would be required to define any such systematic distance dependence and, unfortunately, such data are not available for the SALMON and STERLING events.

Usable data were recorded over a wider distance range (i.e., about 1 to 113 km) for the Azgir III and III-2 explosions, due both to their higher yields and to the fact that the 8 kt III-2 event was only partially decoupled. However, the data were hand-digitized from photographic recordings in this case and a number of

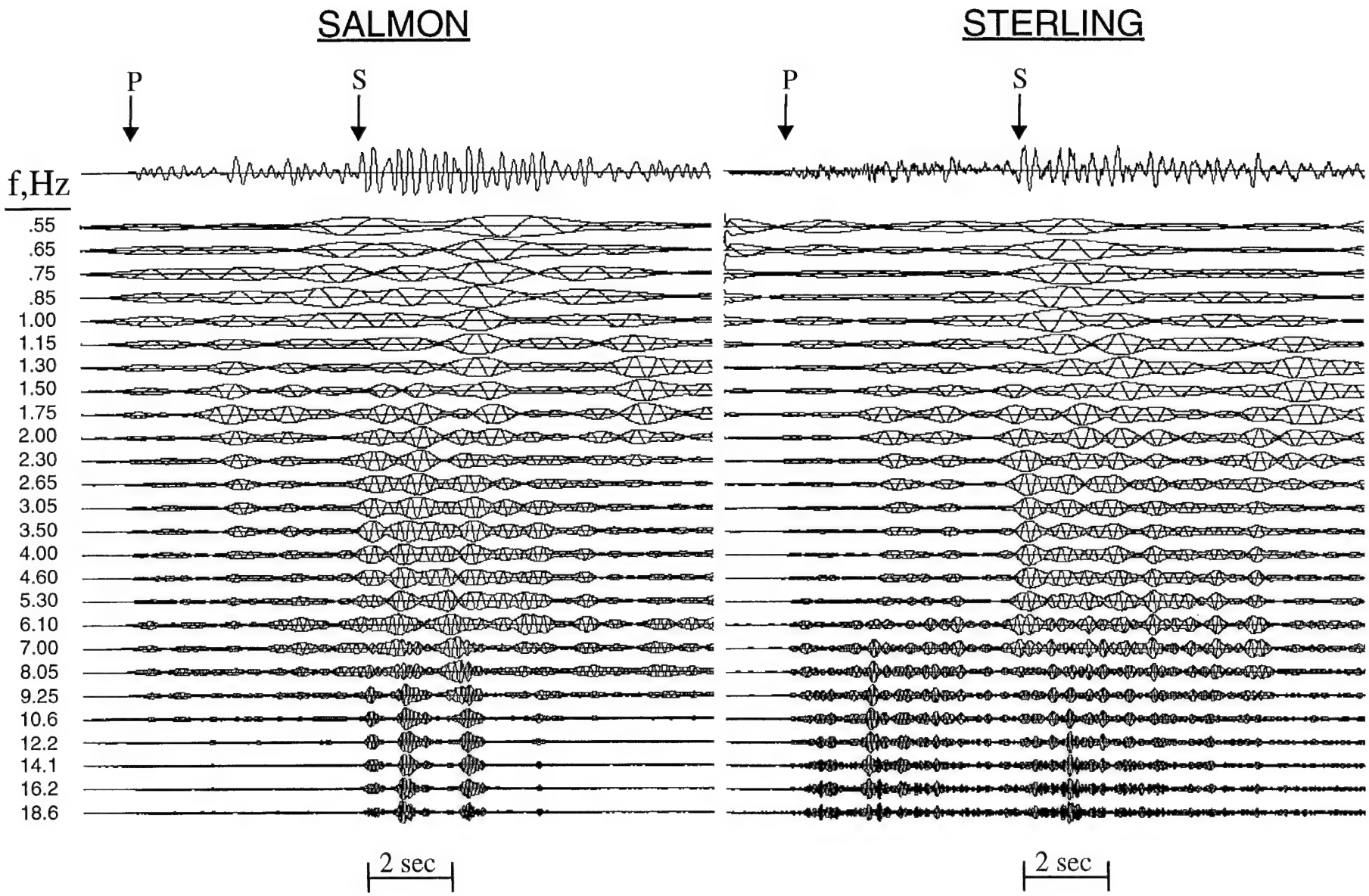

Figure 18. Comparison of vertical component waveforms and associated bandpass filter outputs for the SALMON and STERLING events recorded at station 20S at a range of 32 km.

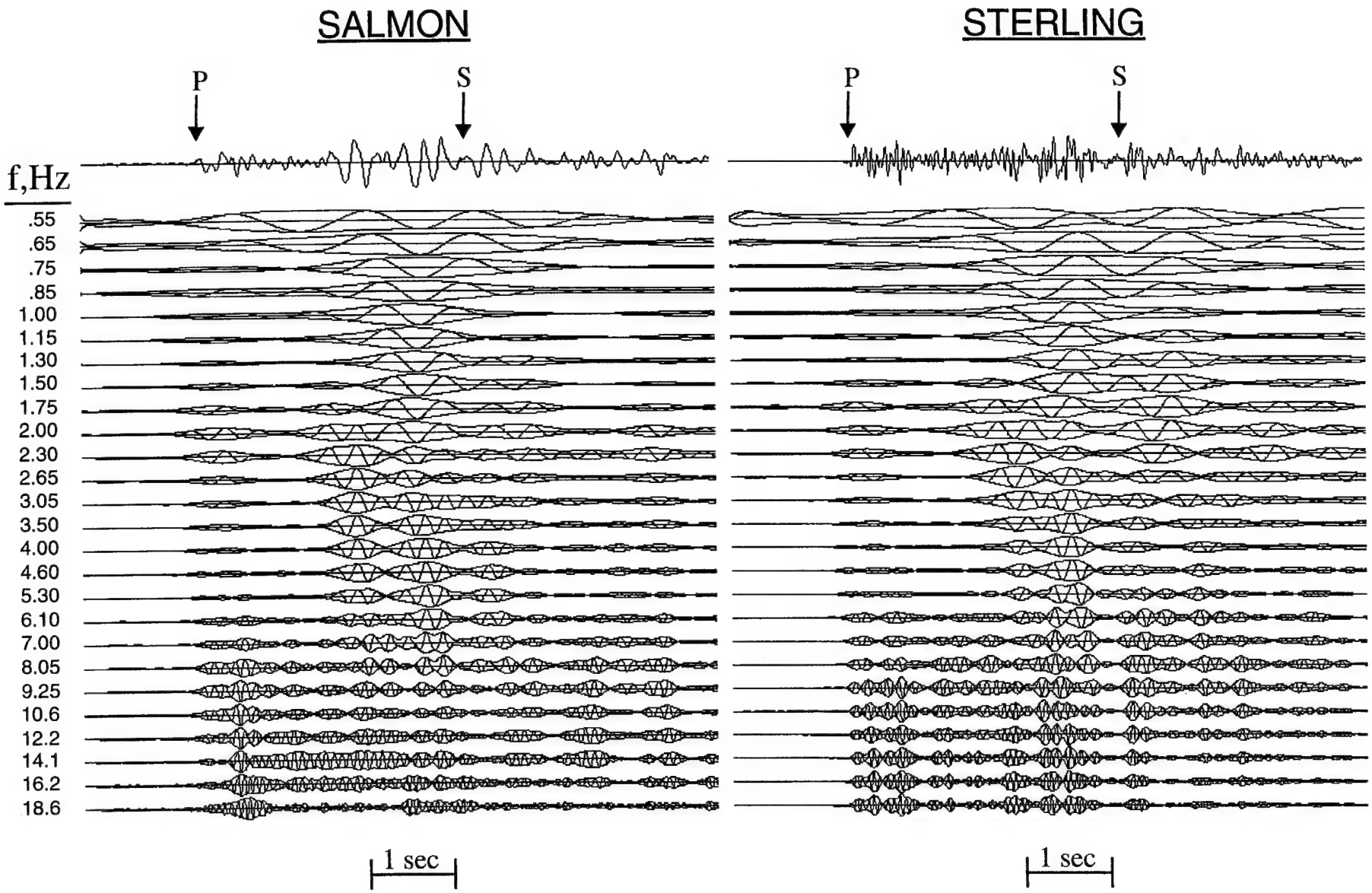

Figure 19. Comparison of vertical component waveforms and associated bandpass filter outputs for the SALMON and STERLING events recorded at station 10S at a range of 16 km.

the resulting digitized waveforms were truncated prior to the expected S arrival times, and such data are not useful for the purposes of the present investigation. As a result, our analysis has been limited to the data recorded at four stations which were located at ranges of 17.8, 18.2, 23.0 and 113 km. Our bandpass filter comparison of the tamped and decoupled Azgir recordings from the 17.8 km distance station analyzed by Blandford (1995) is presented in Figure 20. With reference to Figure 17, it can be seen that our results are very consistent with those obtained by Blandford using a different set of filters, with both showing enhanced S/P ratios for the tamped explosion relative to the decoupled explosion above 3 Hz. Similar comparisons for the data recorded at distances of 18.2 km and 23.0 km are shown in Figures 21 and 22, respectively. Comparing Figures 21 and 20, it can be seen that the results obtained for the 18.2 km station are quite similar to those obtained for the 17.8 km station with respect to the frequency dependent differences in the S/P ratios. On the other hand, the results shown in Figure 22 for the station at 23 km distance appear to be inconsistent with the other two, showing no significant differences in S/P ratios between the tamped and decoupled sources, at least on the filter outputs for frequencies below 5-6 Hz, where the data are considered to be reliable. Thus, as with the SALMON/STERLING comparisons, there is some evidence that the observed frequency dependent differences in S/P ratios between tamped and decoupled nuclear explosions may vary between stations, perhaps in a distance dependent manner.

Additional data, recorded over a broader range of distances would clearly be helpful in testing for any such distance dependence. The only other Azgir III-2 recording which appears to be usable for this purpose is that from a station located at a range of 113 km and, unfortunately, the digitized data from the companion tamped Azgir III explosion from that station were truncated prior to the expected S onset time. Therefore, in order to provide a basis for comparison in this case, data recorded from the tamped 1.1 kt Azgir I explosion of 4/22/66 at stations located in the same distance range have been collected and analyzed. A disadvantage of this approach is that, since the Azgir III-2 and Azgir I explosions were not co-located, variations in propagation paths to the stations could lead to some differences in the recorded seismic signals which might be confused with source differences. On the other hand, because the yield of the Azgir I explosion is significantly lower than that of the Azgir III explosion, the corresponding

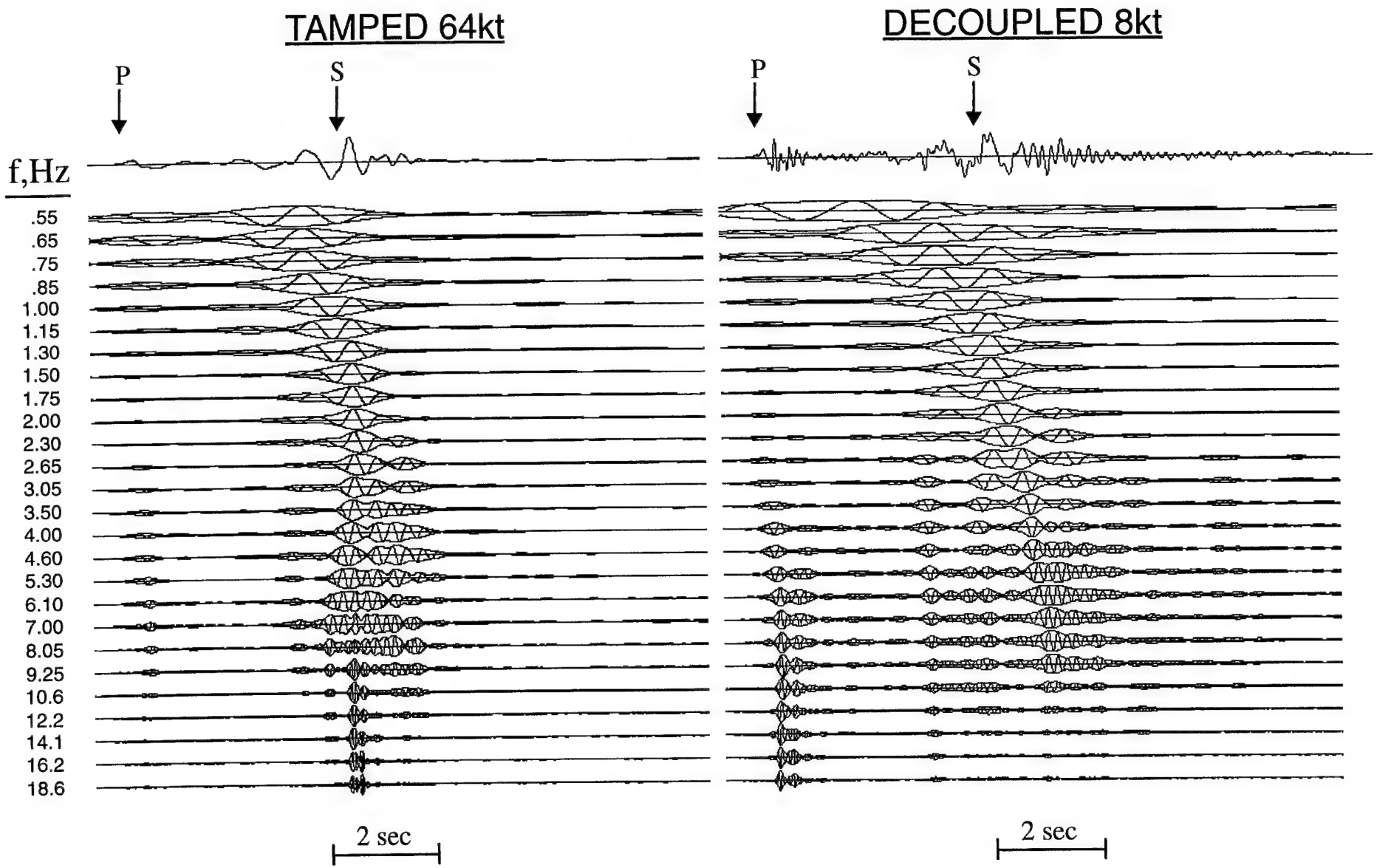

Figure 20. Comparison of vertical component waveforms and associated bandpass filter outputs for the Soviet Azgir tamped (III) and cavity decoupled (III-2) nuclear explosions recorded at a range of 17.8 km.

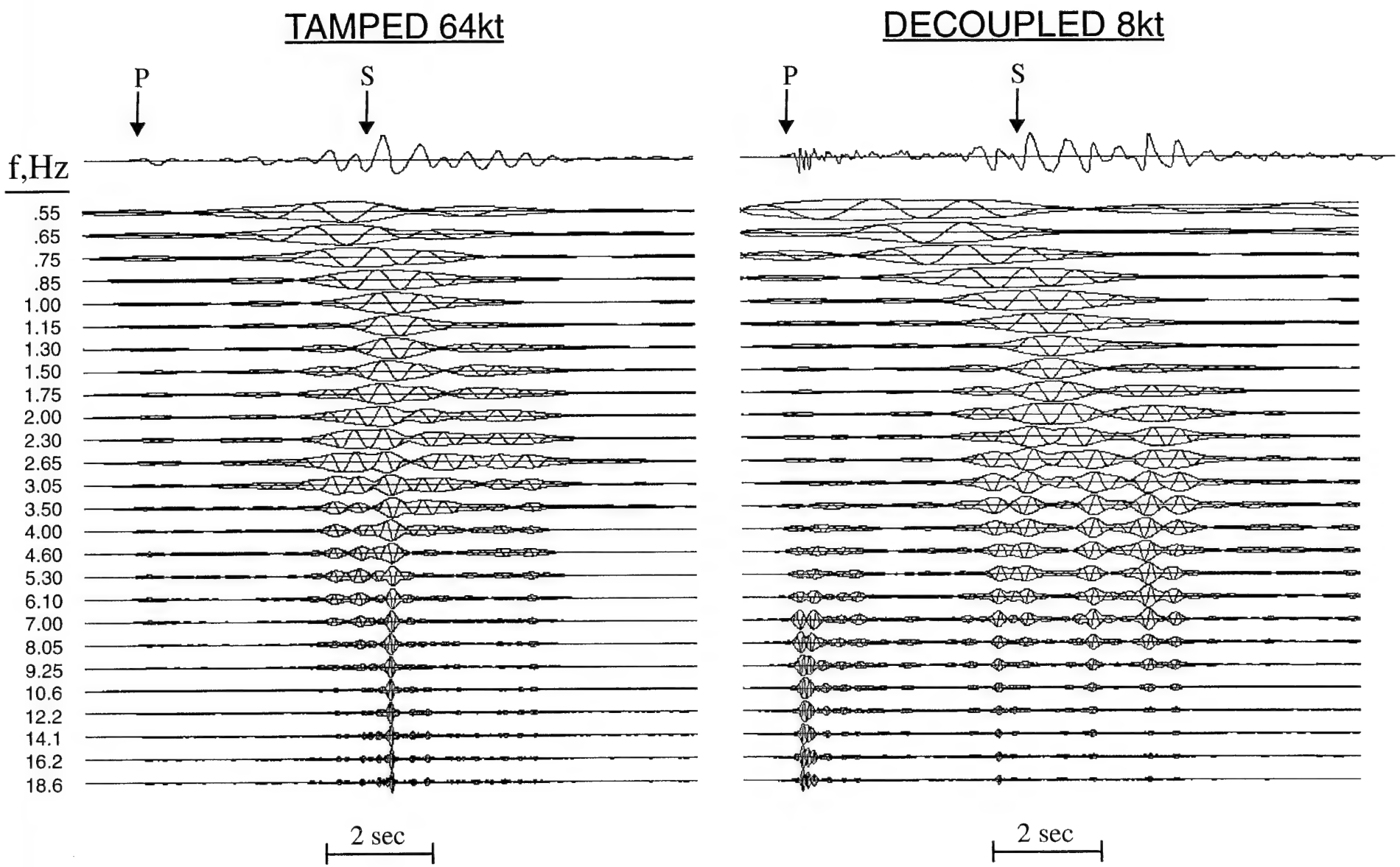

Figure 21. Comparison of vertical component waveforms and associated bandpass filter outputs for the Soviet Azgir tamped (III) and cavity decoupled (III-2) nuclear explosions recorded at a range of 18.2 km.

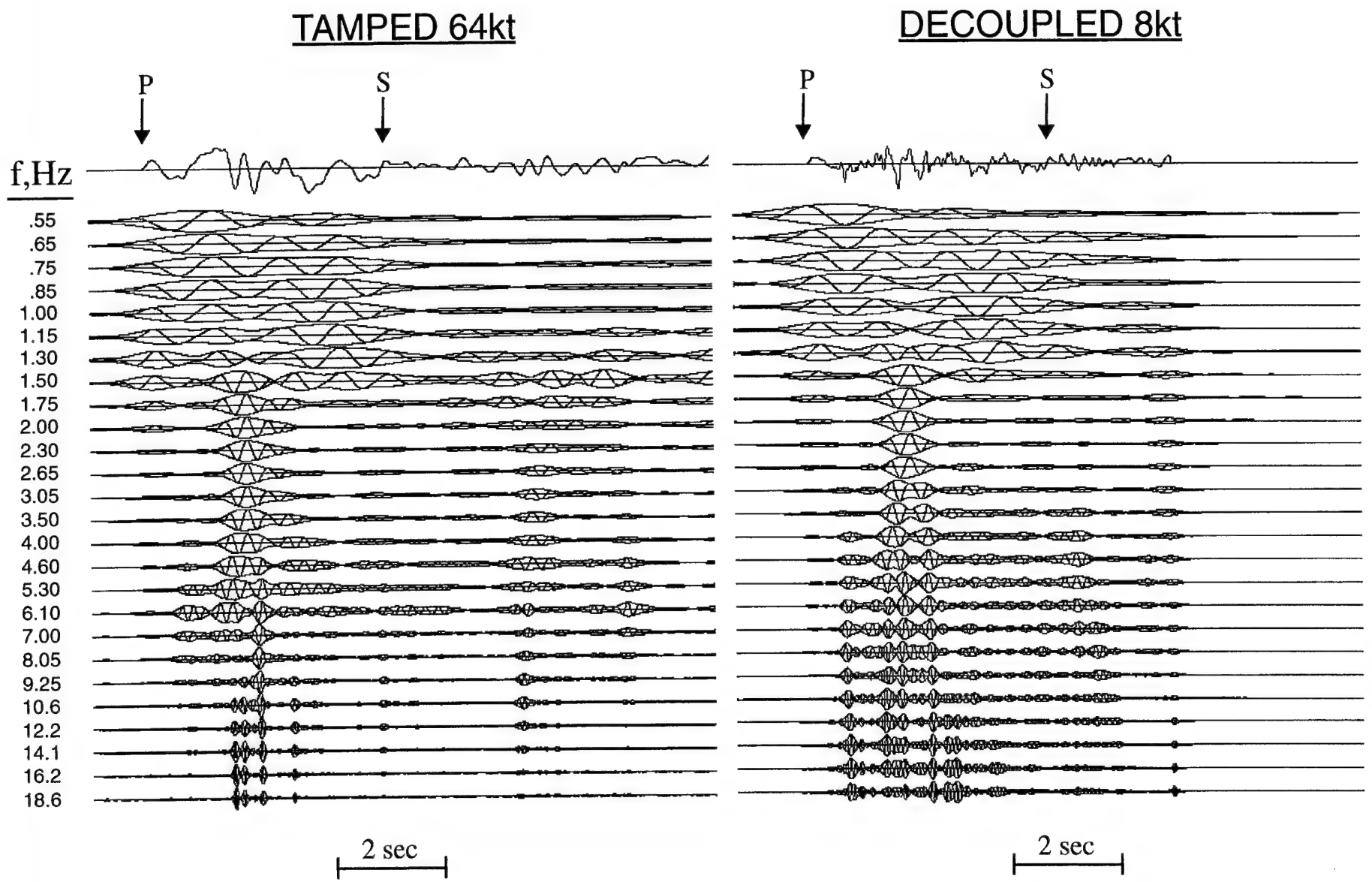

Figure 22. Comparison of vertical component waveforms and associated bandpass filter outputs for the Soviet Azgir tamped (III) and cavity decoupled (III-2) nuclear explosions recorded at a range of 23.0 km.

source corner frequency is higher and, consequently, the Azgir I digitized data are considered to be reliable to somewhat higher frequencies.

The results of bandpass filtering the data recorded from the Azgir III-2 cavity decoupled explosion at a range of 113 km are shown in Figures 23 and 24 where they are compared with the corresponding results of bandpass filtering the data recorded from the tamped Azgir I explosion at distances of 97 and 112 km, respectively. It can be seen from Figure 23 that the tamped explosion recording at a range of 97 km is characterized by an even more impulsive initial P arrival than that of the decoupled explosion recording at a range of 113 km. Moreover, the high frequency S/P ratios for the tamped explosion are observed to be equal to, or perhaps even smaller than, those associated with the decoupled explosion recording at this distance. Similar comments apply to the comparison shown in Figure 24, where it can be seen that the time dependent filter outputs for the tamped and decoupled recordings at this distance are remarkably similar over the entire displayed frequency range.

Thus, these data recorded at distances on the order of 100 km from a cavity decoupled and nearby tamped explosion do not show any systematic differences in frequency dependent S/P ratios which might be considered to be consistent with the Blandford hypothesis. That is, these Azgir data seem to be consistent with the SALMON/STERLING experience to the extent that apparently diagnostic differences in S/P ratios are seen at stations at some distances, but not at others. Clearly, the limited quantity and somewhat questionable quality of the data which are currently available for analysis makes it difficult to draw definitive conclusions at this time. However, in the absence of further data or much improved theoretical understanding, we must tentatively conclude that frequency dependent S/P ratios do not appear to provide a consistent basis for discriminating between tamped and cavity decoupled nuclear explosions.

A final matter of interest with respect to this hypothesis concerns the critical evaluation of possible reasons for frequency dependent differences in the seismic signals recorded from tamped and cavity decoupled explosions. As was noted above, Blandford (1995) has postulated that the greater degree of nonlinear material response and associated cracking induced by tamped explosions might explain an increased S wave generation efficiency at high frequencies. We have

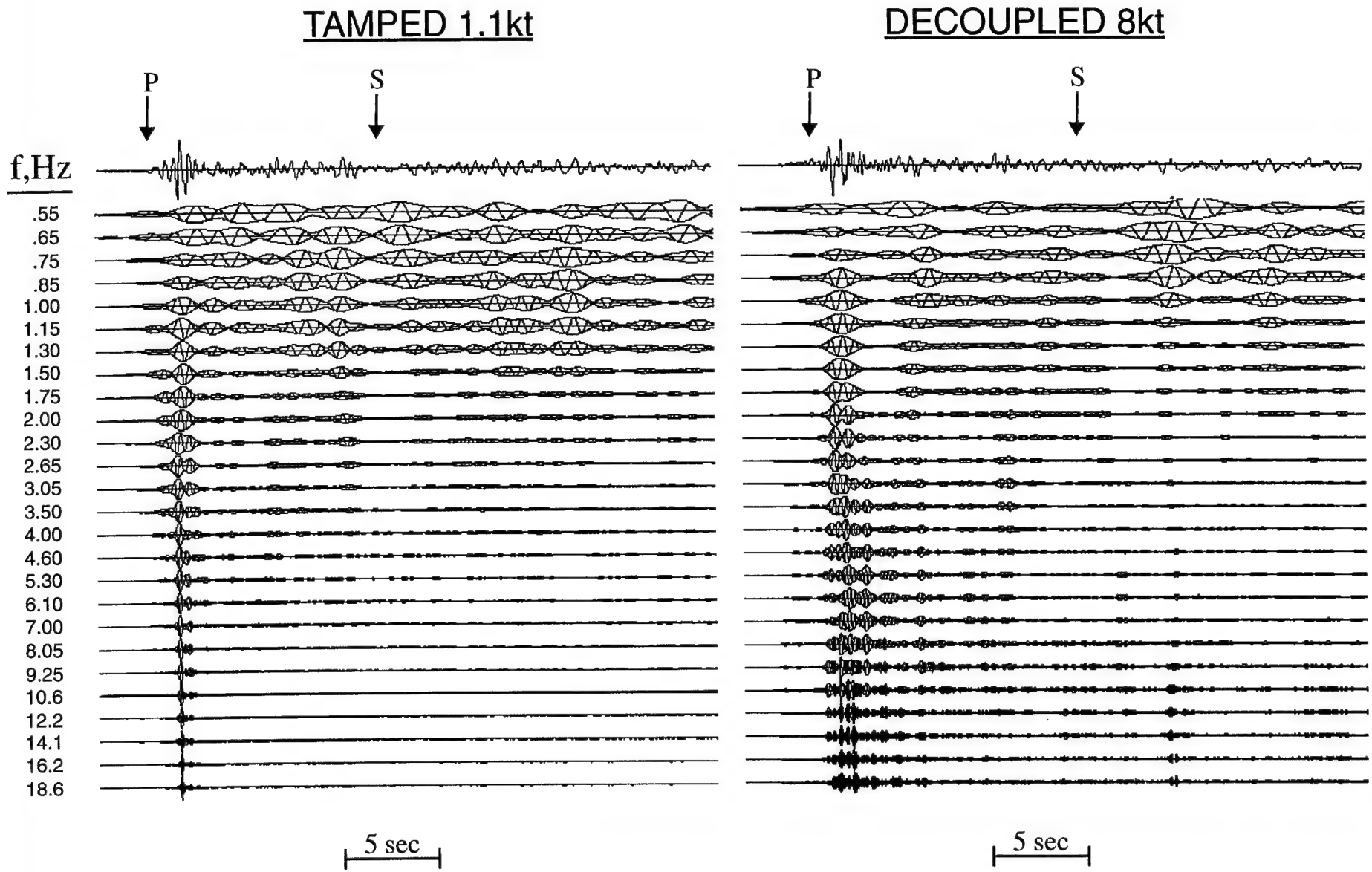

Figure 23. Comparison of vertical component waveforms and associated bandpass filter outputs for the Soviet Azgir tamped (I) and cavity decoupled (III-2) nuclear explosions recorded at ranges of 97 and 113 km, respectively.

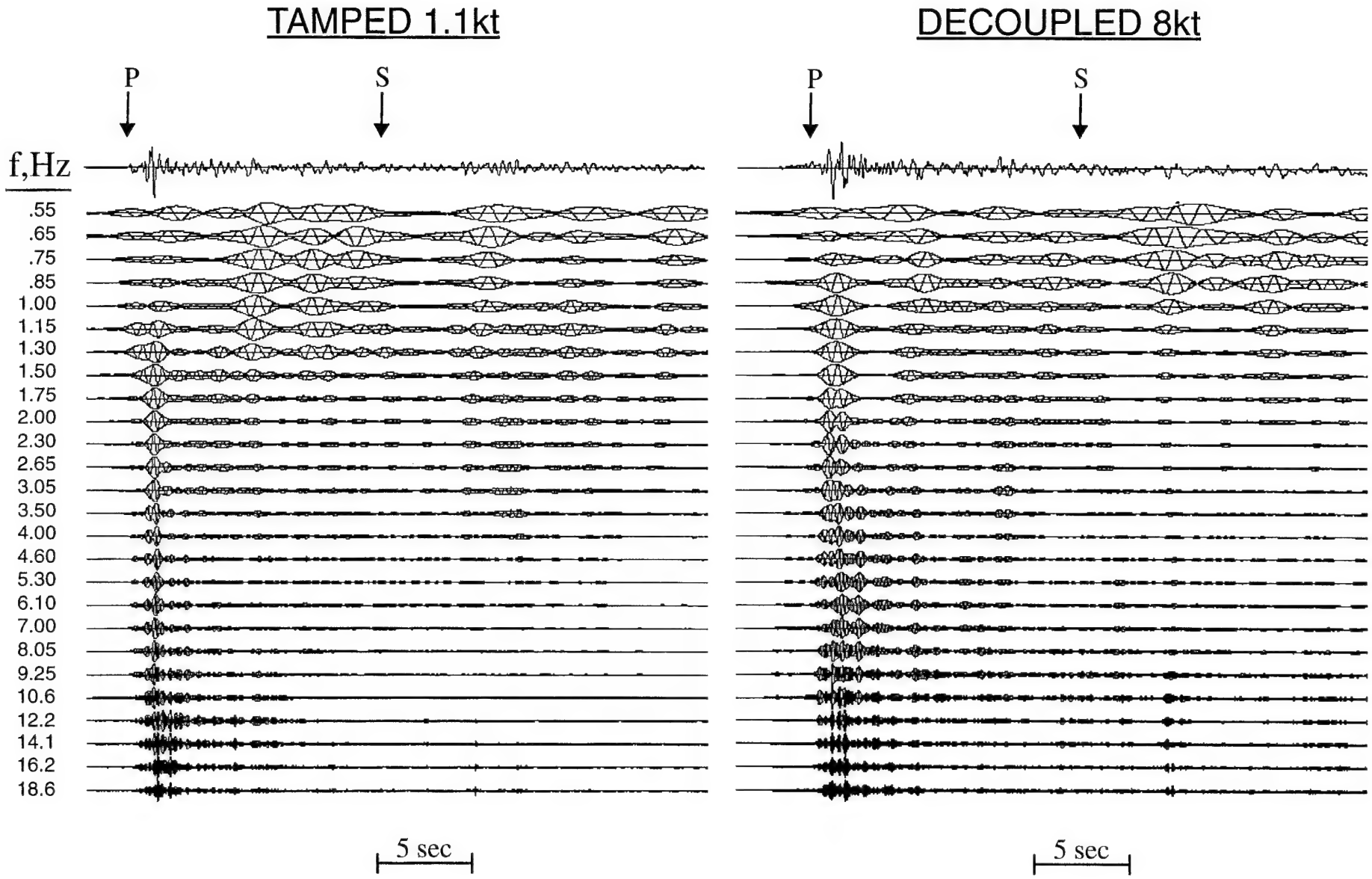

Figure 24. Comparison of vertical component waveforms and associated bandpass filter outputs for the Soviet Azgir tamped (I) and cavity decoupled (III-2) nuclear explosions recorded at ranges of 112 and 113 km, respectively.

evaluated this hypothesis in a preliminary fashion using data recorded from a series of Russian nuclear explosions detonated in a water-filled cavity at Azgir. Since the yields of the six cavity shots in this series varied by more than a factor of 50, comparisons of the observed frequency dependent S/P ratios for these different explosions should provide evidence relevant to the evaluation of the Blandford hypothesis.

On 7/01/68, the 25 kt Azgir II tamped nuclear explosion was detonated at a depth of 597 m in salt. The explosion produced a stable, roughly spherical cavity which subsequently filled with water from the pierced water table above the cap rock. A post-test, downhole survey indicated that this cavity had a maximum horizontal radius of 32.5 m and a total volume of 101,000 m^3. This total volume is equal to that which would be associated with a purely spherical cavity with a radius of 28.9 m. Six nuclear explosions with different yields were subsequently detonated in this water-filled cavity during the period from 1975 to 1979. The source parameters of the seven nuclear tests at this location are listed in Table 1, where it can be seen that the yields of the water-filled cavity explosions varied over a factor of 50, ranging from 0.01 to 0.50 kt. Now a 28.9 m radius, air-filled cavity at a depth of 585 m in salt would be expected to decouple a 1.3 kt nuclear explosion to the same degree as that achieved for the U.S. STERLING explosion. It follows that, if this cavity had been air-filled, all six of the cavity tests listed in Table 1 would have been fully decoupled and the associated seismic signals would have been well below the teleseismic detection threshold. In fact, however, the two largest of these cavity explosions were detected at teleseismic distances, indicating enhanced coupling rather than decoupling over some frequency bands, more consistent with what would be expected for explosions in water (Murphy *et al.*, 1994). Nevertheless, it seems unlikely that the smallest these explosions induced any significant nonlinear response in the cavity walls and, consequently, a comparison of the frequency dependent S/P ratios observed at fixed stations from the explosions of Table 1 should provide a good test of the potential importance of induced cracking as an explanation for high frequency S wave generation by explosive sources.

Table 1. Source Parameters For Azgir Water-Filled Cavity Tests

Emplacement Coordinates: 47.9086N, 47.9119E

Event	Date	Origin Time, UT	Depth, m	Yield, kt*
AII	7-01-68	04 02	597.2	25
AII-2	4-25-75	05 00	582	0.35
AII-3	10-14-77	06 59 59.100	587	0.10
AII-4	10-30-77	06 59.59.069	586.2	0.01
AII-5	9-12-78	04 59 58.494	585	0.08
AII-6	11-30-78	04 59 58.929	586	0.06
AII-7	1-10-79	08 00	590	0.50

*Russian Ministry of Defense (personal communication, Ralph Alewine, 1994)

Photographic recordings of the ground motion data observed from the tamped explosion AII and the first four of the water-filled cavity tests (i.e., AII-2, AII-3, AII-4, AII-5) have now been collected and carefully digitized at the Russian Institute for Dynamics of the Geospheres (IDG) using standardized procedures described by Kitov *et al.* (1994). While these data were digitized at high sampling ratios, the limited dynamic range of the photographic recording medium once again limits the resolution of high frequency energy, particularly for the tamped 25 kt explosion. Thus, the data from the tamped AII explosion are probably not reliable above 8-10 Hz, while the data for the smaller cavity tests may be reliable out to about 15 Hz at some of the closer stations.

Bandpass filter outputs derived from the data recorded from the tamped AII explosion at a distance of 75 km are shown in Figure 25, together with the corresponding bandpass filter outputs derived from the data of the AII-2, AII-3 and AII-4 cavity explosions recorded at that same station. Comparing the time dependent filter outputs for these four events, it can be seen that they appear to be very similar over the entire frequency band represented here. In particular, there are no obvious differences in the frequency dependent S/P ratios between the tamped and cavity tests and no apparent increase of high frequency S wave generation efficiency with increasing yield for the cavity tests. A similar comparison is shown in Figure 26 using data recorded at a station located at a distance of 7.8 km. At this station, data were recorded from all four of the cavity tests digitized by IDG, as well as from the tamped AII explosion. In this

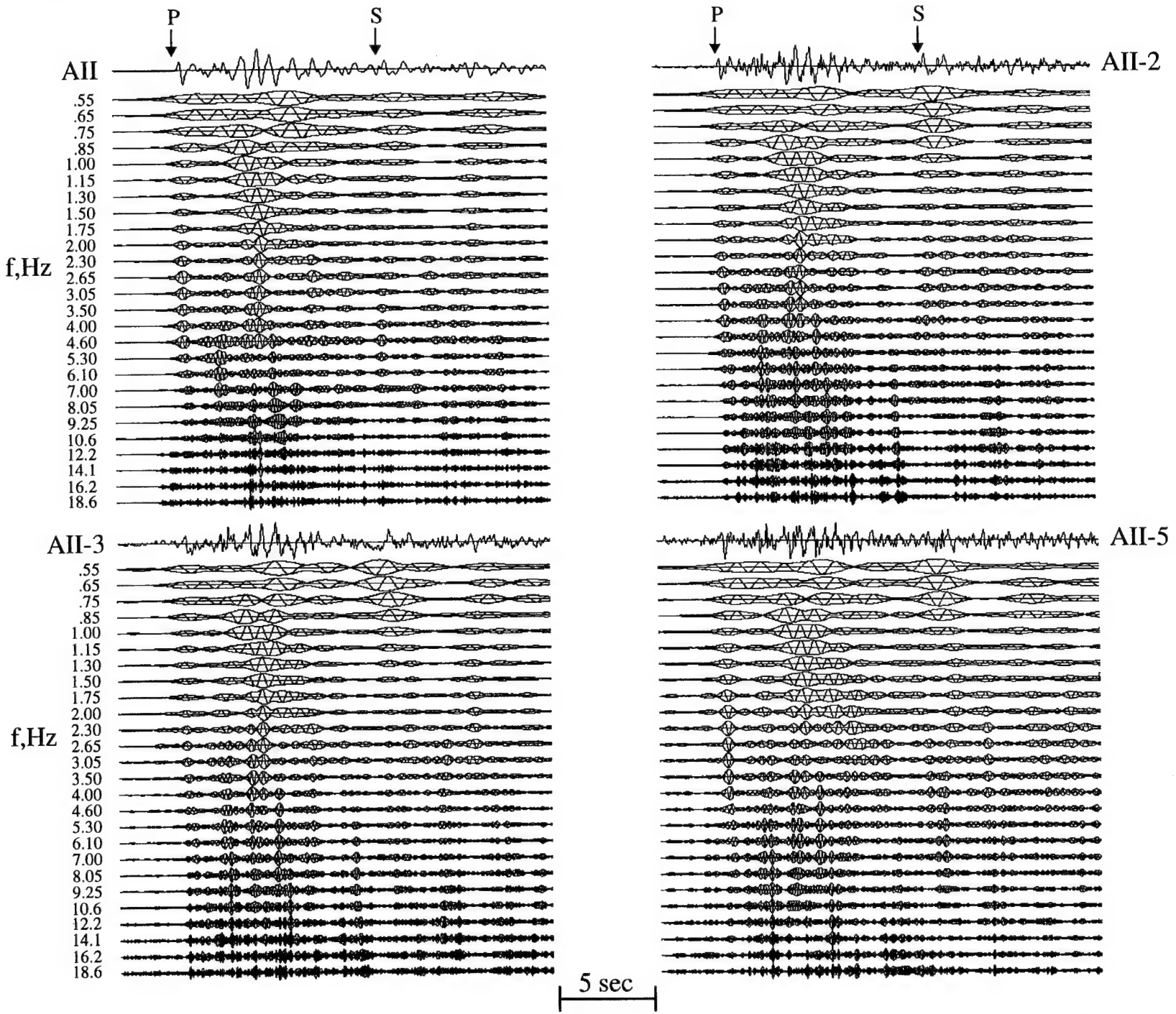

Figure 25. Comparison of bandpass filter outputs for the Azgir II tamped nuclear explosion and three Azgir water-filled cavity tests (AII-2,AII-3,AII-5) derived from ground motion data recorded at a common station at a range of 75 km.

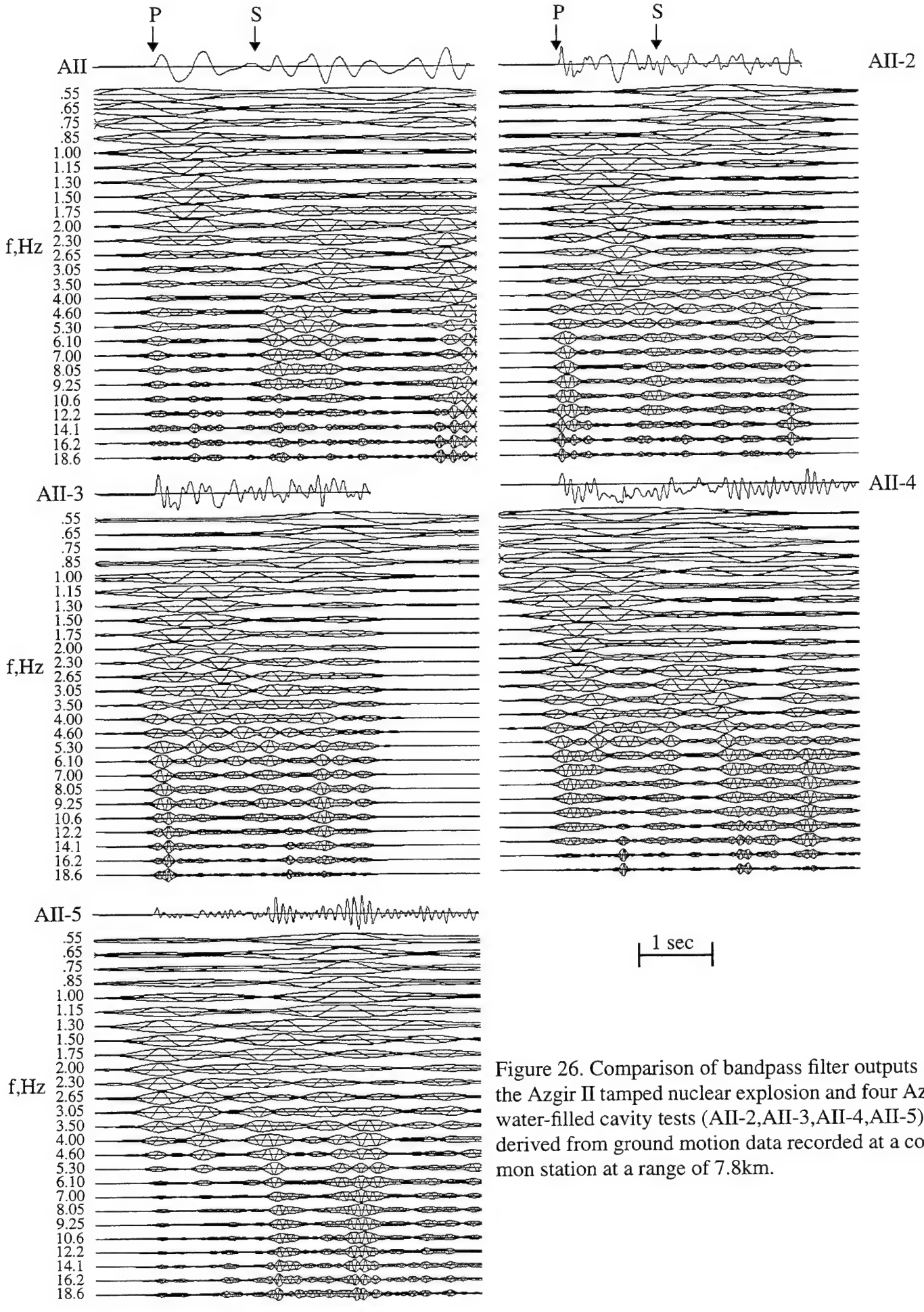

Figure 26. Comparison of bandpass filter outputs for the Azgir II tamped nuclear explosion and four Azgir water-filled cavity tests (AII-2,AII-3,AII-4,AII-5) derived from ground motion data recorded at a common station at a range of 7.8km.

case, there does appear to be some variability in the frequency dependent S/P ratios between the various events. However, this variability does not seem to correlate with the expected intensity of the induced stresses in the surrounding salt medium in any systematic fashion. Thus, for example, the high frequency S/P ratios for the 0.08 kt AII-5 water-filled cavity test appear to be comparable to or larger than those observed from the 25 kt tamped AII explosion at this station. Similarly, the high frequency S wave generation efficiencies for the 0.01 kt AII-4 and 0.10 kt AII-3 cavity tests are not noticeably different in this figure. In fact, the most conspicuous differences on this figure are in the low frequency (< 1.0 Hz) bandpass filter outputs for which the S/P ratios are notably larger for the cavity shots than for the tamped explosion. This may just be an indication that the dominant frequencies of the initial P waves are controlled by the source, while the dominant frequencies of the waves arriving after S (e.g., surface waves) are controlled by the propagation path characteristics which remain constant for all the explosions. Due to the lowpass nature of anelastic attenuation in the earth, such differences would be expected to be much less pronounced at greater distances, and this is found to be the case for these explosions (cf. Figure 25). In any case, the data recorded from this water-filled cavity test series do not support the Blandford hypothesis regarding differences in S wave generation mechanisms between tamped and cavity decoupled nuclear explosions. In fact, most of the data analyzed in this investigation seem to be more consistent with the hypothesis that the seismic source characteristics of these two source types are generally quite similar, at least over the limited frequency band which is typically available for seismic discrimination analysis.

3.3 Seismic Discrimination of Cavity Decoupled Nuclear and Ripple-Fired Chemical Explosions

It was noted previously in Section 2 that the majority of large CE events are near-surface, ripple-fired quarry blasts in which the explosives are distributed over a wide surface area in a large number of shallow drill holes and detonated sequentially in time in a manner designed to simultaneously maximize the efficiency of overburden removal and minimize the ground motion hazard to structures in the vicinity of the mine. The resulting seismic source functions for many such CE events have been observed to have characteristics which reflect

this extended distribution in space and time. Thus, for example, previous studies by Baumgardt and Ziegler (1988), Smith (1989), Hedlin *et al.* (1989, 1990) and others have identified the presence of time-independent bands in the spectrograms of ground motion data recorded from such CE events and have quantitatively related these spectral characteristics to the time-dependent detonation sequences of these ripple-fired explosions. Most recently, Kim *et al.* (1994) have reported on an extensive investigation of the spectral characteristics of near-regional ground motion data recorded from a large sample of over 100 quarry blasts detonated in the northeastern U.S. and Norway. On the basis of their analyses, they concluded that the observation of regular spectral banding at high frequencies is the most reliable seismic discriminant of ripple-fired CE blasts, at least in cases in which good-quality, high-frequency data are available for analysis. However, they also noted that such spectral banding is not a universal feature of all quarry blasts and that, even when present, it can show significant variability between blasts at the same mine. Moreover, they cautioned that such data need to be carefully evaluated, since spectral banding can also be produced by factors which are independent of the source, such as wave reverberations in structures along the propagation path and recording system noise.

One limitation of the studies referenced above is that they typically have not employed direct comparisons with nuclear explosion data. Moreover, much of the mine blast data studied to date have been recorded from mines in only a few areas of the world (primarily the U.S. and Scandinavia) and, consequently, they may not be representative of the blasting conditions in other regions of monitoring interest. In an attempt to circumvent some of these data limitations in the present study, we have used the near-regional ground motion data recorded from selected Azgir nuclear tests, including the Azgir III-2 cavity decoupled test, as the basis for comparisons with the corresponding near-regional ground motion data recorded from several quarry blasts conducted near IRIS station KIV, which is located about 600 km southwest of Azgir. Ground motion data are available from both these source areas over a common distance interval extending from about 20 to 115 km. For example, scaled versions of data recorded in this distance range from Azgir nuclear explosions are displayed in order of increasing distance in Figure 27, where, in this case the data have been theoretically scaled to 1 kt fully decoupled conditions using the procedures described in Section 2. In this figure, waveforms labeled III-2 correspond to scaled versions of recordings

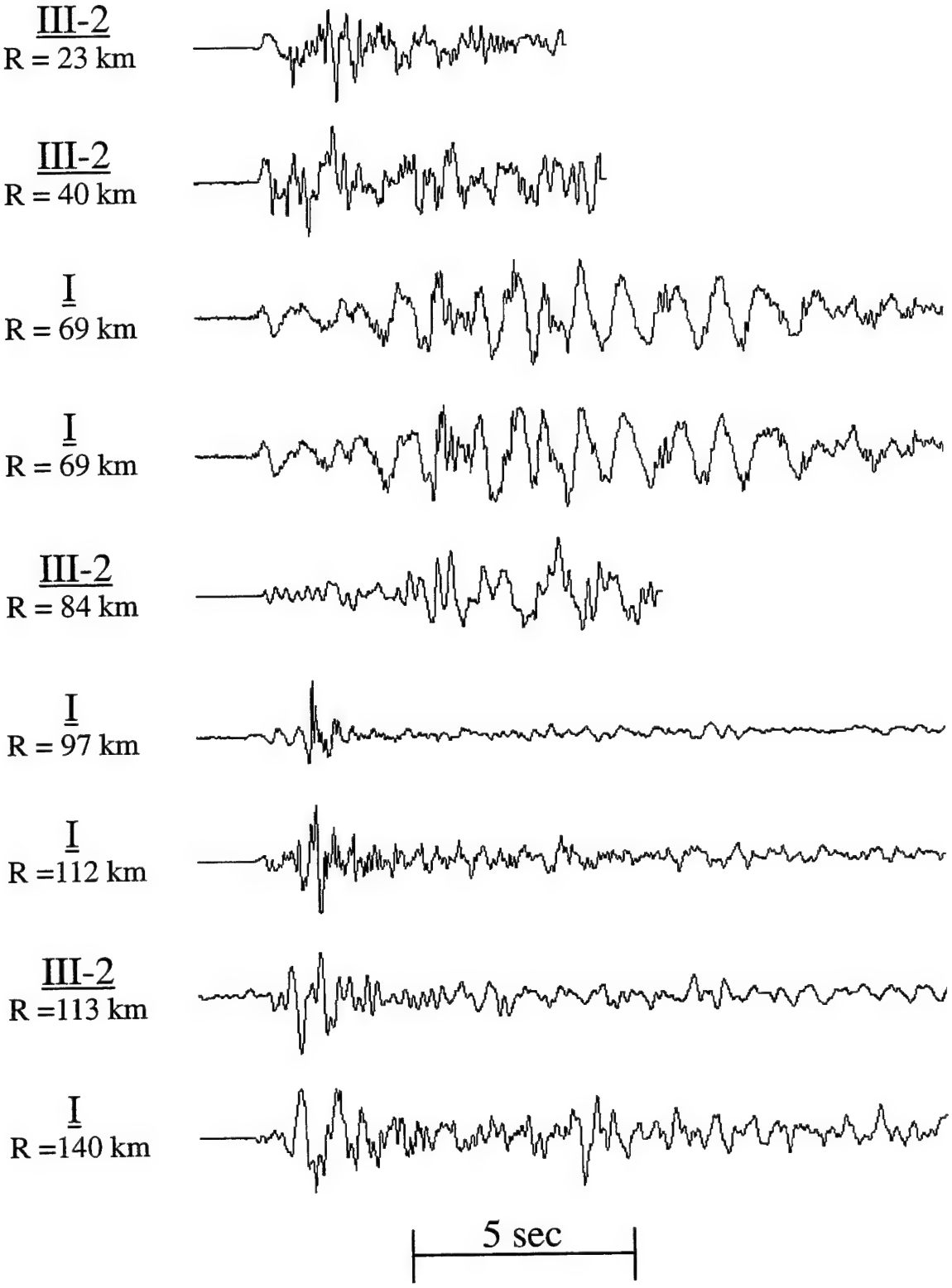

Figure 27. Theoretically scaled vertical component ground motions corresponding to 1 kt fully decoupled nuclear explosions at depths of 987m (III-2) and 161m (I) at the Azgir test site.

from the 8 kt partially decoupled Azgir III-2 explosion at a depth of 987 m, while those labeled I correspond to scaled versions of the 1 kt Azgir I explosion at a depth of 161 m. As was noted previously, although these data were digitized at sampling rates of 200 samples/second or more, the limited dynamic range of the original photographic recording medium limits the usable upper frequency limit to about 10 Hz in this case. The corresponding mine blast data are shown in Figure 28, where here the waveform labels T1, T2 and Z-K denote the Tyrnyauz 1 and 2 and Zhako-Krasnogorskaya mine blasts described previously in Section 2. These data were electronically recorded and digitized at a sampling rate of 125 samples/second and, consequently, should provide usable information over the entire frequency band considered in this investigation, at least in cases where the signal-to-noise ratios are adequate over this band. As was noted previously by Murphy and Barker (1994), direct visual comparisons of the waveforms shown in Figures 27 and 28 reveal no obvious and consistent differences which would permit an analyst to routinely separate the data from these two source types. Therefore, in the following analysis, a variety of more sophisticated signal processing procedures will be applied to these data in an attempt to assess the applicability of different discrimination procedures.

It was noted above that the observation of regular spectral banding at high frequencies is generally considered to be the most reliable indicator of a ripple-fired quarry blast source. Therefore, we began our identification analysis of our sample of such events by computing spectrograms from the quarry blast and nuclear decoupled ground motion waveforms of Figures 27 and 28. Following Kim *et al.* (1994), we have computed velocity spectra as a function of time using a series of overlapping time windows and have displayed the resulting spectral amplitudes as a function of time and frequency in the form of wire-frame diagrams. The resulting spectrograms for the Tyrnyauz 1 and 2 quarry blast data recorded at six common stations are presented in Figures 29 and 30, while those derived from the four Zhako-Krasnogorskaya quarry blast recordings are shown in Figure 31. Examination of these figures reveals the presence of some isolated, time-independent spectral modulation patterns, but no consistent spectral banding between stations for any one event. Moreover, it seems clear that the data should be adequate to delineate any such features if they are present, in that a rather narrowband noise source at about 15 Hz at station KUB produces clearly identifiable ridges beginning before the signal onset time and continuing

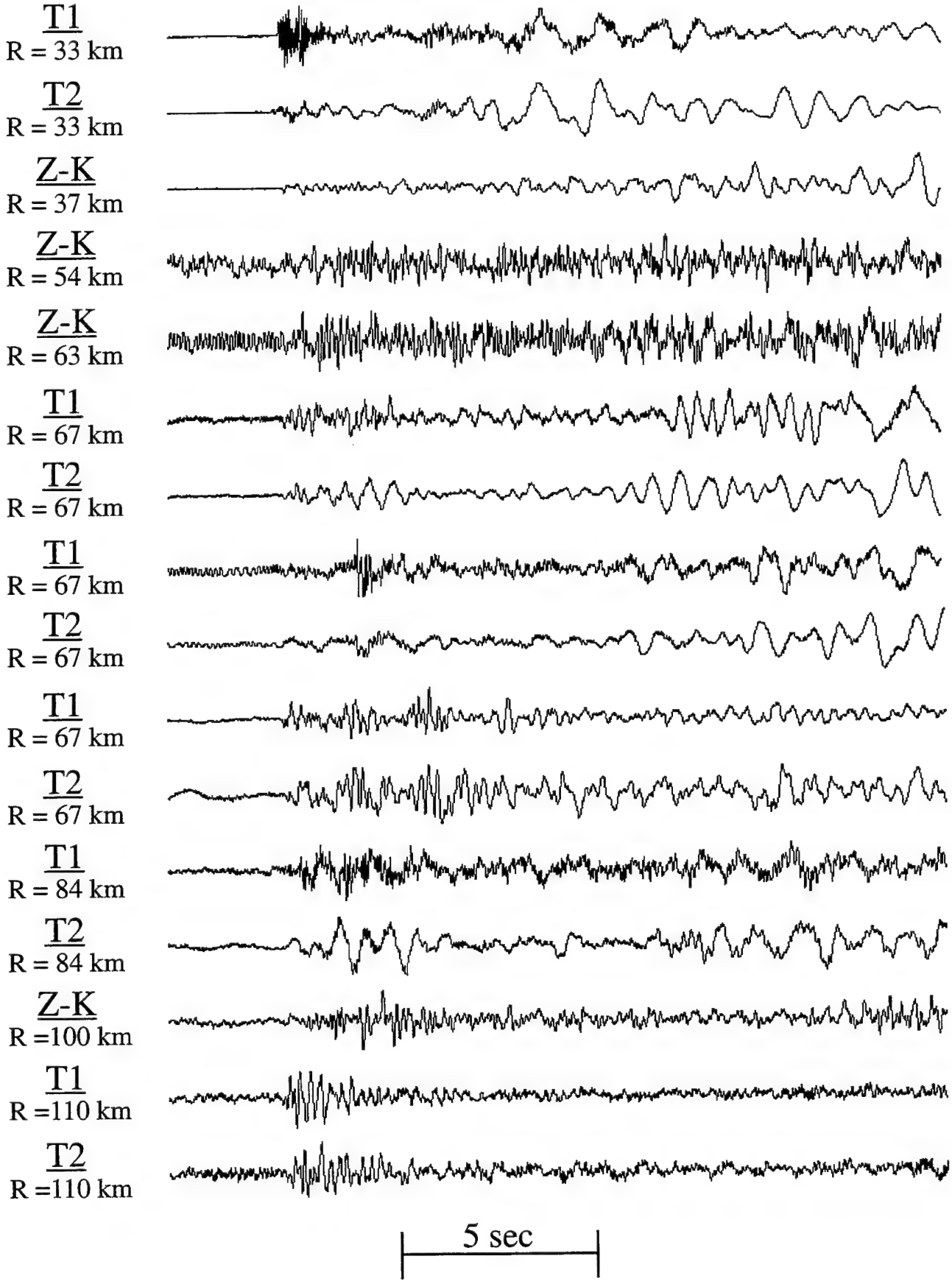

Figure 28. Vertical component ground motions recorded at the KIV station array from mine blasts at the Tyrnyauz (T1, T2) and Zhako-Krasnogorskaya (Z-K) mines.

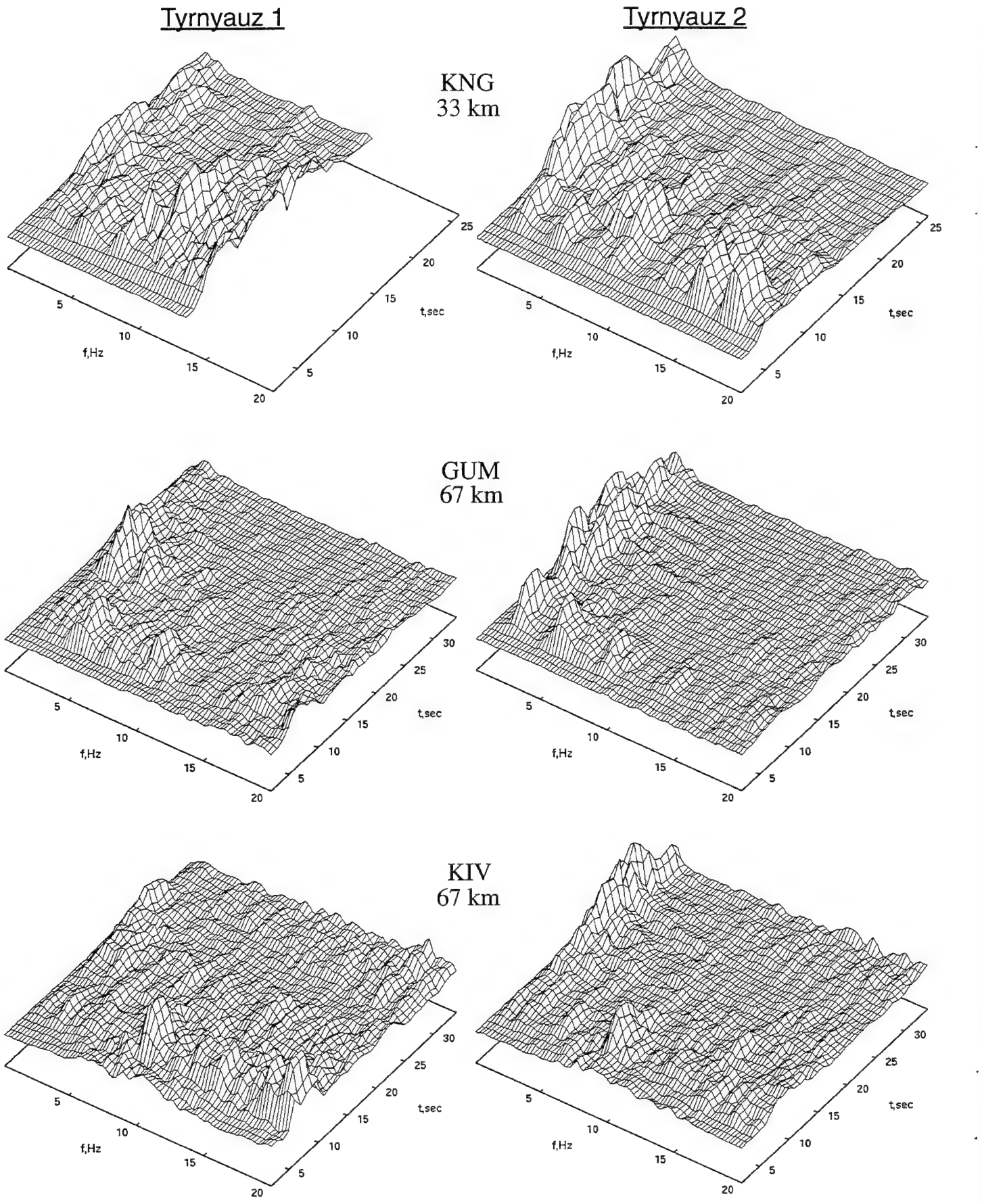

Figure 29. Spectrograms of Tyrnyauz 1 and 2 mine blast recordings at IRIS temporary stations KNG, GUM and KIV.

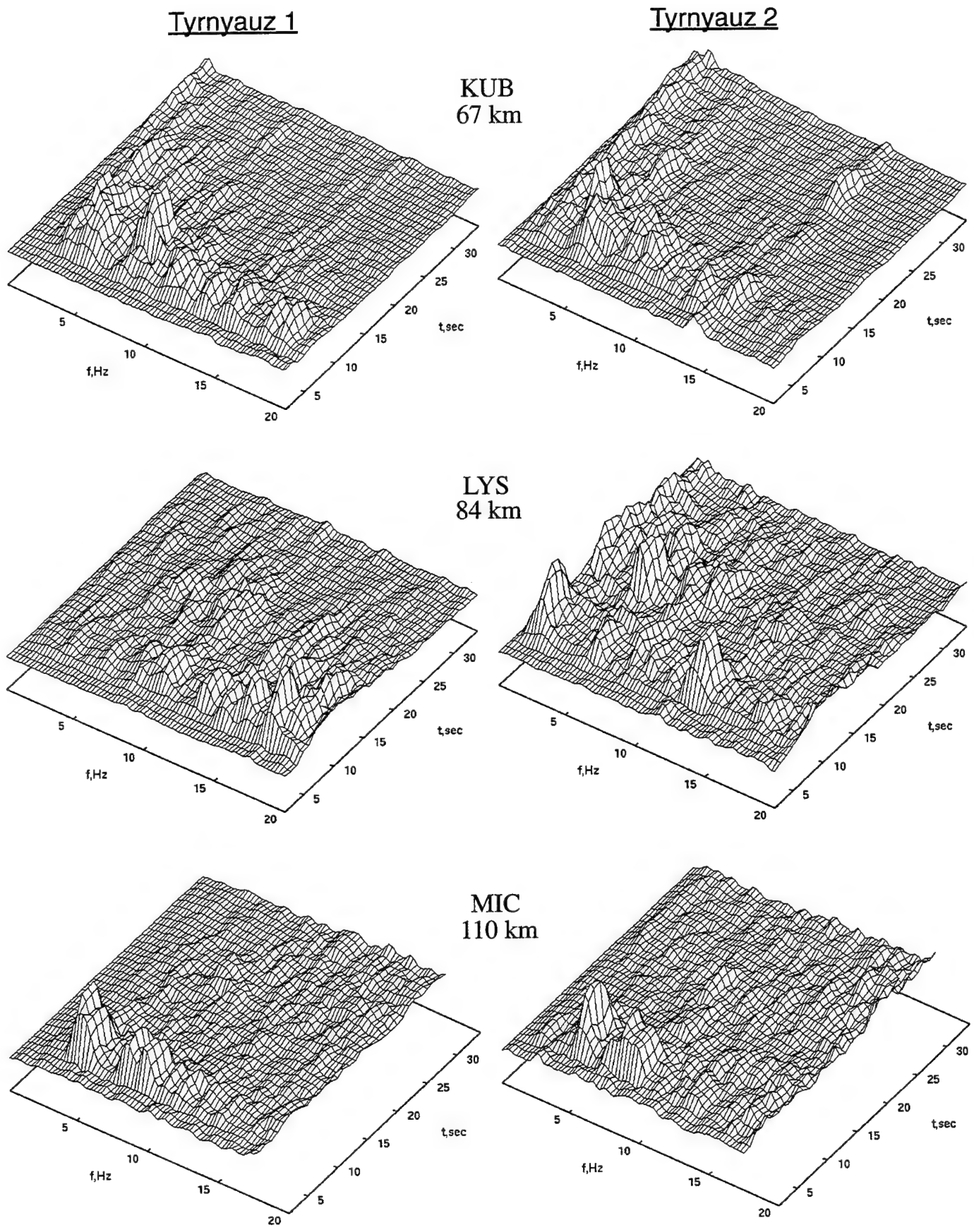

Figure 30. Spectrograms of Tyrnyauz 1 and 2 mine blast recordings at IRIS temporary stations KUB, LYS and MIC.

Zhako-Krasnogorskaya

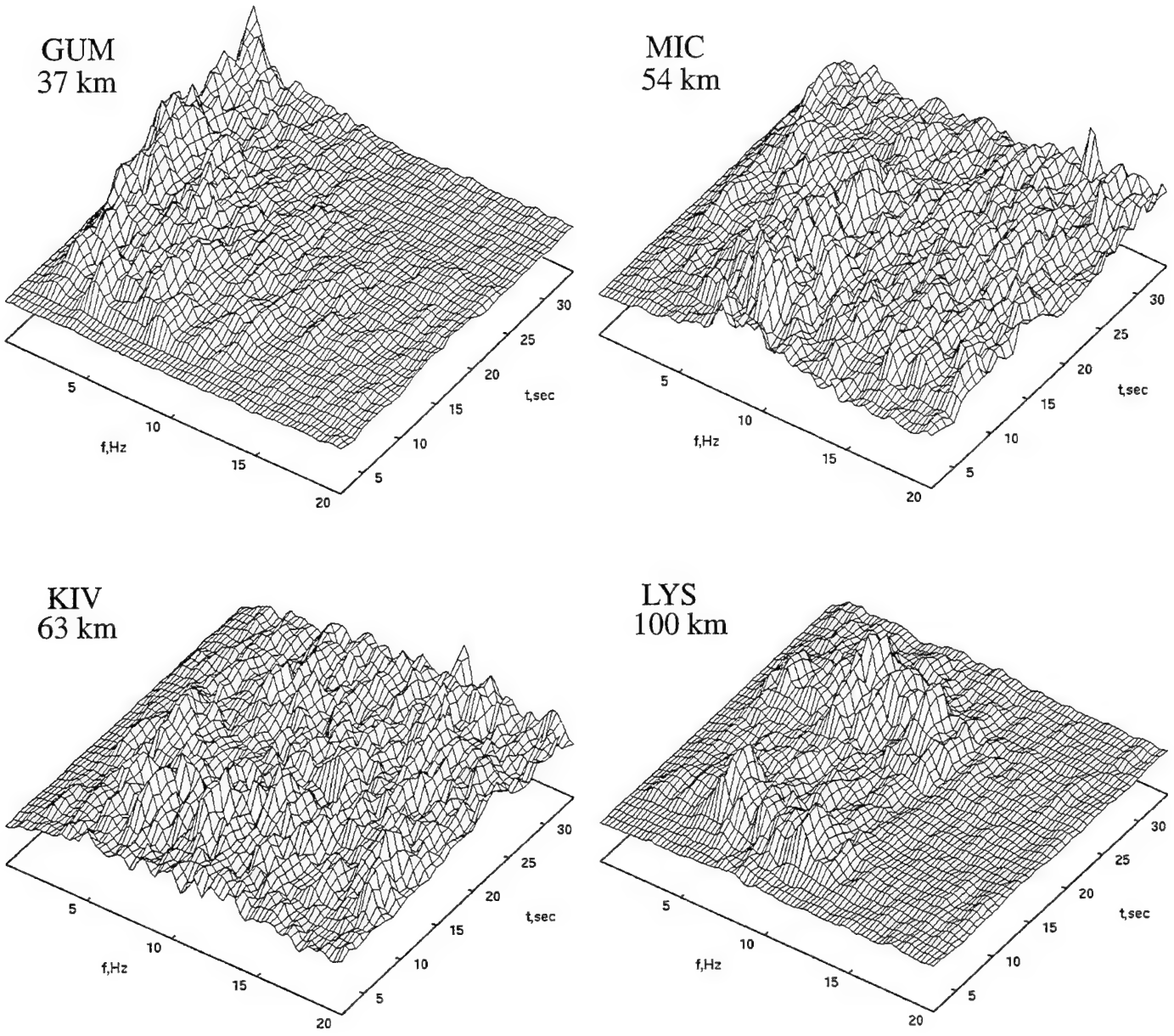

Figure 31. Spectrograms of Zhako-Krasnogorskaya mine blast recordings at IRIS temporary stations GUM, MIC, KIV and LYS.

throughout the recording on the spectrograms corresponding to the two Tyrnyauz recordings shown at the top of Figure 30. While these negative results are disappointing, they are not completely surprising in that Kim *et al.* (1994) and others have pointed out that spectral banding is not a universal feature of all quarry blasts and, in particular, that it is often not observed in cases where the delay times between the individual charges in the blast are small. While it is known that the mine blasts represented in Figures 29-31 were ripple-fired (Rivière-Barbier, 1993), the specific delay times for the cases shown here are not known and it may be that they were sufficiently short that the finite duration characteristics of the source can not be identified in this case using data limited to frequencies below 20 Hz.

Corresponding spectrograms for the Azgir nuclear explosion data of Figure 27 are shown in Figures 32 and 33. Here the results have been segregated so that the spectrograms corresponding to the scaled Azgir III-2 recordings, which are representative of a source depth of 987 m, are shown in Figure 32, while the spectrograms corresponding to the scaled Azgir I recordings, which are representative of a source depth of 161 m, are shown in Figure 33. It can be seen from these figures that there is again no consistent evidence of spectral banding in the computed spectrograms, in accord with what would be expected for these instantaneous nuclear sources. In some cases, these spectrograms do show some very "explosion-like" qualities, such as the impulsive, broadband first arrivals at the 97 km distance station shown in Figure 33. In other cases, however, such as with the 69 km distance stations of Figure 33, the spectrograms are fairly complex and appear to be rather similar to some of the corresponding quarry blast spectrograms shown in Figures 29-31. Therefore, it must be concluded that spectrogram data alone are not sufficient to distinguish between ripple-fired quarry blasts and cavity decoupled nuclear sources, in this case.

Another way of looking at the nuclear explosion and mine blast data of Figures 27 and 28 is through the bandpass filter processing described in Section 3.2 above in conjunction with the comparison of the cavity decoupled and tamped nuclear seismic source functions. In this representation, information regarding the frequency dependence of the relative phase excitation functions (e.g., S/P) is emphasized, at the expense of suppressing information concerning the relative spectral composition of any one particular phase. For the purposes of this

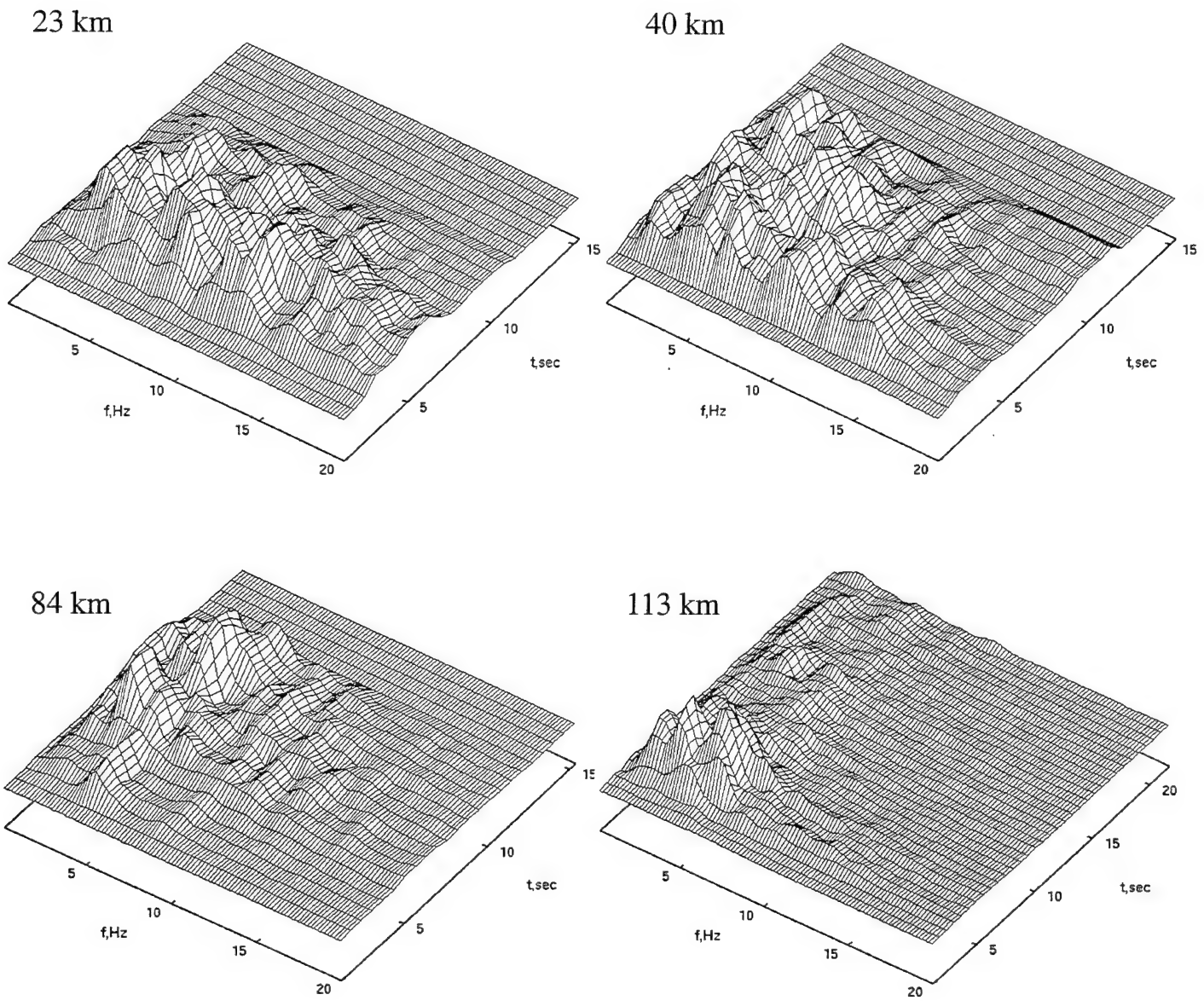

Figure 32. Spectrograms of scaled Azgir III-2 recordings corresponding to a 1 kt fully decoupled explosion at a depth of 987m.

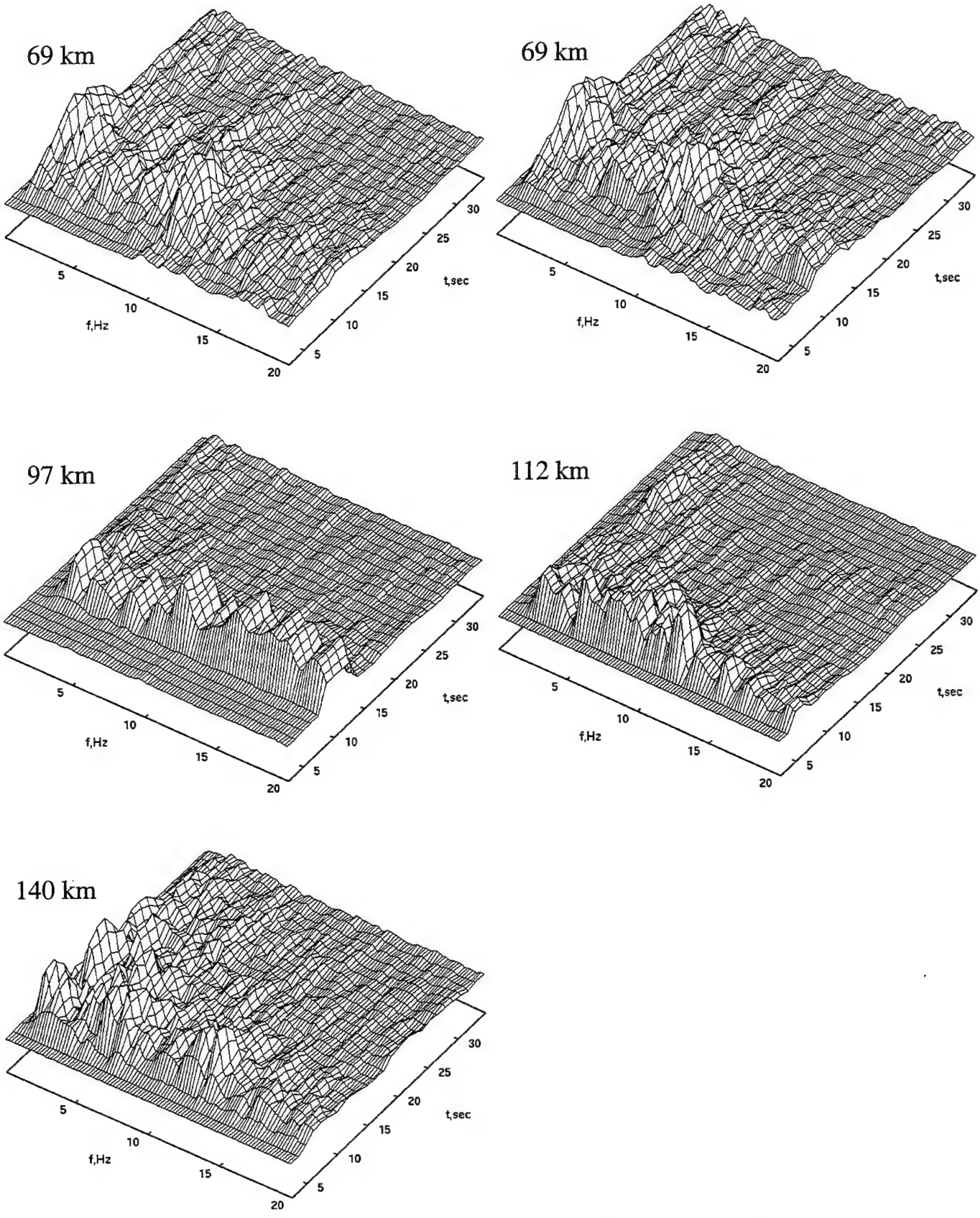

Figure 33. Spectrograms of scaled Azgir I recordings corresponding to a 1 kt fully decoupled explosion at a depth of 161m.

analysis of the seismic data recorded from the two source types, the available data have been grouped into four distinct distance ranges: $23 < \Delta < 40$ km, $63 < \Delta < 69$ km, $\Delta = 84$ km and $97 < \Delta < 113$ km. The time dependent bandpass filter outputs for the nuclear explosion and mine blast recordings in the first of these distance groupings are shown in Figure 34, where the vertical arrows above each set of filter outputs denote the approximate expected onset times of S at those ranges. In the discussion of this and subsequent bandpass filters displays in this section, the term "S/P ratio" is defined to be the ratio of the maximum amplitude after this expected S onset to the maximum amplitude prior to this S onset on the individual, time-dependent filter outputs. It can be seen from this figure that the filter outputs for the three mine blast recordings (labeled T1, T2 and ZK) in this distance range show fairly consistent patterns, with S/P > 1 for frequencies below about 1 Hz and S/P $\approx$ 1 or larger between 2 and 10 Hz. The two sets of filter outputs corresponding to the nuclear explosion recordings at 23 and 40 km, on the other hand, do not show a consistent pattern at high frequencies in that S/P < 1 for the former and S/P $\approx$ 1 for the latter between about 2 and 10 Hz. In fact, for frequencies above 2 Hz, the bandpass filter outputs corresponding to the nuclear explosion recording at a distance of 40 km appear to be quite similar to those for the ZK mine blast recording at 37 km. The only consistent differences which can be seen in the bandpass filter outputs for these data are for frequencies below about 1 Hz, where the S/P ratios are greater than one for the mine blast data and less than one for the nuclear explosion data.

In the second distance interval, which extends from 63 to 69 km, there are two Azgir nuclear explosion recordings and six mine blast recordings available for analysis. The bandpass filter outputs corresponding to these data are shown in Figures 35 and 36, where the output for the two nuclear explosion recordings are repeated at the top of the figures to facilitate the comparisons. It can be seen from these figures that the two nuclear explosion recordings in this distance range give consistent results, with S/P $\approx$ 1 for frequencies below 1.5 Hz and above 5 Hz, and S/P < 1 over the intervening band between 1.5 and 5 Hz. The mine blast data, on the other hand, show significant variability between events in this case, with the Tyrnyauz data having S/P ratios of less than one between 5 and 12 Hz, while S/P $\approx$ 1 over the same band for the ZK data. That is, these data are consistent with those from the first distance grouping in that they show overlap in the high frequency S/P ratios between the data from the two source types. Once

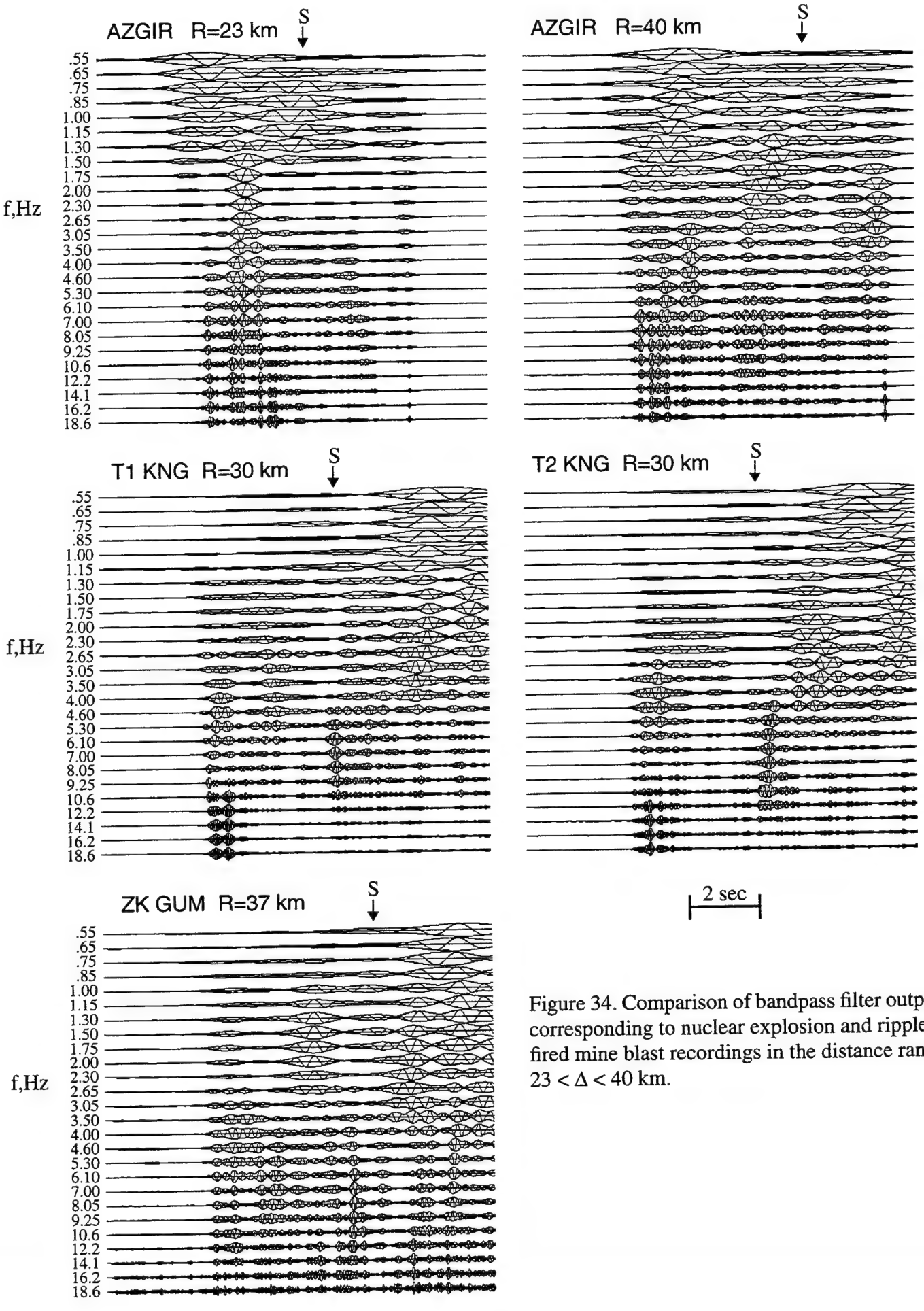

Figure 34. Comparison of bandpass filter outputs corresponding to nuclear explosion and ripple-fired mine blast recordings in the distance range $23 < \Delta < 40$ km.

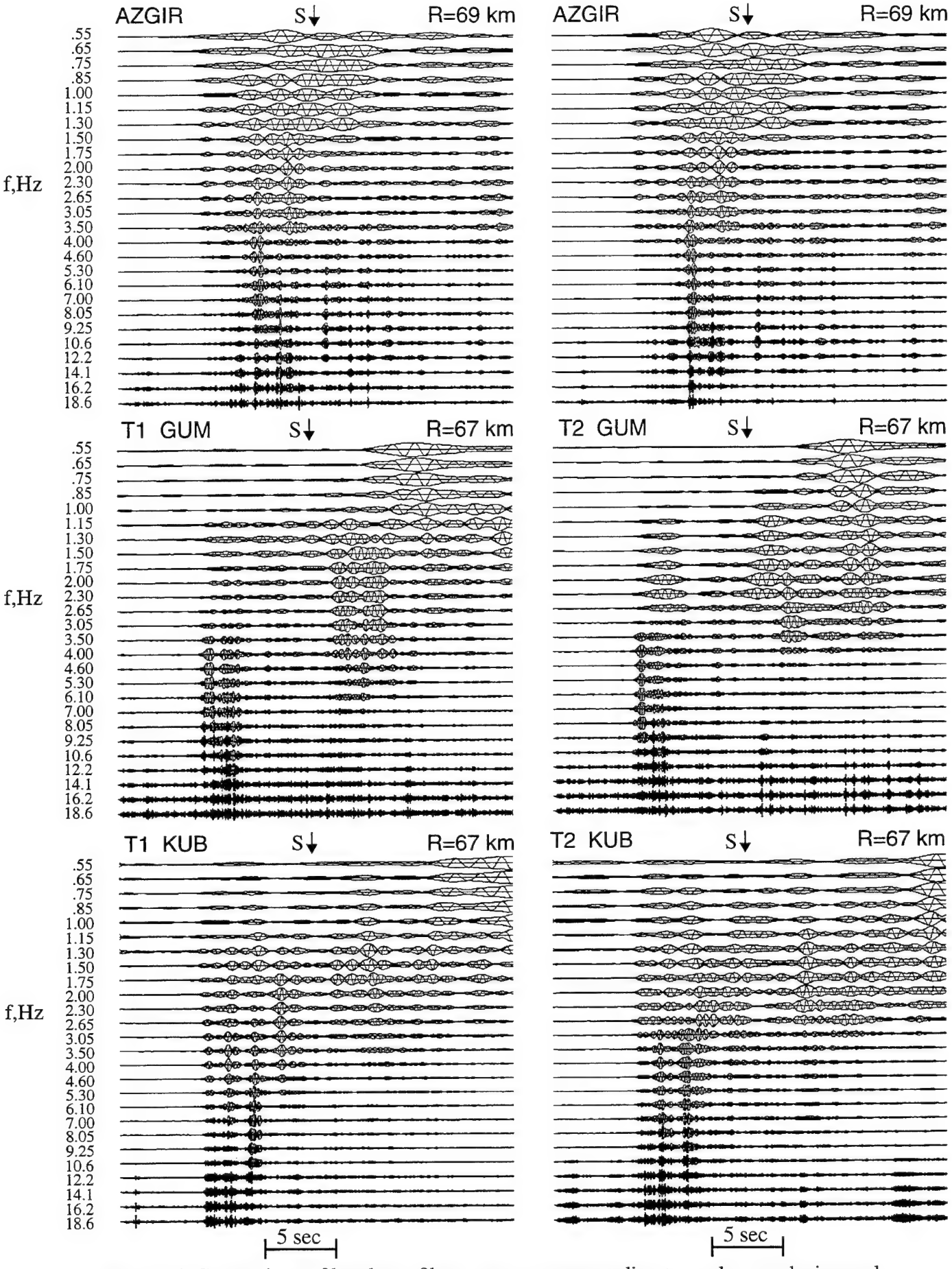

Figure 35. Comparison of bandpass filter outputs corresponding to nuclear explosion and ripple-fired mine blast recordings in the distance range $67 < \Delta < 69$ km.

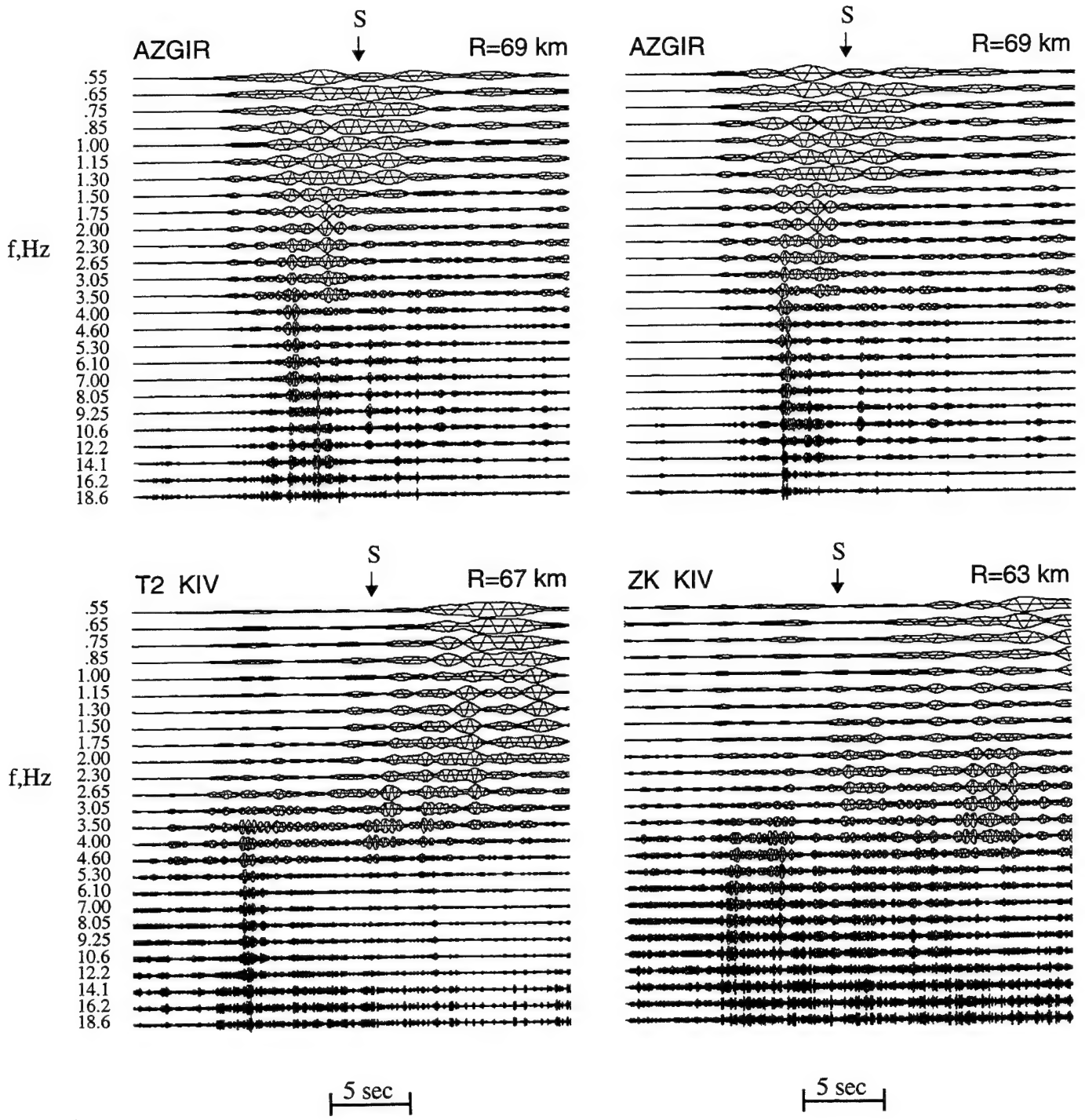

Figure 36. Comparison of bandpass filter outputs corresponding to nuclear explosion and ripple-fired mine blast recordings in the distance range $63 < \Delta < 69$ km.

again, the most consistent differences in this distance interval are seen at frequencies below about 1 Hz where S/P $\approx$ 1 for the nuclear recordings and S/P > 1 for the mine blast recordings.

The bandpass filter outputs corresponding to the one nuclear and two mine blast recordings in the third distance grouping at 84 km are shown in Figure 37, where it can be seen that they are all quite similar, with S/P $\approx$ 1 over most of the frequency band from 0.55 to 10 Hz. The only notable exception to this generalization is for the T2 mine blast data over the limited frequency band extending from about 3 to 7 Hz, for which the S/P ratios are significantly greater than one. That is, the nuclear explosion and T1 mine blast data appear to be quite similar with respect to the frequency dependence of the S/P ratios in this case, while the data for the two blasts at the same mine show some significant differences. Notice also that the bandpass filter outputs at frequencies below 1 Hz are quite similar for the two source types in this case, in contrast to the results obtained for the two closer distance groups.

The fourth and final distance grouping includes three nuclear explosion and three mine blast recordings from the distance interval 97 < Δ < 113 km, and the bandpass filter outputs corresponding to these data are shown in Figure 38. Comparing the three sets of nuclear explosion bandpass filter outputs shown in the left column of this figure, it can be seen that they are fairly consistent in this distance range, showing S/P $\approx$ 1 for frequencies below about 1 Hz and S/P < 1 over the frequency band extending from about 1.5 to 10 Hz. With regard to the corresponding mine blast data shown in the right hand column of this figure, it can be seen that the bandpass filter outputs for the two Tyrnyauz blasts are quite comparable to those for the nuclear explosions, showing S/P $\approx$ 1 for frequencies below about 2 Hz and S/P < 1 in the higher frequency band extending from about 2 to 10 Hz. That is, the high frequency S/P ratio is not a reliable discriminant between the two source types for these recordings. On the other hand, the bandpass filter outputs corresponding to the ZK mine blast recording are observed to be quite different from those of the other five recordings in this distance group, with S/P > 1 in the intermediate frequency band extending from about 1.5 to 3 Hz and S/P $\approx$ 1 for frequencies above 3 Hz. This latter characteristic seems to be a consistent feature of all the ZK data which have been analyzed, and it once again illustrates the fact that the variations between the

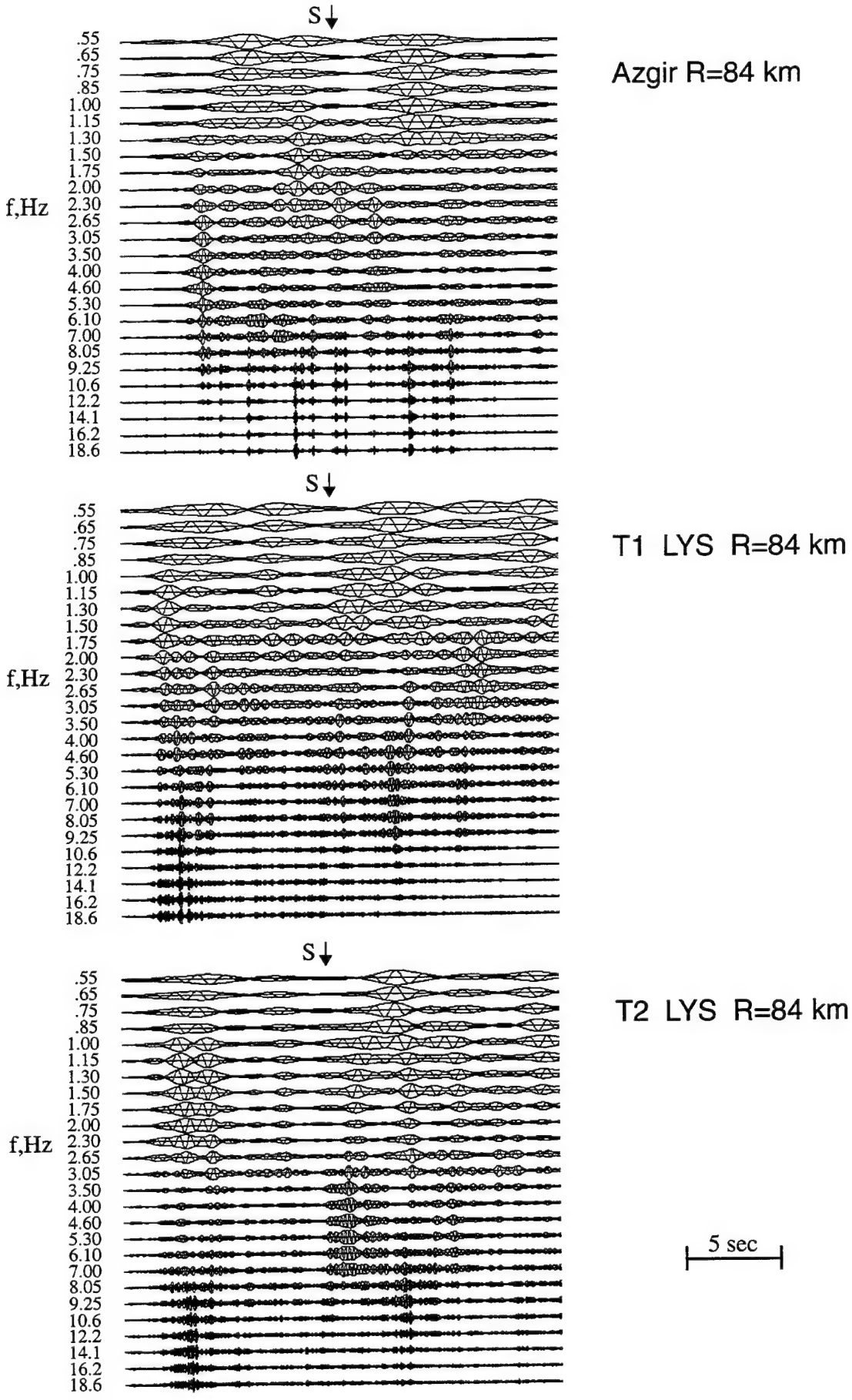

Figure 37. Comparison of bandpass filter outputs corresponding to nuclear explosion and ripple-fired mine blast recordings at a distance of 84 km.

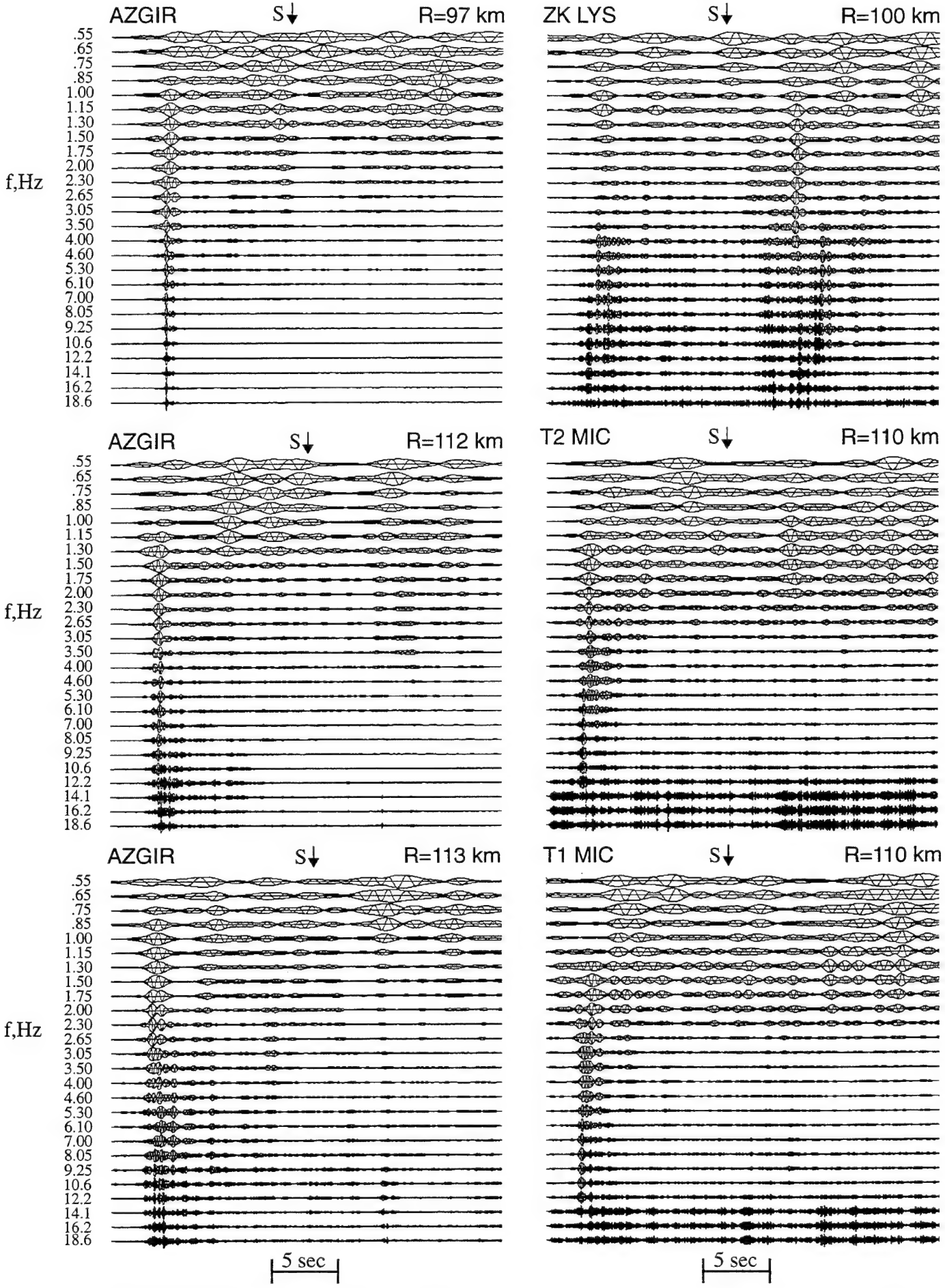

Figure 38. Comparison of bandpass filter outputs corresponding to nuclear explosion and ripple-fired mine blast recordings in the distance range $97 < \Delta < 113$ km.

frequency dependent S/P ratios for different mine blasts can be more pronounced than those observed between some nuclear explosion and mine blast recordings. Note also from Figure 38 that the low frequency S/P ratios are approximately equal to one for all the recordings in this distance group, consistent with the observations at the 84 km distance range, but in contrast to the observations for the two closer distance groups.

Thus, the data of Figures 34-38 are not consistent with any simple characterization of possible differences in the frequency dependent S/P ratios between nuclear explosion and ripple-fired mine blast sources. Rather, they seem to indicate that the effects of varying observation distances, propagation paths and seismic source characteristics of individual mine blast events can obscure any consistent differences between the two source types which might be isolated using the kind of time-dependent, narrowband filter technique employed in this analysis.

A more quantitative and direct technique for assessing frequency dependent variations in S/P excitation ratios is through comparisons of S/P spectral ratios determined from data recorded at comparable distances from different source types. Such ratios have been computed for the nuclear explosion and mine blast data of Figures 34-38, and the resulting S/P spectral ratio data for the four distance groupings are summarized in Figures 39-42. The results derived from the data recorded in the distance range $23 < \Delta < 40$ km are shown in Figure 39, where the ratios corresponding to the three mine blast recordings are separately compared with the ratios determined from the nuclear explosion recordings at 23 km (left) and at 40 km (right). It can be seen from this figure that these spectral ratio data are generally consistent with the results of previous discrimination studies (e.g., Bennett *et al.*, 1994) to the extent that the high frequency S/P ratios for the nuclear explosion data are less than 1.0, while those for the mine blast data are typically equal to or greater than 1.0. However, as was noted previously in conjunction with the discussion of Figure 34, these two populations do not appear to be very strongly separated in some cases, particularly with respect to the nuclear explosion recording at a distance of 40 km, for which the S/P spectral ratio for one of the mine blast recordings (i.e., ZK at 37 km) intersects the nuclear explosion spectral ratio at frequencies above 5 Hz.

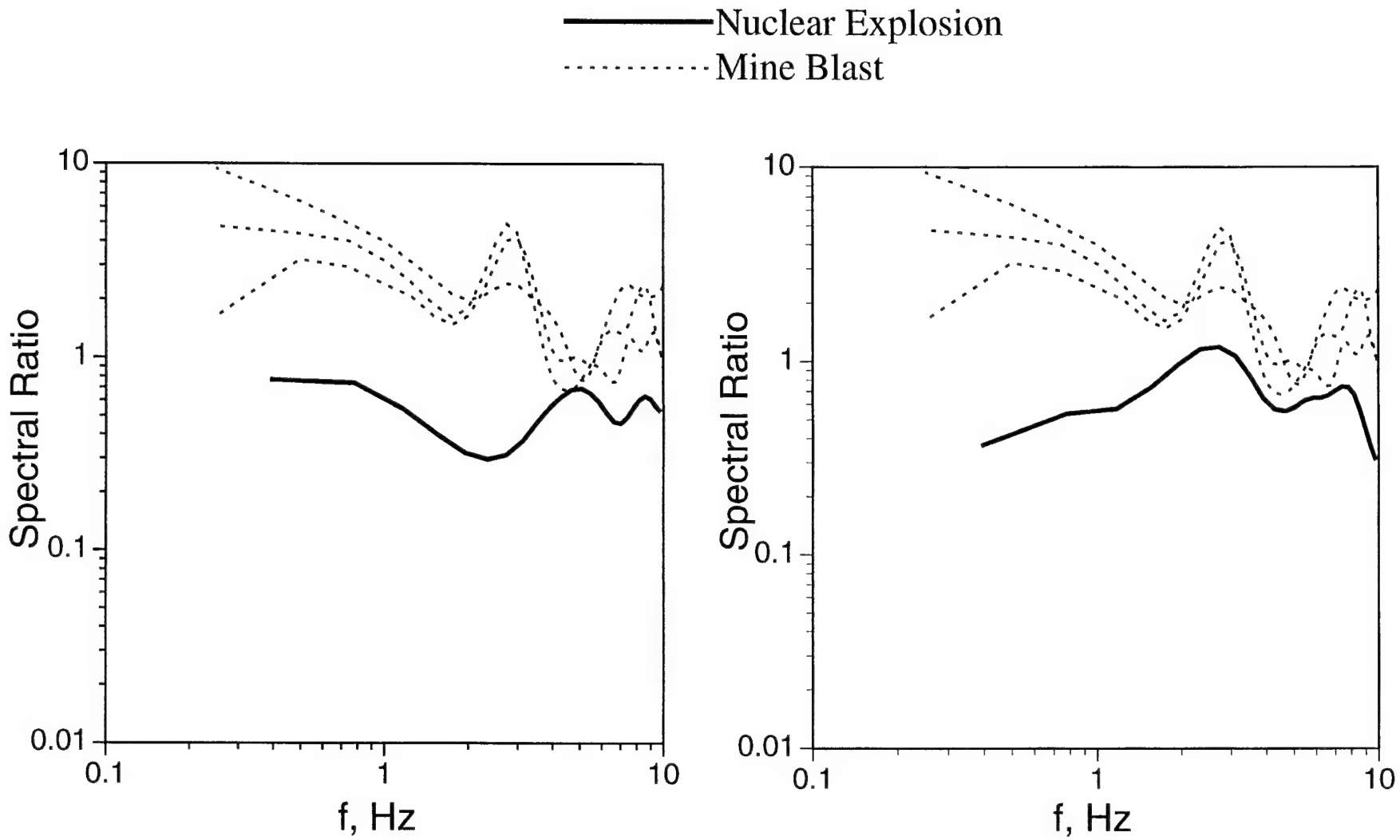

Figure 39. Comparison of S/P spectral ratios corresponding to nuclear explosion and ripple-fired mine blast recordings in the distance range $23 < \Delta < 40$ km.

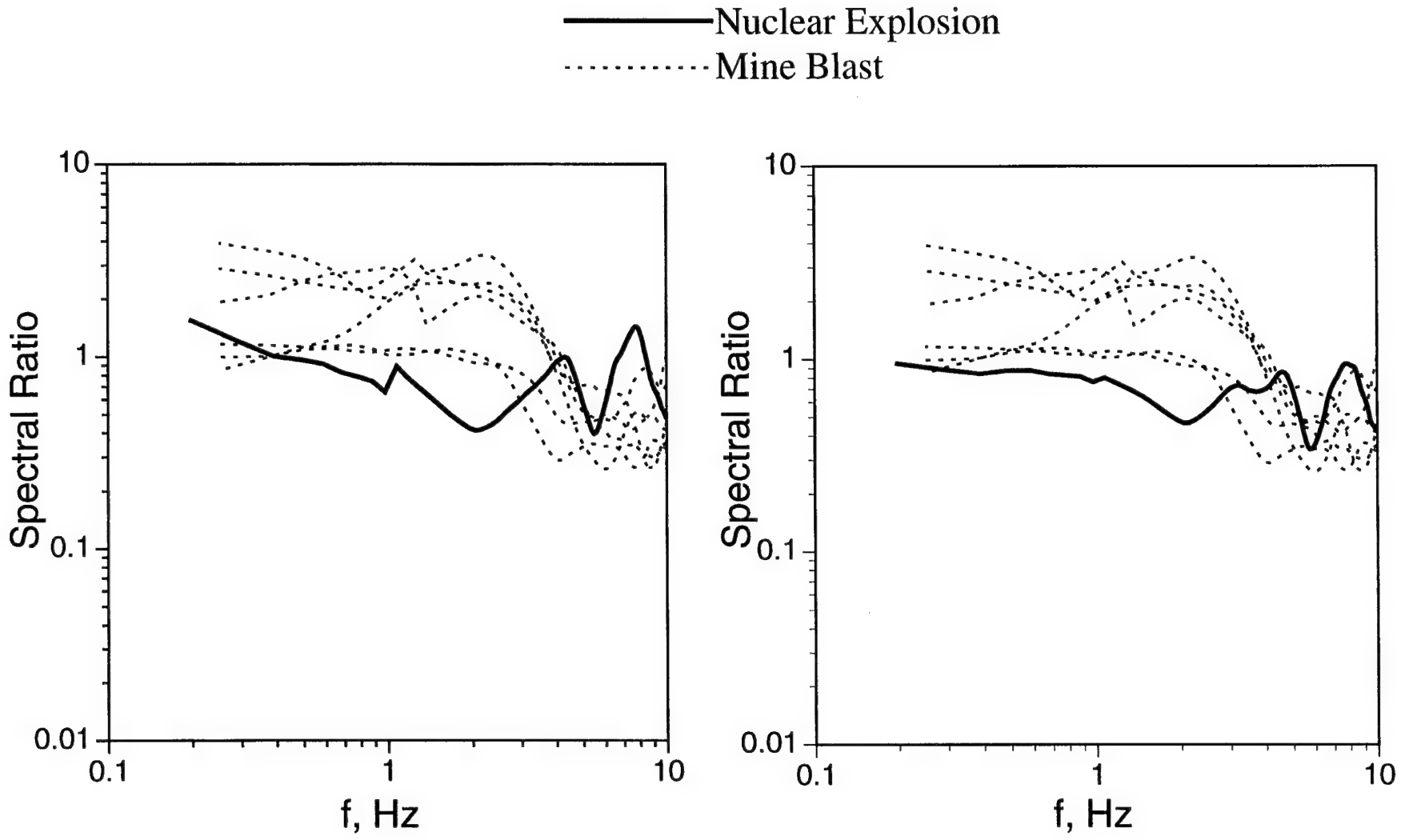

Figure 40. Comparison of S/P spectral ratios corresponding to nuclear explosion and ripple-fired mine blast recordings in the distance range $63 < \Delta < 69$ km.

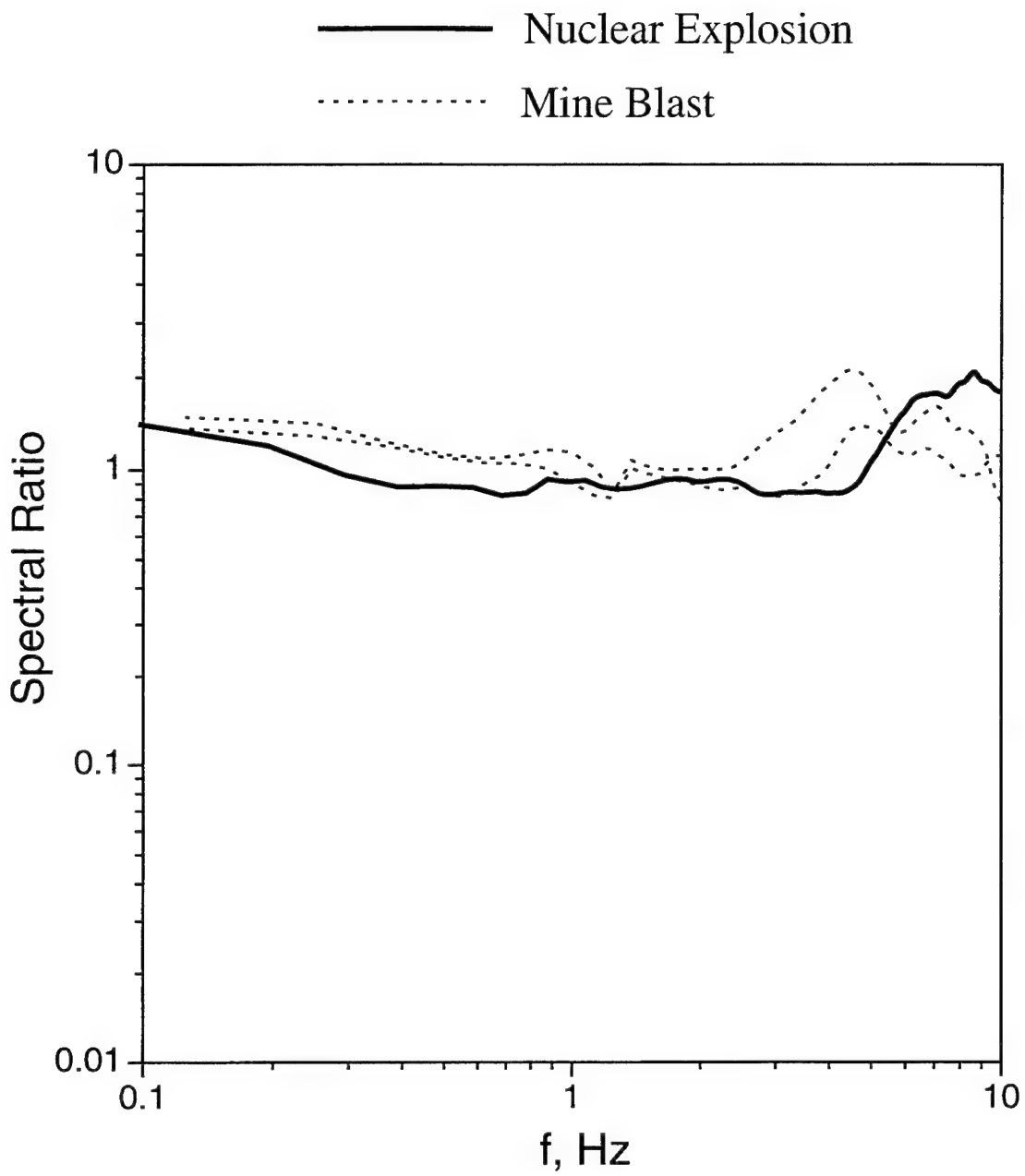

Figure 41. Comparison of S/P spectral ratios corresponding to nuclear explosion and ripple-fired mine blast recordings at a distance of 84 km.

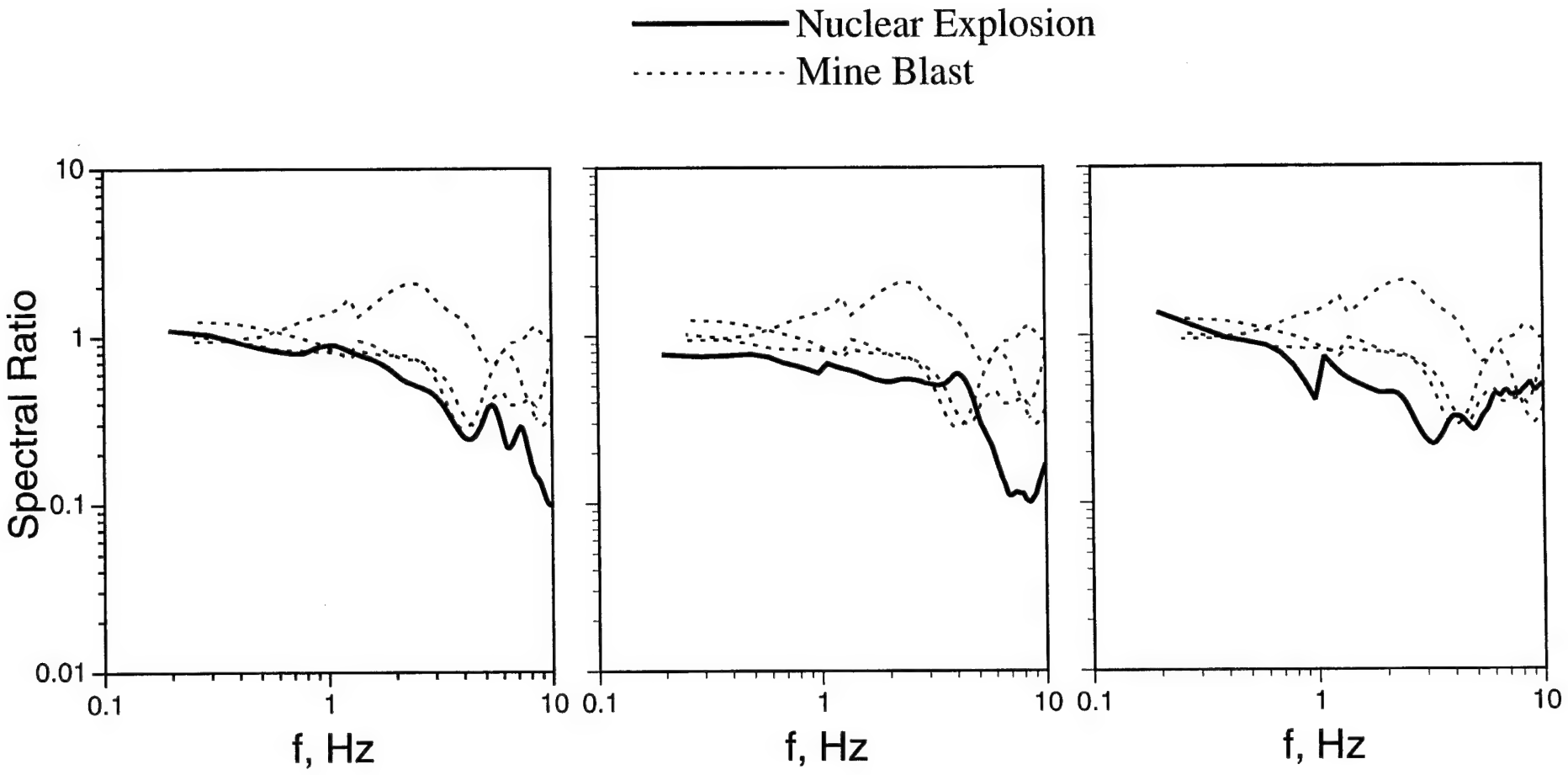

Figure 42. Comparison of S/P spectral ratios corresponding to nuclear explosion and ripple-fired mine blast recordings in the distance range $97 < \Delta < 113$ km.

The S/P spectral ratios derived from the data recorded in the distance range $63 < \Delta < 69$ km are shown in Figure 40, where the six mine blast ratios are separately compared with each of the two nuclear explosion ratios. It can be seen that for these data, the nuclear explosion spectral ratios average to a value of about 1.0 in the high frequency band between 5 and 10 Hz, while five of the six mine blast spectral ratios are significantly less than 1.0 over this same band. That is, these data show opposite trends, as a function of source type, than those noted for the closer distance grouping shown in Figure 39. The one mine blast spectral ratio which does not fit this pattern corresponds to the ZK recording at a range of 63 km, for which the high frequency S/P spectral ratio is nearly identical to those for the two nuclear explosion recordings. Very much the same pattern is observed for the 84 km distance S/P ratios shown in Figure 41. For this distance grouping, the S/P spectral ratios corresponding to the two source types are found to be remarkably similar over the entire displayed frequency range from 0.5 to 10 Hz.

Finally, the S/P spectral ratios corresponding to the three mine blast recordings in the distance range $97 < \Delta < 113$ km are presented in Figure 42 where they are separately compared with each of the three nuclear explosion spectral ratios from this distance grouping. In this case, all three of the nuclear explosion ratios and two of the three mine blast ratios tend toward values which are significantly less than 1.0 at high frequencies, with some overlap evident between the ratios corresponding to the two source types at both low and high frequencies. Once again, the significant outlier on these plots corresponds to the ZK mine blast recording at a range of 100 km, for which $S/P \approx 1.0$, independent of frequency.

Thus, these more detailed S/P spectral ratio comparisons are consistent with the previous bandpass filter analysis results in that they show significant variability as functions of source conditions, epicentral distance and propagation path characteristics. These results indicate that high frequency S/P ratios do not consistently separate the near-regional ground motions recorded from ripple-fired mine blasts and nuclear explosions, at least for the data set considered in this analysis.

4. SUMMARY AND CONCLUSIONS

4.1 Summary

Given that the feasibility of the cavity decoupling evasion scenario has been experimentally confirmed, it follows that conclusive monitoring of any eventual CTBT will necessarily involve identification analyses of signals recorded from small seismic events with magnitudes approaching a lower threshold which is on the order of m_b = 2.0. At such low magnitudes, seismic activity associated with naturally occurring earthquakes is supplemented by seismic events of similar size which are associated with chemical explosions (CE) which are routinely being carried out in most developed areas of the world in conjunction with a variety of quarrying, mining and construction projects. For this reason, it is important to characterize the types and sizes of the CE events which will have to be detected and identified in order to effectively monitor a CTBT. The investigations summarized in this report have centered on a variety of comparative analyses of observed and simulated seismic data corresponding to decoupled nuclear explosions and different types of CE events. In particular, data recorded from cavity decoupled nuclear tests in both the U.S. and former Soviet Union have been used as points of reference for evaluating potential seismic discriminants which might be used to differentiate such sources from CE events occurring in the same source regions.

The relative seismic coupling efficiencies of cavity decoupled nuclear explosions and different types of CE events were addressed in Section 2, where the phenomenology of cavity decoupling was reviewed and used as a basis for defining some simple scaling procedures applicable to the simulation of seismic signals corresponding to fully decoupled nuclear explosions of different yields. These scaling procedures were then applied to the broadband, near-regional seismic data recorded from tamped and partially decoupled Soviet Azgir nuclear explosions to obtain estimates of the ground motions to be expected from fully decoupled 1 kt explosions at that test site. Comparisons of these simulated nuclear data with ground motion data recorded from both tamped and near-surface, ripple-fired CE events were then used as a basis for estimating the relative seismic coupling efficiencies of these different source types. On the basis of this analysis, it was concluded that, for ripple-fired mine blasts at two mines

located near IRIS station KIV, explosions with total yields in the 70-100 ton range can be expected to produce near-regional ground motions with amplitude levels comparable to those expected from fully decoupled 1 kt nuclear explosions at Azgir. The corresponding equivalent yield for tamped CE events was estimated to be on the order of 7 tons. That is, it was concluded that tamped CE events couple about twice as well as tamped nuclear explosions of the same yield, while the average low frequency seismic coupling efficiencies of ripple-fired mine blasts at the two mines considered in this study were found to be factors of 5 to 7 lower than those of tamped nuclear explosions of comparable yield.

The seismic identification of cavity decoupled nuclear explosions and CE events was considered in Section 3 where, once again it was found to be necessary to differentiate between tamped and ripple-fired CE events. With regard to seismic discrimination of tamped CE events, data recorded from the U.S. NPE and STERLING HE explosions were reviewed and it was concluded that, at least in some cases, the seismic source characteristics of tamped CE events appear to be indistinguishable from those of tamped nuclear explosions over the entire frequency range of interest in seismic monitoring. Moreover, comparisons of seismic signals observed from tamped and cavity decoupled nuclear explosions at common stations were presented which indicated that, while potentially diagnostic differences between these two source types may be detectable in the data from isolated locations, their seismic source characteristics generally appear to be quite similar at most stations. It follows that unambiguous seismic identification of fully decoupled nuclear explosions at the 1 kt level will likely be very difficult in any regions where tamped CE events with yields on the order of 10 tons are conducted in conjunction with underground mining activities. Some combination of nonseismic monitoring methods and on-site inspections may be required to insure treaty compliance at that level in such areas.

A seismic identification analysis of near-surface, ripple-fired quarry blasts was also presented in Section 3, where it was noted that, while the identification of such explosions is often represented as a solved problem, there remain a number of practical issues of concern for CTBT monitoring. Thus, over the past 6 or so years, a number of studies have been published in which potentially diagnostic spectral banding has been detected in the seismic signals recorded from significant numbers of quarry blast sources. However, it is important to

recognize that rather broadband data were typically required to confidently detect this spectral banding, as evidenced by the fact that high sample rate data recorded at distances of a few hundred kilometers or less have generally been used in these studies. Since the station spacing in any likely CTBT monitoring network will be much larger than this, it is appropriate to question whether the high frequency data required to implement this discriminant will be routinely available for analysis, particularly in regions where the anelastic attenuation is relatively high. Moreover, it has been noted by a number of investigators that, even when good data are available, spectral banding is not observed to be a universal feature of all quarry blasts, particularly for those ripple-fired explosions which employ short delay times. For these reasons, it is appropriate to explore a wider range of potential discriminants of such events and, in our analysis, we attempted to do this using direct comparisons of scaled nuclear explosion data with seismic data recorded from selected ripple-fired quarry blasts conducted at two mine sites located west of the Caspian Sea near IRIS station KIV. Spectrogram analyses of these mine blast data revealed no consistent banding in the seismic data recorded from these events at stations in the near-regional distance range extending from about 33 to 110 km, presumably due to some combination of data bandwidth limitations and short delay times in these selected ripple-fired explosions. Similarly, it was found that the high frequency S/P spectral ratio discriminant, which has been found to consistently separate earthquake and nuclear explosion sources, did not reliably separate the data recorded from this sample of nuclear explosion and ripple-fired CE events. Consequently, it was concluded that additional research will be required before it will be possible to routinely discriminate between these two source types in cases where spectral banding can not be confidently identified.

4.2 Conclusions

The research summarized above supports the following principal conclusions regarding the seismic identification of small, cavity decoupled nuclear explosions.

(1) Fully decoupled 1 kt nuclear explosions can be expected to produce seismic signals consistent with teleseismic body wave magnitudes in the range $2.1 < m_b < 2.6$, depending upon the tectonic environment in the source region.

(2) A completely reliable CTBT monitoring network will be required to have the capability to routinely detect and identify tamped CE events with yields greater than about 5 tons and near-surface, ripple-fired mine blasts with yields greater than about 50 tons, at least in regions where cavity decoupling is considered to be feasible at the 1 kt level.

(3) The seismic source characteristics of at least some tamped CE events appear to be indistinguishable from those of tamped nuclear explosions over the entire frequency range of interest in seismic monitoring.

(4) High frequency S/P spectral ratios for tamped nuclear explosions are observed to be significantly larger than those for cavity decoupled nuclear explosions in some instances. However, this is not consistently found to be the case and such data do not appear to provide a reliable basis for discriminating between these two source types.

(5) Spectral banding is not a universal feature of ripple-fired quarry blast sources and spectrogram data alone are not sufficient to discriminate between broadband seismic data recorded from cavity decoupled nuclear explosions and ripple-fired mine blasts for our selected sample of events located in the Caspian Sea region.

(6) High frequency S/P spectral ratios derived from data recorded from nuclear explosion sources are typically lower than those observed for other types of seismic sources. However, the S/P spectral ratios determined from our selected sample of ripple-fired quarry blasts show significant variability as functions of epicentral distance, propagation path and the specific explosive configurations at the source, and tend to overlap the corresponding ratios associated with Azgir nuclear explosions.

(7) Seismic discrimination between small cavity decoupled nuclear explosions and CE events remains as a major challenge to effective CTBT monitoring.

REFERENCES

Adushkin, V. V., I. O. Kitov and D. D. Sultanov (1992), Experimental Results of USSR Nuclear Explosion Decoupling Measurements," Paper presented at the 14th Annual PL/DARPA Seismic Research Symposium, PL-TR-92-2210, ADA256711.

Barker, T. G., K. L. McLaughlin and J. L. Stevens (1992), "Numerical Simulation of Quarry Blast Sources," S-CUBED Technical Report to DARPA, SSS-TR-93-13859.

Baumgardt, D. R. and K. A. Ziegler (1988), "Spectral Evidence for Source Multiplicity in Explosions: Application to Regional Discrimination of Earthquakes and Explosions," *Bull. Seism. Soc. Am.*, *78*, 1773-1795.

Bennett, T. J., B. W. Barker and J. R. Murphy (1994), "Investigation of Regional Seismic Discrimination Issues for Small or Decoupled Nuclear Explosions," S-CUBED Technical Report SSS-DTR-94-14821 (PL-TR-94-2260), ADA292744.

Blandford, R. R. (1995), "Discrimination of Mining, Cratering, Tamped, and Decoupled Explosions Using High Frequency S-to-P Ratios," AFTAC-TR-95-002.

Brode, H. L. (1968), "Review of Nuclear Weapons Effects," *Annual Review of Nuclear Science*, *18*, p. 153.

Denny, M., P. Goldstein, K. Mayeda and W. R. Walter (1995), "Seismic Results from DoE's Non-Proliferation Experiment: A Comparison of Chemical and Nuclear Explosions," *Seismological Research Letters*, *66*, No. 2.

Glenn, L. A. and P. Goldstein (1994), "Seismic Decoupling with Chemical and Nuclear Explosions in Salt," *Journal of Geophysical Research*, Vol. 99, No. B6, p. 11,723.

Hedlin, M. A., J. B. Minster, and J. A. Orcutt (1989), "The Time-frequency Characteristics of Quarry Blasts and Calibration Explosions Recorded in Kazakhstan, USSR," *Geophys. J. Int.*, 99, 109-121.

Hedlin, M. A., J. B. Minster, and J. A. Orcutt (1990), "An Automatic Means to Discriminate Between Earthquakes and Quarry Blasts," *Bull. Seism. Soc. Am.*, *80*, 2143-2160.

Kim, W. Y., D. W. Simpson and P. G. Richards (1994), "High-Frequency Spectra of Regional Phases from Earthquakes and Chemical Explosions," *Bull. Seism. Soc. Am.*, *84*, 1365-1386.

Kitov, I. O., V. V. Adushkin, V. N. Kostuchenko, O. P. Kuznetsov and D. D. Sultanov (1994), "Procedures for Photographic Paper Record Digitizing," Scientific Report Number 1 on S-CUBED Contract 911412, August.

Latter, A. L., R. E. Lelevier, E. A. Martinelli and W. G. McMillan (1961), "A Method of Concealing Underground Nuclear Explosions," *J. Geophys. Res.*, *66*, p. 2929.

Mueller, R. A. and J. R. Murphy (1971), "Seismic Characteristics of Underground Nuclear Detonations. Part I. Seismic Spectrum Scaling," *Bull. Seism. Soc. Am.*, *61*, 1975.

Murphy, J. R. and B. W. Barker (1994), "Seismic Identification Analyses of Cavity Decoupled Nuclear and Chemical Explosions," S-CUBED Technical Report SSS-TR-94-14399 (PL-TR-94-2036), ADA280947.

Murphy, J. R., I. O. Kitov, J. L. Stevens, D. D. Sultanov, B. W. Barker, N. Rimer and M. C. Friedman (1994), "Analyses of the Seismic Characteristics of U.S. and Russian Cavity Decoupled Explosions," PL-TR-94-2295, ADA292881.

Office of Technology Assessment (1988), "Seismic Verification of Nuclear Testing Treaties," OTA-SC-361, Government Printing Office, Washington, DC.

Perret, W. R. (1968a), "Free-Field Particle Motion from a Nuclear Explosion in Salt, Part I," Sandia Laboratory Report VUF-3012.

Perret, W. R. (1968b), "Free-Field Ground Motion Study, Project Sterling," Sandia Laboratory Report SC-RR-68-410.

Richards, P. G., D. A. Anderson, and D. W. Simpson (1992), "A Survey of Blasting Activity in the United States," *Bull. Seism. Soc. Am.*, *82*, 1416-1433.

Rimer, N., W. Proffer, E. Halda and R. Nilson (1933), "Containment Related Phenomenology from Chemical Kiloton," S-CUBED Technical Report to DNA, SSS-DTR-94-14405.

Rivière-Barbier, F. (1993), "Status Report on the Cooperative Research Program Between the EME and the CSS for Exchange and Analysis of Seismic Data from Quarry Blasts in Russia and in the U.S.," DARPA Center for Seismic Studies Report C93-01.

Rodean, H. C. (1971), "Cavity Decoupling of Nuclear Explosions," UCRL-51097.

Smith, A. T. (1989), "High-Frequency Seismic Observations and Models of Chemical Explosions: Implications for the Discrimination of Ripple-Fired Mining Blasts," *Bull. Seism. Soc. Am., 79*, 1089-1110.

Springer, D., M. Denny, J. Healy and W. Mickey (1968), "The Sterling Experiment: Decoupling of Seismic Waves by a Shot-Generated Cavity," *J. Geophys. Res., 73*, pp. 5995-6011.

Stevens, J. L., J. R. Murphy and N. Rimer (1991), "Seismic Source Characteristics of Cavity Decoupled Explosions in Salt and Tuff," *Bull. Seism. Soc. Am., 81*, 4 pp. 1272-1291.

Stump, B. W., D. C. Pearson and R. E. Reinke (1994), "Source Comparisons Between Nuclear and Chemical Explosions Detonated at Rainier Mesa Nevada Test Site," Los Alamos CTBT R&D Program, LAUR-94-4073.

Sykes, L. R. (1994), "Dealing With Decoupled Nuclear Explosions Under a Comprehensive Test Ban Treaty," PL-TR-94-2301, ADA290740.

Walter, W. R., H. J. Patton and K. M. Maid (1994), "Regional Seismic Observations of the NPE at the Livermore NTS Network," U.S. Department of Energy, Non-Proliferation Experiment Symposium, Rockville, Maryland, April.

Prof. Thomas Ahrens
Seismological Lab, 252-21
Division of Geological & Planetary Sciences
California Institute of Technology
Pasadena, CA 91125

Prof. Keiiti Aki
Center for Earth Sciences
University of Southern California
University Park
Los Angeles, CA 90089-0741

Prof. Shelton Alexander
Geosciences Department
403 Deike Building
The Pennsylvania State University
University Park, PA 16802

Prof. Charles B. Archambeau
University of Colorado
JSPC
Campus Box 583
Boulder, CO 80309

Dr. Thomas C. Bache, Jr.
Science Applications Int'l Corp.
10260 Campus Point Drive
San Diego, CA 92121 (2 copies)

Prof. Muawia Barazangi
Cornell University
Institute for the Study of the Continent
3126 SNEE Hall
Ithaca, NY 14853

Dr. Jeff Barker
Department of Geological Sciences
State University of New York
at Binghamton
Vestal, NY 13901

Dr. Douglas R. Baumgardt
ENSCO, Inc
5400 Port Royal Road
Springfield, VA 22151-2388

Dr. Susan Beck
Department of Geosciences
Building #77
University of Arizona
Tuscon, AZ 85721

Dr. T.J. Bennett
S-CUBED
A Division of Maxwell Laboratories
11800 Sunrise Valley Drive, Suite 1212
Reston, VA 22091

Dr. Robert Blandford
AFTAC/TT, Center for Seismic Studies
1300 North 17th Street
Suite 1450
Arlington, VA 22209-2308

Dr. Stephen Bratt
ARPA/NMRO
3701 North Fairfax Drive
Arlington, VA 22203-1714

Dale Breding
U.S. Department of Energy
Recipient, IS-20, GA-033
Office of Arms Control
Washington, DC 20585

Dr. Lawrence Burdick
C/O Barbara Wold
Dept of Biology
CA Inst. of Technology
Pasadena, CA 91125

Dr. Robert Burridge
Schlumberger-Doll Research Center
Old Quarry Road
Ridgefield, CT 06877

Dr. Jerry Carter
Center for Seismic Studies
1300 North 17th Street
Suite 1450
Arlington, VA 22209-2308

Dr. Martin Chapman
Department of Geological Sciences
Virginia Polytechnical Institute
21044 Derring Hall
Blacksburg, VA 24061

Mr Robert Cockerham
Arms Control & Disarmament Agency
320 21st Street North West
Room 5741
Washington, DC 20451,

Prof. Vernon F. Cormier
Department of Geology & Geophysics
U-45, Room 207
University of Connecticut
Storrs, CT 06268

Prof. Steven Day
Department of Geological Sciences
San Diego State University
San Diego, CA 92182

Dr. Zoltan Der
ENSCO, Inc.
5400 Port Royal Road
Springfield, VA 22151-2388

Dr. Stanley K. Dickinson
AFOSR/NM
110 Duncan Avenue
Suite B115
Bolling AFB, DC 20332-6448

Prof. Adam Dziewonski
Hoffman Laboratory, Harvard University
Dept. of Earth Atmos. & Planetary Sciences
20 Oxford Street
Cambridge, MA 02138

Prof. John Ebel
Department of Geology & Geophysics
Boston College
Chestnut Hill, MA 02167

Dr. Petr Firbas
Institute of Physics of the Earth
Masaryk University Brno
Jecna 29a
612 46 Brno, Czech Republic

Dr. Mark D. Fisk
Mission Research Corporation
735 State Street
P.O. Drawer 719
Santa Barbara, CA 93102

Prof. Donald Forsyth
Department of Geological Sciences
Brown University
Providence, RI 02912

Dr. Cliff Frolich
Institute of Geophysics
8701 North Mopac
Austin, TX 78759

Dr. Holly Given
IGPP, A-025
Scripps Institute of Oceanography
University of California, San Diego
La Jolla, CA 92093

Dr. Jeffrey W. Given
SAIC
10260 Campus Point Drive
San Diego, CA 92121

Dr. Indra N. Gupta
Multimax, Inc.
1441 McCormick Drive
Landover, MD 20785

Dan N. Hagedon
Pacific Northwest Laboratories
Battelle Boulevard
Richland, WA 99352

Dr. James Hannon
Lawrence Livermore National Laboratory
P.O. Box 808, L-205
Livermore, CA 94550

Prof. Danny Harvey
University of Colorado, JSPC
Campus Box 583
Boulder, CO 80309

Prof. Donald V. Helmberger
Division of Geological & Planetary Sciences
California Institute of Technology
Pasadena, CA 91125

Prof. Eugene Herrin
Geophysical Laboratory
Southern Methodist University
Dallas, TX 75275

Prof. Robert B. Herrmann
Department of Earth & Atmospheric Sciences
St. Louis University
St. Louis, MO 63156

Prof. Lane R. Johnson
Seismographic Station
University of California
Berkeley, CA 94720

Prof. Thomas H. Jordan
Department of Earth, Atmospheric &
Planetary Sciences
Massachusetts Institute of Technology
Cambridge, MA 02139

Prof. Alan Kafka
Department of Geology & Geophysics
Boston College
Chestnut Hill, MA 02167

U.S. Dept of Energy
Max Koontz, NN-20, GA-033
Office of Research and Develop.
1000 Independence Avenue
Washington, DC 20585

Dr. Richard LaCoss
MIT Lincoln Laboratory, M-200B
P.O. Box 73
Lexington, MA 02173-0073

Dr. Fred K. Lamb
University of Illinois at Urbana-Champaign
Department of Physics
1110 West Green Street
Urbana, IL 61801

Prof. Charles A. Langston
Geosciences Department
403 Deike Building
The Pennsylvania State University
University Park, PA 16802

Jim Lawson, Chief Geophysicist
Oklahoma Geological Survey
Oklahoma Geophysical Observatory
P.O. Box 8
Leonard, OK 74043-0008

Prof. Thorne Lay
Institute of Tectonics
Earth Science Board
University of California, Santa Cruz
Santa Cruz, CA 95064

Dr. William Leith
U.S. Geological Survey
Mail Stop 928
Reston, VA 22092

Mr. James F. Lewkowicz
Phillips Laboratory/GPE
29 Randolph Road
Hanscom AFB, MA 01731-3010(2 copies)

Prof. L. Timothy Long
School of Geophysical Sciences
Georgia Institute of Technology
Atlanta, GA 30332

Dr. Randolph Martin, III
New England Research, Inc.
76 Olcott Drive
White River Junction, VT 05001

Dr. Robert Masse
Denver Federal Building
Box 25046, Mail Stop 967
Denver, CO 80225

Dr. Gary McCartor
Department of Physics
Southern Methodist University
Dallas, TX 75275

Prof. Thomas V. McEvilly
Seismographic Station
University of California
Berkeley, CA 94720

Dr. Art McGarr
U.S. Geological Survey
Mail Stop 977
U.S. Geological Survey
Menlo Park, CA 94025

Dr. Keith L. McLaughlin
S-CUBED
A Division of Maxwell Laboratory
P.O. Box 1620
La Jolla, CA 92038-1620

Stephen Miller & Dr. Alexander Florence
SRI International
333 Ravenswood Avenue
Box AF 116
Menlo Park, CA 94025-3493

Prof. Bernard Minster
IGPP, A-025
Scripps Institute of Oceanography
University of California, San Diego
La Jolla, CA 92093

Prof. Brian J. Mitchell
Department of Earth & Atmospheric Sciences
St. Louis University
St. Louis, MO 63156

Mr. Richard J. Morrow
USACDA/IVI
320 21st St. N.W.
Washington , DC 20451

Mr. Jack Murphy
S-CUBED
A Division of Maxwell Laboratory
11800 Sunrise Valley Drive, Suite 1212
Reston, VA 22091 (2 Copies)

Dr. Keith K. Nakanishi
Lawrence Livermore National Laboratory
L-025
P.O. Box 808
Livermore, CA 94550

Prof. John A. Orcutt
IGPP, A-025
Scripps Institute of Oceanography
University of California, San Diego
La Jolla, CA 92093

Prof. Jeffrey Park
Kline Geology Laboratory
P.O. Box 6666
New Haven, CT 06511-8130

Dr. Howard Patton
Lawrence Livermore National Laboratory
L-025
P.O. Box 808
Livermore, CA 94550

Dr. Frank Pilotte
HQ AFTAC/TT
1030 South Highway A1A
Patrick AFB, FL 32925-3002

Dr. Jay J. Pulli
Radix Systems, Inc.
6 Taft Court
Rockville, MD 20850

Dr. Robert Reinke
ATTN: FCTVTD
Field Command
Defense Nuclear Agency
Kirtland AFB, NM 87115

Prof. Paul G. Richards
Lamont-Doherty Earth Observatory
of Columbia University
Palisades, NY 10964

Mr. Wilmer Rivers
Teledyne Geotech
1300 17th St N #1450
Arlington, VA 22209-3803

Dr. Alan S. Ryall, Jr.
Lawrence Livermore National Laboratory
P.O. Box 808, L-205
Livermore, CA 94550

Dr.Chandan K. Saikia
Woodward Clyde- Consultants
566 El Dorado Street
Pasadena, CA 91101

Dr. Richard Sailor
TASC, Inc.
55 Walkers Brook Drive
Reading, MA 01867

Prof. Charles G. Sammis
Center for Earth Sciences
University of Southern California
University Park
Los Angeles, CA 90089-0741

Prof. Christopher H. Scholz
Lamont-Doherty Earth Observatory
of Columbia University
Palisades, NY 10964

Dr. Susan Schwartz
Institute of Tectonics
1156 High Street
Santa Cruz, CA 95064

Mr. Dogan Seber
Cornell University
Inst. for the Study of the Continent
3130 SNEE Hall
Ithaca, NY 14853-1504

Secretary of the Air Force
(SAFRD)
Washington, DC 20330

Office of the Secretary of Defense
DDR&E
Washington, DC 20330

Thomas J. Sereno, Jr.
Science Application Int'l Corp.
10260 Campus Point Drive
San Diego, CA 92121

Dr. Michael Shore
Defense Nuclear Agency/SPSS
6801 Telegraph Road
Alexandria, VA 22310

Dr. Robert Shumway
University of California Davis
Division of Statistics
Davis, CA 95616

Dr. Matthew Sibol
Virginia Tech
Seismological Observatory
4044 Derring Hall
Blacksburg, VA 24061-0420

Prof. David G. Simpson
IRIS, Inc.
1616 North Fort Myer Drive
Suite 1050
Arlington, VA 22209

Donald L. Springer
Lawrence Livermore National Laboratory
L-025
P.O. Box 808
Livermore, CA 94550

Dr. Jeffrey Stevens
S-CUBED
A Division of Maxwell Laboratory
P.O. Box 1620
La Jolla, CA 92038-1620

Prof. Brian Stump
Los Alamos National Laboratory
EES-3
Mail Stop C-335
Los Alamos, NM 87545

Prof. Jeremiah Sullivan
University of Illinois at Urbana-Champaign
Department of Physics
1110 West Green Street
Urbana, IL 61801

Prof. L. Sykes
Lamont-Doherty Earth Observatory
of Columbia University
Palisades, NY 10964

Dr. Steven R. Taylor
Los Alamos National Laboratory
P.O. Box 1663
Mail Stop C335
Los Alamos, NM 87545

Prof. Tuncay Taymaz
Istanbul Technical University
Dept. of Geophysical Engineering
Mining Faculty
Maslak-80626, Istanbul Turkey

Prof. Clifford Thurber
University of Wisconsin-Madison
Department of Geology & Geophysics
1215 West Dayton Street
Madison, WS 53706

Prof. M. Nafi Toksoz
Earth Resources Lab
Massachusetts Institute of Technology
42 Carleton Street
Cambridge, MA 02142

Dr. Larry Turnbull
CIA-OSWR/NED
Washington, DC 20505

Dr. Gregory van der Vink
IRIS, Inc.
1616 North Fort Myer Drive
Suite 1050
Arlington, VA 22209

Dr. Karl Veith
EG&G
2341 Jefferson Davis Highway
Suite 801
Arlington, VA 22202-3809

Prof. Terry C. Wallace
Department of Geosciences
Building #77
University of Arizona
Tuscon, AZ 85721

Dr. Thomas Weaver
Los Alamos National Laboratory
P.O. Box 1663
Mail Stop C335
Los Alamos, NM 87545

Dr. William Wortman
Mission Research Corporation
8560 Cinderbed Road
Suite 700
Newington, VA 22122

Prof. Francis T. Wu
Department of Geological Sciences
State University of New York
at Binghamton
Vestal, NY 13901

Prof Ru-Shan Wu
University of California, Santa Cruz
Earth Sciences Department
Santa Cruz, CA 95064

ARPA, OASB/Library
3701 North Fairfax Drive
Arlington, VA 22203-1714

HQ DNA
ATTN: Technical Library
Washington, DC 20305

Defense Technical Information Center
8725 John J. Kingman Road
Ft Belvoir, VA 22060-6218
(2 copies)

TACTEC
Battelle Memorial Institute
505 King Avenue
Columbus, OH 43201 (Final Report)

Phillips Laboratory
ATTN: XPG
29 Randolph Road
Hanscom AFB, MA 01731-3010

Phillips Laboratory
ATTN: GPE
29 Randolph Road
Hanscom AFB, MA 01731-3010

Phillips Laboratory
ATTN: TSML
5 Wright Street
Hanscom AFB, MA 01731-3004

Phillips Laboratory
ATTN: PL/SUL
3550 Aberdeen Ave SE
Kirtland, NM 87117-5776 (2 copies)

Dr. Michel Bouchon
I.R.I.G.M.-B.P. 68
38402 St. Martin D'Heres
Cedex, FRANCE

Dr. Michel Campillo
Observatoire de Grenoble
I.R.I.G.M.-B.P. 53
38041 Grenoble, FRANCE

Prof. Hans-Peter Harjes
Institute for Geophysic
Ruhr University/Bochum
P.O. Box 102148
4630 Bochum 1, GERMANY

Prof. Eystein Husebye
IFJF
Jordskjelvstasjonen
Allegaten, 5007 BERGEN NORWAY

David Jepsen
Acting Head, Nuclear Monitoring Section
Bureau of Mineral Resources
Geology and Geophysics
G.P.O. Box 378, Canberra, AUSTRALIA

Ms. Eva Johannisson
Senior Research Officer
FOA
S-172 90 Sundbyberg, SWEDEN

Dr. Peter Marshall
Procurement Executive
Ministry of Defense
Blacknest, Brimpton
Reading FG7-FRS, UNITED KINGDOM

Dr. Bernard Massinon, Dr. Pierre Mechler
Societe Radiomana
27 rue Claude Bernard
75005 Paris, FRANCE (2 Copies)

Dr. Svein Mykkeltveit
NTNT/NORSAR
P.O. Box 51
N-2007 Kjeller, NORWAY (3 Copies)

Prof. Keith Priestley
University of Cambridge
Bullard Labs, Dept. of Earth Sciences
Madingley Rise, Madingley Road
Cambridge CB3 OEZ, ENGLAND

Dr. Jorg Schlittenhardt
Federal Institute for Geosciences & Nat'l Res.
Postfach 510153
D-30631 Hannover , GERMANY

Dr. Johannes Schweitzer
Institute of Geophysics
Ruhr University/Bochum
P.O. Box 1102148
4360 Bochum 1, GERMANY

Trust & Verify
VERTIC
Carrara House
20 Embankment Place
London WC2N 6NN, ENGLAND

Prof. Dr. M. Namik YALCIN
Dept. of Earth Sciences
P.O. Box 21,
41470
GEBZE-KOCAELI, TURKEY